

DEGREE PROGRAMME IN MECHANICAL ENGINEERING

## **MASTER THESIS**

### **Optimisation model for a ship's hybrid energy system with a Flettner rotor**

Author	Alessandro Maruccia
Supervisor	Prof. Kari Tammi
Advisor	M. Sc. Janne Huotari

May, 2019





---

**Author** Alessandro Maruccia

---

**Title of thesis** Optimisation model for a ship's hybrid energy system with a Flettner rotor

---

**Master programme** Mechanical Engineering

**Code** ENG25

---

**Thesis supervisor** Prof. Kari Tammi

---

**Thesis advisor(s)** M.Sc. Janne Huotari

---

**Date** 26.05.2019

**Number of pages** 81

**Language** English

---

## Abstract

This thesis attempts to investigate the effect of the implementation of Flettner rotors in the topology of the cruise ship *Silja Serenade*, which, in the year of this thesis dissertation, travels from Helsinki to Stockholm. The aim is the implementation of simulation models written in Matlab that simulate the behaviour of the ship topologies' components, with the goal of minimising the global fuel consumption. The models refer to a particular time period defined by the provided data, but the structure is completely general and can be applied to the most different data and time periods, and for every ship. The topologies will consider the presence of a battery and a shaft generator.

In the first part of this work, the literature part is described, covering the reasons of fuel consumption's restrictions, the Flettner rotor's old and recent history, the fundamentals of the ships' topologies and a brief introduction to the optimisation theory. Those chapters are essential in order to comprehend what are the motivations for the research topic and how the work is developed.

The second part includes the building of the optimisation models, the logic that they follow and the results. Each component of the topologies is explained separately, clarifying the assumptions taken over them and explaining why they are reasonable. The optimisation models are explained step by step, discussing why each decision is taken and how they influence the final results.

In the final part, final conclusions are drawn. Results compare the case of different topologies in order to establish firmly the impact of the various topologies arrangements on the total fuel consumption, with a special focus on the effects that the Flettner rotors' implementation has on it.

---

**Keywords** Flettner rotors, Optimisation, Matlab, Ship topology, Fuel consumption reduction

---

# Acknowledgments

In the first place, I would like to express my gratitude to my supervisor Prof. Kari Tammi and to my advisor Janne Huotari, who constantly supported me during my researches and encouraged me to widen my researches. To them goes my thanking, for their unstoppable patience, professionalism, motivation and huge knowledge. I would like to immensely thank my hosting University of Aalto for having increased my practicalities and skills and having provided me the tools that resulted to be essential for this work.

Equally, I would immensely like to express my thanks to my Italian supervisor Prof. Eleonora Atzeni for her fundamental contribution and the Polytechnic University of Turin for giving support during my exchange and for having furnished to me all the knowledge needed for this work.

I would like to express my gratitude to my parents that never stopped supporting and encouraging me, for the better or for the worse, and to my brother Tommaso. I would like to thank my wide net of friends and colleagues that supported me during this process of growing, with a special mention for Alessandra, Arturo, Eleonora, Eliana, Giovanni, Guido and Michela, my project manager and friend Alekski and my flatmates Gabriele and Marco. To them, but also to all the others, goes all my gratitude for having improved me as a person. Thank you.

# Table of contents

Abstract.....	II
Acknowledgments .....	III
Table of contents.....	III
List of tables.....	IV
List of figures.....	V
Abbreviations.....	VI
Nomenclature.....	VII
1 Introduction.....	1
1.1 Research motivation .....	2
1.2 Research purpose .....	5
2 Background.....	7
2.1 History of the Flettner rotors .....	7
2.2 Recent history .....	9
2.3 Challenges.....	13
3 How a cruise ship works.....	15
3.1 The ship's propulsion system .....	15

3.2 The naval diesel engine.....	15
3.2.1 ICE efficiency.....	18
3.3 The ship’s topologies.....	20
4 Basics of optimisation theory.....	25
5 Application of the optimisation model on Silja Serenade.....	28
5.1 Assumptions over the system’s topology – the propulsion unit.....	28
5.2 Assumptions over the system’s topology – the auxiliary unit.....	30
5.3 The diesel engines.....	32
5.4 Energy Storage System – the battery.....	37
5.5 The Flettner rotors.....	40
6 Models implementation.....	44
6.1 Matlab optimisation model.....	44
6.2 Models variables.....	46
6.3 Objective function.....	46
6.4 Constraints.....	51
6.5 Implementation of the model with the shaft generator.....	53
6.6 Optimised model with the Flettner rotor.....	54
7 Optimised results for the hybrid power system.....	56
7.1 Results for the propulsion power unit.....	56
7.2 Results for the auxiliary power unit.....	58
7.3 Results with the implementation of the shaft generator.....	62
7.4 Effects of the Flettner rotor on the propulsion system.....	66
7.5 Effects of the FR on the shaft generator’s powering topology.....	69
8 Conclusions.....	74
References.....	76

## List of tables

Table 1: Silja Serenade details.....	5
Table 2: SFOC data for ME.....	33
Table 3: SFOC data for AE.....	35
Table 4: Evaluation of the peaks.....	38
Table 5: AT6700 module data.....	40
Table 6: Fuel consumptions and savings for different solutions.....	74

## List of figures

Figure 1: Hybrid system solution example.....	1
Figure 2: WHO headquarters, in Geneva.....	3
Figure 3: Fuel consumption rate of different types of maritime engines.....	4
Figure 4: The Buckau with Flettner rotors.....	8
Figure 5: The ship Baden-Baden [27].....	9
Figure 6: Global Fossil Carbon Emissions from 1750 to 2000 .....	10
Figure 7: Polar diagram for the E-ship1: speed of 16 kn, true wind of 24 kn .....	11
Figure 8: The E-ship 1 [39].....	11
Figure 9: Slide from the ENERCON's 4th Conference on Ship Efficiency .....	12
Figure 10: Scheme of two-stroke diesel engine.....	16
Figure 11: Ideal Diesel cycle on the PV diagram .....	17
Figure 12: Indicated cycle for diesel engines .....	20
Figure 13: Diesel-electric plant [65].....	22
Figure 14: First type of ship topology .....	23
Figure 15: Second type for ship topology.....	24
Figure 16: All-electric propulsion system .....	24
Figure 17: Propulsion Power Demand.....	28
Figure 18: Propulsion power demand compared to the ship speed profile.....	29
Figure 19: Auxiliary power demand .....	31
Figure 20: Silja Serenade journey.....	32
Figure 21: SFOC for ME from data.....	33
Figure 22: FFR for the ME with maximum power of 8125 kW.....	34
Figure 23: FFR for the ME with maximum power of 7500 kW .....	35
Figure 24: SFOC for AE from data .....	36
Figure 25: FFR from data for AE with maximum power of 2400 kW .....	36
Figure 26: FFR from data for AE with maximum power of 3200 kW .....	37
Figure 27: Graph related to the fifth peak.....	39
Figure 28: Silja Serenade's polar diagram for the speed of 18 kn .....	41
Figure 29: Interpolated polar diagram values in 2D .....	42
Figure 30: 3D data representation – first view .....	42
Figure 31: 3D data representation – second view.....	43
Figure 32: Interpolated FFR and SFOC for ME with max power 8125 kW .....	48
Figure 33: Interpolated FFR and SFOC for ME with max power 7500 kW .....	48
Figure 34: Interpolated FFR and SFOC for the AEs with max power of 3200 kW .....	49
Figure 35: Interpolated FFR and SFOC for the AEs with max power of 2400 kW .....	50
Figure 36: Interpolated SFOC for MEs and AEs.....	50
Figure 37: Propulsion and auxiliary power demand.....	54
Figure 38: Data for the case of FR installation.....	55
Figure 39: Results for the propulsion power unit simulation .....	57
Figure 40: Optimised power plotted for each propeller-driving engine .....	57
Figure 41: Results for the auxiliary power unit simulation .....	58
Figure 42: Optimised power plotted for each motor-driving engine .....	59
Figure 43: Battery SOC .....	60
Figure 44: Results for the auxiliary power unit simulation for the evaluated time .....	61
Figure 45: Optimised power for each motor-driving engine for the evaluated time .....	61
Figure 46: Battery SOC for the evaluated time .....	62

Figure 47: Optimised propulsion engines with shaft generator .....	63
Figure 48: Optimised MEs powers with shaft generator .....	64
Figure 49: Optimised auxiliary AEs and battery with shaft generator .....	64
Figure 50: Optimised AEs and battery powers with shaft generator .....	65
Figure 51: Power converted through the shaft generator (input).....	65
Figure 52: Optimised battery SOC with the shaft generator .....	66
Figure 53: FR's thrust contribution .....	67
Figure 54: Powers related to the system .....	67
Figure 55: Optimised MEs in case of FR installation.....	68
Figure 56: Behaviour of MEs in case of FR installation .....	69
Figure 57: Optimised MEs in case of shaft generator and FR installation .....	70
Figure 58: Behaviour of MEs in case of shaft generator and FR installation.....	70
Figure 59: Optimised shaft power in case of shaft generator and FR installation.....	71
Figure 60: Optimised AEs in case of shaft generator and FR installation.....	71
Figure 61: Behaviour of AEs in case of shaft generator and FR installation .....	72
Figure 62: SOC trend in case of shaft generator and FR installation .....	72

## Abbreviations

AC	Alternate Current
AE	Auxiliary Engine
DC	Direct Current
DE	Diesel-electric engines
ESS	Energy Storage System
FR	Flettner rotor
FRR	Fuel Flow Rate
GHG	Green House Gases
HFO	Heavy Fuel Oil
ICE	Internal Combustion Engine
LP	Linear Problem
ME	Engine driving propeller
MILP	Mixed Integer Linear Program
PWM	Pulse Width Modulation
SFOC	Specific Fuel Oil Consumption
SOC	State Of Charge
WHO	World Health Organisation

## Nomenclature

$i$	Time step index
$j$	Engine index
$k$	Operating engine region index
$I$	Set of time steps
$J$	Set of engines
$K$	Set of engine operation regions

$C_{rate,cha}$	Charging C-rate
$C_{rate,dis}$	Discharging C-rate
$E_{B,max}$	Maximum battery energy
$E_B$	Battery Energy
$m_{add}$	Starting additional equivalent mass of fuel
$P_{B,cha}$	Battery Charging Power
$P_{B,dis}$	Battery discharge power
$P_D$	Demanded Power
$P_{E,max}$	Maximum engine power
$P_{E,min}$	Minimum engine power
$P_E$	Engine Power
$P_{E,aux}$	Auxiliary engine power
$P_{E,prop}$	Propulsion engine power
$P_{shaft}$	Shaft generator power
$P_{thrusters}$	Bow thrusters power demand
$\eta_{cha}$	Battery charging efficiency
$\eta_{dis}$	Battery discharging efficiency
$\eta_{shaft}$	Shaft generator efficiency
engOn	On/off engine's status
TurnOn	Turning on engine's status
$\theta_{max}$	Engine's working region upper threshold
$\theta_{min}$	Engine's working region lower threshold
$\Delta t$	Time step
$t$	Absolute time



# 1 Introduction

The European Union climate and energy package adopted by the European Union is the very first strong step for the European Commission toward a rigid control of the wasted energy and the related pollution. Overcoming for the first time in history the individual oppositions of the member states, the European Commission faced directly the incumbent danger that pollution represents for the European Union and, in general, for the whole world. It is also called the “20-20-20” directive as it aims at “smart, sustainable, inclusive growth” by reducing greenhouse gas emissions by 20%, increasing the efficiency of systems by 20% and increase the use of renewable energies by 20% [1].

While it seems likely that this target will be reached in the near future for conventional systems, for transports it seems to be harder, above all as far as naval transport is concerned. Due to the modality of transportation itself, the system governing the ship motion results to be very tough to control in order to reduce emissions. Furthermore, the big quantities of energy involved in a ship transport operation does not allow the battery to store the energy required to be feasible for large cruise ships, differently from what happens in the case of electric cars or small vessels.

Otherwise, it is possible to use hybrid systems, for example using a system of battery and conventional Internal Combustion Engines (ICEs) for the auxiliary power supply system and conventional Internal Combustion Engines for the propulsion: the largest amount of the required energy is supplied by the ICEs, while the battery supplies energy when the power requirement oscillates or there it presents peaks [2]. A simple scheme is shown in Figure 1.

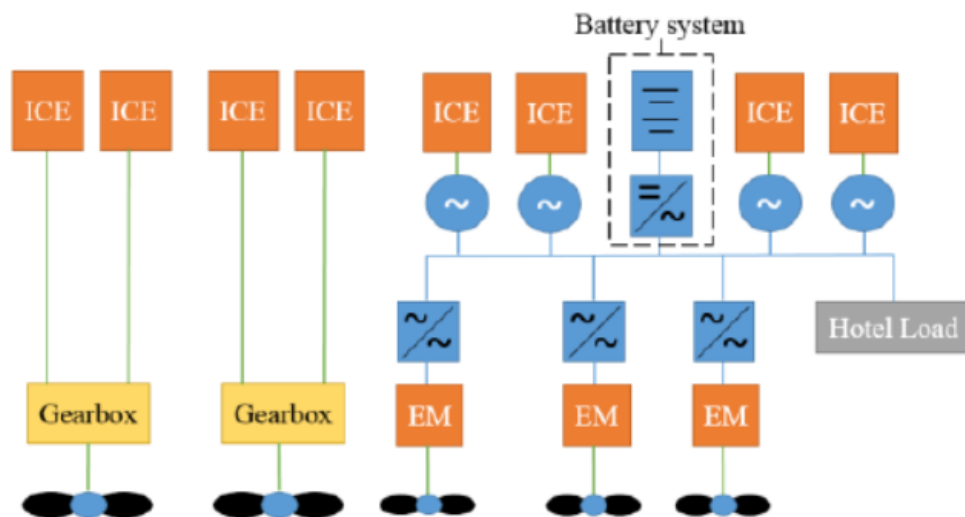


Figure 1: Hybrid system solution example [2]

One other way of reducing the vessel's fuel consumption – and subsequently the pollution derived from it – is to use the battery system not only in order to supply the auxiliary power, but also to shave the peaks of essential power for the vessel. They occur each time that the ship calls at a port: in this case, auxiliary propellers are turned on in order to turn the ship in close spaces. In fact, inside the port, vessels of big sizes are not able to move nimbly and they could face multiple problems if they count only on the rear propellers [3]. The basic idea behind the battery logic is that the peaks of power could be supplied by the battery rather than by the generators, as the battery efficiency is higher than the diesel engines, which are used to drive the generators.

Furthermore, two other aspects have to be taken into consideration from this point of view: firstly, it is not efficient to turn on one engine in order to supply additional power for a relatively short amount of time, as the engine would be working at partial load, which makes the efficiency drop. On the other hand, the battery is often charged for long periods without using the potential power that it can supply, resulting in a waste of free additional energy that could be provided to the main shafts [4]. An ideal model would consider an optimised use of the battery, supplying energy during the peaks of requirement and recharging when its use is not needed.

The main purpose of the battery is not only to reduce the consumption through the discharging of the battery, but also to maximise the efficiency of the generators allowing engines to work stably at their point of maximum efficiency. The combination of these two aspects brings to a significant reduction in fuel consumption.

## 1.1 Research motivation

Climate change is real. It involves not only people of the future, in a world that does not belong to us, in an abstract universe, but above all our generation. Despite the fact that some people negate the existence of a climate change, or that some people do not feel the problem as a today issue, its effects are tangible. Dozens of thousands of scientific researches show that, if humanity does not change dramatically the situation about emissions and polluting, it will suffer from the consequences. An article from the worldwide famous newspaper The Guardian affirms that global pollution kills nine millions of earth citizen a year, causes trillions of dollars of damages and threatens 'survival of human societies', to put it bluntly [5]. The same article claims that the number of deaths and the costs of the environmental damages are probably underestimated, as further researches are discovering new links between illnesses and pollution. Furthermore, it reports that air and water pollution are respectively the first and second biggest killers in the world.

A report from the WHO (World Health Organisation) states that 'The health effects of air pollution are serious - one out of three of deaths from stroke, lung cancer and heart disease are due to air pollution' [6]. In addition to this, it asserts that nine people out of ten in the world, at this moment, breathe polluted air. Air pollution is closely linked to climate change, which in turn is mainly caused by the fossil fuel combustion. It releases in the air a huge quantity of toxic substances, such as the well-known NO<sub>x</sub>, the sulphur dioxide and heavy metals, which are dangerous for the human life, besides the Green House Gases (GHG, which are mainly CO<sub>2</sub> and CH<sub>4</sub> [7].

The same WHO, which is really sensitive to the issue of climate change, organised the First WHO Global Conference on Air Pollution and Health, in the days 30<sup>th</sup> October – 1<sup>st</sup> November 2018, with the financial support of France, Germany, Monaco, Norway and Switzerland. It took place in the WHO headquarter, in the city of Geneva, Switzerland. The conference had the target to define the strategy to reach the goal of reducing the deaths from air pollution of two thirds by 2030. It included big-scale efforts with the setup of at least 500 BreatheLife cities in 20 countries by 2020, the development of independent solutions to reduce the fossil fuel burning, the redesign of cities to minimise the losses of energy, efforts to protect the most vulnerable portions of citizens, such as children and elders, the improvement of the air quality in the cities, the access of the clean energy, etcetera [8]. Those, alongside with the European Union climate and energy package, are only few but strong example of how the world is becoming more and more concerned about the environment issue.



*Figure 2: WHO headquarters, in Geneva [8]*

The briefly presented hybrid system has been developed in response to the need for the society to increase the technology that allows mechanical systems to save fuel, increase the global energy efficiency and reduce the air and water pollution. The long report from the International Maritime Organisation for the Green House Gasses (GHG) led in 2014 by organisations from USA, China, India, UK, Japan, Canada and Finland has calculated that, for the period 2007-2012, shipping accounted for 3.1% of annual global CO<sub>2</sub> emissions and 2.8% of annual global equivalent CO<sub>2</sub> emissions regarding GHGs combining CO<sub>2</sub>, CH<sub>4</sub> and N<sub>2</sub>O [9]. Among this, 2.6% of global CO<sub>2</sub> emission and 2.4% of global equivalent CO<sub>2</sub> for the above-mentioned gases belongs to the so-called international shipping, indicating the shipping between ports of different countries (excluding military and fishing vessels).

In order to reduce water and air pollution, companies tried to come up with different types of solutions, aiming at the increase of the efficiency or the reduction of the fuel consumption [10]. For example, solar panels and wind turbines have been set on the deck of the vessel in order to gain free energy directly from the surrounding environment [11]. In this direction, e.g., the Japanese company Eco Marine Power made great efforts and progresses in order to study the effect of renewable energy systems directly installed on the vessel. In fact, they used an intelligent system that is able to collect information about weather condition through an integrate sensors system and set the devices on board in order to maximise the energy performance [12]. Further studies have been made also in order to analyse the functionality of Lithium-ion batteries that store the power gained and are connected to a Battery Management System to ensure a safe and optimal operation. Another important option involved in maximising energy performance is to run the engines at their optimal load. Unfortunately, in most cases the high variability of the power required results in the engines running at sub-optimal operating points, but requires also a continuous turn off and turn on of the engines. Generally, for cruise ships, at least two engines are always turned on and hence if one fails for some reason, the other is available to supply the required power at least partially. The working load influences considerably the efficiency of the generator. As can be seen in Figure 3, the efficiency increases up to the maximum point when the power is at around 85% of the maximum load. If the power increases further, the efficiency slightly decreases.

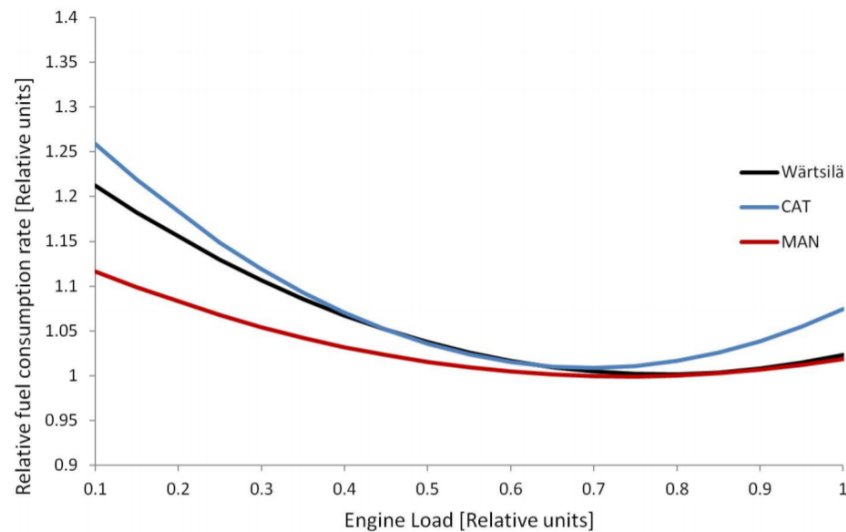


Figure 3: Fuel consumption rate of different types of maritime engines [13]

Finally, the list of efforts invested to increase the energy performance of a ship comprehends the use of Flettner rotors, or rotor sails. The Flettner rotor is a smooth cylinder of variable height, composed of high-performing composite materials. The cylinder is based on the deck of the ship and rotates along its longitudinal axis: the relative slip between the surface of the rotor and the wind, bumping into the surface of the cylinder with a specific angle in respect to the direction of the ship, generate a thrust on the ship [14]. The Flettner rotors are suitable for numerous type of vessels, e.g. bulk carriers, tankers, cruise ships, roll-on/roll-off ships, as far as there is enough flat space

on the deck to install the rotor. Generic studies on Flettner rotors has pointed out that the presence of this type of device decreases the ship’s fuel consumption from 3% to 15%, with some exceptional cases up to 35% [15].

## 1.2 Research purpose

The proposed item was studied and developed in the research department of Aalto University in Espoo (FI) in collaboration with the main local ship companies. Born with the target to approach a global and accurate study for shipping models, it presents one branch related to the study of the amount of fuel consumption savings in relation to the use of Flettner rotors. The subject of this research is the use of Flettner rotor by the ships, the creation of a model for its operation and the creation of an optimised model for global energy performance. The ship taken into consideration is the *Silja Serenade*, a Ro/Ro passenger ship travelling from Helsinki to Stockholm, passing from the port of Mariehamn. The characteristics of the vessel are shown in Table 1.

Name	Silja Serenade
IMO	8715259
MMSI	230184000
Maritime call sign	OJCS
Flag of convenience (FOC)	Finland [FI]
AIS Vessel Type	Passenger
Gross Tonnage	58376 t
Net Tonnage	3779 t
Length Overall	203 m
Breadth Extreme	31.93 m
Year of building	1990

*Table 1: Silja Serenade details [14]*

Ordered in 1987 by the Finnish shipping company Efofa for the ferryboat brand *Silja Line*, operating from November 1990, the MS (Motor Ship) *Silja Serenade* can carry up to nearly 3000 passengers and 450 cars at time. It was built by the STX Finland Oy Company, owned by the South-Korean holding company STX Corporation, in the shipyards of Turku. Today this majestic ship of 203 m of length, able to reach 23 knots (43 km/h), is owned by the Estonian company Tallink Group, that is the largest passenger and cargo ship company in the Baltic Sea region [16].

It is worth to notice that the vessel was the first to be characterised by a main central multi-deck promenade: this architectonic solution, which would characterized subsequently other cruise ferries built by STX Finland, consists in a main horizontal atrium. This arrangement allows almost every cabin, located in the upper part of the structure, to feature one window facing the port/starboard side or the interior of the structure. Furthermore, it creates an optic effect of free space and it has been studied to maximise the sensation of comfort and order for a trip that lasts up to 12 hours.

The aim of this research project is to create a generalizable fuel consumption model and to analyse the role of Flettner rotors in order to understand what is its impact is on

the global fuel consumption of the ship. The model will consider a hybrid power system installed on the ship MS Silja Serenade and will simulate it considering:

- 4 engines type ME (Engine driving propeller), Tier II, Heavy Fuel Oil (HFO), equals in pairs.
- 4 engines type AE (Auxiliary engine driving generator), Tier II, HFO, equals in pairs.
- Energy Storage System comprehending one battery of an arbitrary feasible number of modules.
- Flettner rotors.
- Arbitrary efficiency for the battery (97% for charging, 98% for discharging)
- Interpolated graphs SFOC/Power supplied for the engines derived from the brochures by the major manufacturers.

The first simulation will be held in order to test the hybrid model, without considering the effect of the Flettner rotor. Actually, it will help to understand the function of the various parts of the simulation, which need some approximation. What is essential is to understand the meaning of the approximations and to demonstrate why they can be applied, how they simplify the model and how they could affect the results. Many efforts will be dedicated to this purpose, as it can be very difficult, if not impossible, to simulate the behaviour of such complex structure considering the real physics of the parts. However, when it is possible, the approximations will consider the worse conditions or data from the power-needed point of view. The model will run the engines and the battery in order to pursue the minimum fuel consumption for the track run by the vessel; the Silja Serenade's specification will be briefly explained in Chapter 5, while the optimisation model will be explained in Chapter 6.

Finally, the Flettner rotors' influence will be taken into consideration. Considering the polar diagrams furnished by Norsepower, and taking into account the data of the ship direction and wind blowing, the optimised model will include also the additional thrust generated by the rotor. The Flettner rotor model will be explained in Paragraph 6.6 and it will finally be implemented in the final optimisation model, which will evaluate the given thrust by the rotors. The fuel consumptions in the two cases will be compared in order to draw conclusions about the worth of the rotor installation on this particular ship. The simulations will consider also the presence or absence of a shaft generator. It is to be noted that the results of the simulations can be very different depending on the type, weight and route of the vessel.

## 2 Background

### 2.1 History of the Flettner rotors

Differently from what can be thought, the Flettner rotor is not a recent idea. Effectively, the idea of a spinning cylinder posed in a vertical position for supplying thrust to a ship came up in 1921 to the German naval engineer Anton Flettner, who patented the Flettner rotor in 1922 [17]. He attempted to build a first prototype of rotor ship assisted by such important German engineers like Albert Betz, pioneer of the wind turbine technology, Jacob Ackeret, considered the top aeronautics expert of his period, and Ludwig Prandtl, known among students above all for the famous number that was named after him. The first rotor ship, which had two rotors, was the elegant schooner Buckau and sailed to the seas starting from October 1924 [18]. It was furnished of two metal cylinders of more than 12 m of height and almost 3 m of diameter, topped by a flat disc of 3.6 m that maximise the thrust. The cylinders were spinning by the action of two electrical engines supplying a power of 11 kW each, through an alimentation current of 220 V provided by a DC generator. The maximum spinning velocity of the rotors, which were driven autonomously, was 125 rpm.

In the beginning, the general overview from engineers was sceptical. In fact, they discussed strongly about the efficacy of rotors on the ships. It has to be considered that the Magnus effect, that is the effect that supplies thrust to the rotors, was still partly unexplained and this was one of the reasons for the sceptical thoughts of several engineers and ships experts. Moreover, specialists' doubts were connected to the capacity of the rotors to be dynamically stable during its functioning: in fact, a long cylinder, with an aspect ratio of almost 5, was considered to be critically unstable if subjected to strong wind. To face all these critics and uncertainty, Flettner appealed to all his grit and prestige [19].

Fortunately for the history of the Flettner rotor, indeed, he was already famous and rich for his previous works, the most famous of which were the servo tab (evolved into the trim tab, which is still used in all airplane and several ships [20]) and the famous Flettner rotary ventilator, a free-energy cooling-assistant widely used on cars, vans, public transports, campervans and boats. Counting on his fame and money, he commissioned the study of the fluid profile generated around a spinning cylinder to the Aerodynamische Versuchsanstalt in Göttingen, Germany, which was one of the most important centres of study for aerodynamics [21]. The results of the experiments undergone there have been described as surprising, above all the wind tunnel tests, which results overcame by far the best forecasts.

Due to the improvements in the laminar theory and the experiments in Göttingen, Anton Flettner managed to find some partners, which were the Germania shipyards in Kiel and the Hamburg-America Lines, interested in the rotor ship after the results in the wind tunnel. Soon the advantages against the masts and veils were revealed to the community [22]. Firstly, the axial symmetry of the rotating cylinder made less critic the problem of exploitation of the wind, as the frontal area met by the wind is always the same. In this way, ideally, the direction of the thrust is the same for every direction, at the same relative velocity between the ship and the wind and at the same angle

between the ship direction and the wind: only the thrust value changes. Furthermore, the cylinders occupy less space than sails and masts and are easier to regulate. The more manoeuvrability is also due to the fact that it is enough to spin the cylinder in the opposite verse to change diametrically the direction of the resulting thrust [23]. To people arguing that the wind pressure on the rotor could capsize the ship, the engineers answered that, with the increasing speed of the wind, the rotors on the Buckau made less resistance than the Buckau's rigging itself.

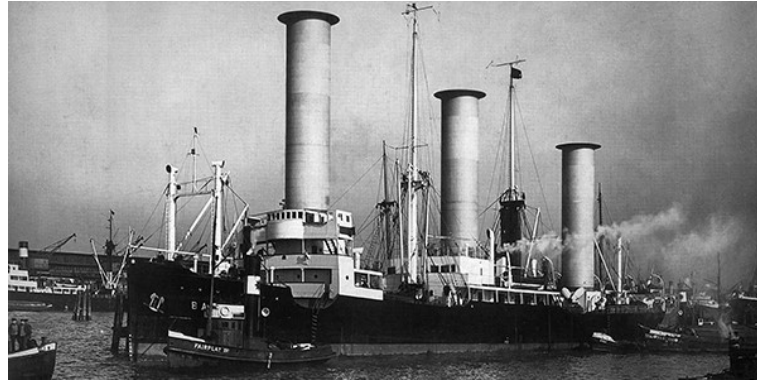


*Figure 4: The Buckau with Flettner rotors [24]*

After positive tests in the wind tunnel, the schooner Buckau became a rotor ship. At the trial, in November 1924, all the promises made by the wind tunnel tests were kept. It was a success celebrated by the most important German naval and aerodynamic engineers. In the January 1925, the Buckau had finished its first series of trials, consisting in 62 tests. In most of the tests the rotor was used alone or combined to the ship's 120 kW Diesel engine [19]. It resulted that, in most of the cases, the combination of power supplied by the Diesel motor and the cylinder had a way better efficiency than the only use of the Flettner rotors. The rotors were able to deliver up to 27 kW, but it has to be considered that the speed of the cylinder was slightly greater than the speed of optimal value, decreasing the efficiency.

The ship became famous for its good results and its new concept of power supply. The uncommon shape and the innovative technology, linked to the new models of fluid dynamics discovered in that period, attracted the worldwide attention: in 1926, a demonstration was taken in America, under the new name of Baden-Baden. Therefore, the Buckau was a success for the engineering development at that time, demonstrating how new discoveries in the field of matters could improve the technology [25]. This can be seen as an example of how, in the global 20<sup>th</sup> century, technology development has been strongly related to the scientific knowledge and progress in the field of the engineering expertise. It was the very first demonstration of how the technology development could bring to a greater competitive position and how the innovation and constant research is the key for overcoming the problems that society has to face [26].



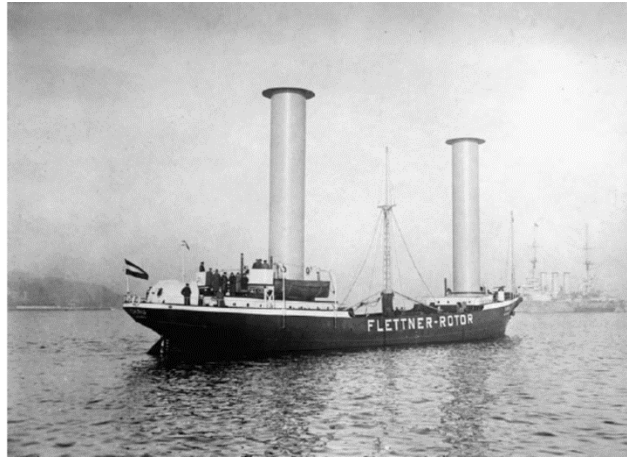


*Figure 5: The ship Baden-Baden [27]*

In the same year of the demonstration in America, the German Admiralty commissioned a new bigger rotor ship called Barbara. It was built by the shipyard A.G. Weser in Bremer. It was driven by two 6-cylinder Diesel engines connected in series, supplying a total power of 745 kW and resulting in a maximum velocity of 19 km/h [21]. Three electric motors supplied energy to three rotors that had bigger dimensions than the Buckau, but had the same architecture and a similar aspect ratio. Spinning at a maximum angular velocity of 160 rpm, they were connected to one generator and supplied a maximum power of 45 kW. Even though the performance was completely positive and it was considered as an engineering master of piece, the Barbara had high costs of investments that it did not manage to amortize during her period of working, transporting decomposable products for the Sloman Line from the Mediterranean Sea to German [28]. When the Great Depression came, in 1929, it reduced considerably the costs of the fuel, and the owners understood that the costs for maintenance would be similar, if not overcome, the spared fuel costs with the rotors. As a result, in the following years, both Buckau and Barbara were finally deprived of the rotors and continued working as conventional vessels.

## 2.2 Recent history

After the Great Depression, the rotor thought and realized by Flettner disappeared from sight for 60 years. In fact, during the years of the world economic and social recovery, followed by a spread of unprecedented wellness, the society and scientists were not concerned with the problem of energy optimisation as today. Investors and leaders preferred to invest in other means instead of trying to optimise the ones that they already had.

However, in the 1980s, during what technology historians call the beginning of the third industrial revolution, the game changed. The diffuse digitalisation introduced digital control concepts that were unthinkable before. One concept introduced during this phase of technology history was based on the attention to the environmental problems [29]. It was possible due to the activity of the Romanian economist Nicholas Georgescu-Roegen, in 1971 [30], and, above all, thanks to the American economist Herma Edwar Daly, in 1973 [31]. As can be seen from the picture below, from the starting of XIX century exponentially increasing quantities of carbon, oil, natural gas

was combusted pouring in the atmosphere, in the seas and in the soil toxic waste products.

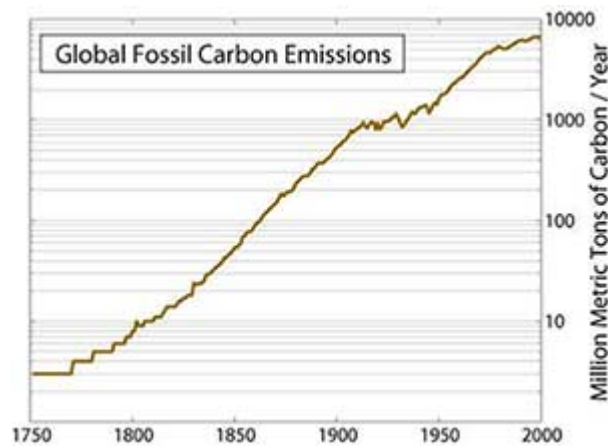


Figure 6: Global Fossil Carbon Emissions from 1750 to 2000 [32]

The International Labour Office and the United Environmental Program of the United Nations introduced the term “green economy” in order to point out a model of eco-friendly economy growth [33]. This approach is based on the integration of public policies aiming to the issues of environmental protection, climate change and energy, technologies and products with low environmental impact, managerial practices and responsible consumer behaviour. Among the industrial sectors linked to the green economy there are renewable energies (solar, wind, biomass, geothermal and micro-hydroelectric) [34], solutions for energy efficiency, mobility and sustainable construction, new markets for CO<sub>2</sub> exchange, the preservation of ecosystems, forestation, organic farming, remediation of contaminated sites, and all operational and service activities that have as their object the protection of the natural environment [35]. The nuclear energy has not been defined as renewable by the UE [36].

This new topic and the increasing in the oil price after the crisis in the 1980s revived the interest in rotor sails. The decisive leap forward was made in 2008, with the launch of the hybrid rotor vessel E-Ship 1. Like the previous ships, also the E-Ship 1 was a Roll-on/Roll-off cargo ship, composed of four Flettner rotors that were able to produce a considerable amount of power thrust. The rotors supported a fuelling system composed of two Mitsubishi diesel engines of 3.5 MW [37]. This ship, destined to make the history of Flettner rotors, was launched by the historical energy company Enercon GmbH, the third largest wind turbine manufacturer in the world, with facilities spread in every continent, counted on Lindenau Werft for its building.

When it was delivered, in 2010, the container ship counted 130 m of length, 22.5 m of width and 10500 of deadweight tonnage. The fuelling system was able to train the ship up to a speed of 17.5 knots (equal to a speed of 32.4 km/h) [38]. According to the polar diagrams furnished by ENERCON, with an optimal value of direction of the wind, i.e. at 90° from the direction of the vessel, the rotors manage to supply up to 40 % of the power required by the ship.

**Power saved in [%] vs. Wind (true) = 24kn/6 BFT  
estimated  
Ship Speed = 16,0kn**

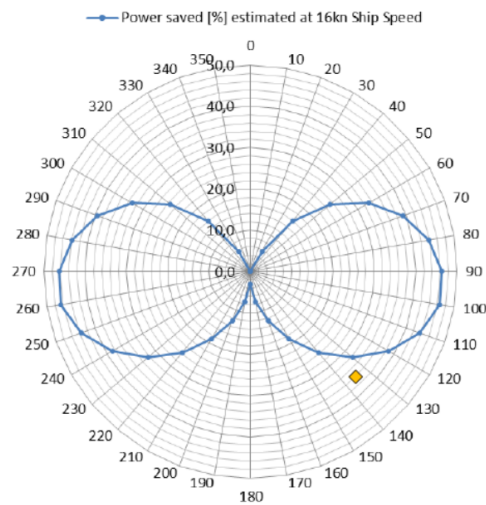


*Figure 7: Polar diagram for the E-ship1: speed of 16 kn, true wind of 24 kn [37]*

As can be thought, a real trip will never reach this target for the high changeability of the direction and strength of the wind. Nevertheless, in ideal conditions, it was a high value of fuel saving, and this shows why the E-Ship 1 reached huge popularity. The Flettner rotors are 27-metres high and have a diameter of 4 m each. As already implemented by Flettner during his experiments, they have an ending plate on top, whose diameter is considerably greater than the rotors: its purpose is to optimise the thrust given by the effect of the wind in a rotating surface.




**Figure 8: The E-ship 1 [39]**

The ENERCON itself tested the rotors in a wind gallery, with CFD (Computational Fluid Dynamics) and validation with measurement data. As specified in the document relative to the 4<sup>th</sup> Conference on ship efficiency done in Hamburg in the dates 23-24 September 2013, several tests have been simulated or physically done on the rotors in

order to maximise their efficiency [37]. Static and dynamic behaviour, thermal behaviour and balancing of rotors are only some of the characteristics that have been investigated [40] by the company in order to optimise the global efficiency of the ship. State-of-the-art systems have been involved in a huge project for maximising the performance of the vessel. Control Technology and Power Management System have been developed and integrated to make the E-Ship 1 one of the most innovative and efficient ships in the world [41].

Finally, the behaviour of the ship in motion has been tested with simulations, updated with the recent discoveries. It can be stated that, for the previous reasons, the E-Ship 1 took inspiration by the historical rotor ships (e.g. the Buckau), but the new technology system of measurements, control and simulation made the two types of ship deeply different as long as performance is concerned.

## E-Ship 1 - Technology and Innovation

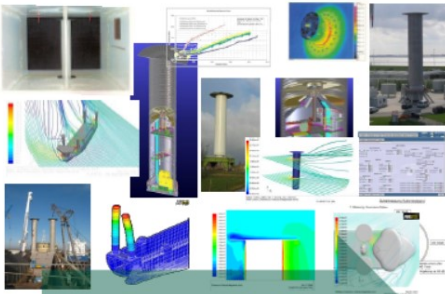


4<sup>th</sup> Conference on Ship Efficiency  
Hamburg, 23-24. September 2013

### Green-Shipping Innovation: Rotor-Sail System / Flettner Rotor



1924 "Buckau"  
First Trails Anton Flettner





2010  
MV „E-Ship 1“

**2000: First ideas for a wind-assisted propulsion cargo vessel**  
**2000: Start of research and first case studies**  
**2002: 1<sup>st</sup> Enercon Test Rig for Evaluation of Flettner-Rotor Technology**  
**2004: Concepts for E-Ship 1 starts to get shape**  
**2007: 2<sup>nd</sup> Enercon Test Rig for Evaluation and Optimization of Flettner-Rotors. „Full-Scale Test“**  
**2007: Keel laying, Lindenau Werft Kiel**  
**2008: Launching and christening**  
**2010: First Commerical operation of E-Ship 1**

12

Figure 9: Slide from the ENERCON's 4th Conference on Ship Efficiency [37]

More recently, in 2015, the Finnish company Norsepower installed twin rotor sails on the MS Estraden, belonging to the Finnish shipping company Bore [42]. Like for the previous rotor ships, also Estraden is a Ro/Ro vessel. Initially, in a test sail a little rotor was installed on a vessel and it resulted to save 2.6% of savings, which in that case meant a PBP (Pay Back Period) of 4 years. After the successful test, the rotors were installed on the MS Estraden. In the moment of the installation, the engineers calculated a fuel saving of 5%, increasing up to the 20% after the implementation of supporting systems.

The Norsepower CEO Tuomas Riski stated: “The successful trials of our wind technology are a ground-breaking moment not only for Norsepower, and also the wider

development of wind propulsion technology for shipping. The results suggest that when Norsepower technology is implemented at scale, it can produce up to 20% net savings in fuel costs with a payback period of less than four years at current fuel prices, confirming that wind technologies are commercially-viable solutions that reduce fuel and carbon emissions in the industry” [43]. Fundamental in this progress was the funding, the measurement from maritime data analysis, the software and the services offered by the NAPA [44] and the VTT Technical Research Centre of Finland [45]. Due to the success of this initiative, Norsepower won the Innovation of the Year Award (June 2016) [46] and received €2.6 M funding from the European Commission and the Finnish Government’s funding agency to further studies in the field of Flettner rotors (August 2016) [47].

## 2.3 Challenges

The Flettner rotors field seems to be full of applications for the future [39]. Nowadays, there are at least four big Flettner rotors manufacturers that share a market that is spreading more and more in time [48] and the researches for saving energy and increasing the efficiency of vessels motors has been increasing in the last thirty years, following an exponential trend. But traditional companies are not the only example of targets for this innovative way of using wind power. In 2008, a group of researchers led by Prof. Salter from Edinburg University proposed to build a fleet composed of automatic fleet driven entirely by Flettner rotors [49]. Their purpose would have been the increase of albedo effect in cloud formation through the use of a powerful ejection of elaborated fine salt grains derived directly from the sea. If spread out in the right proportions, those ejections should have affected the environment creating cloud condensation clusters that, according to the research group, could reflect the sunlight incident on the Earth up to 2% [17]. The final scope, in fact, would have been the reduction of global mean temperature.

The previous experiments, which were never realized, shows clearly how the application for Flattener rotors does not limit to the traditional use for cargo ship propulsion. Developments have to be undergone in order to increase the efficiency and the range of application for Flettner rotors. A problem arises when it comes to small sailing boats: in fact, the big dimensions of the rotor can destabilize the boat in case of rolling and make it difficult to pass in narrow spaces, like the case of passing under bridges [50]. One solution that has been thought is to make the rotor foldable, in order to reduce its height when it is not useful or when a specific situation causes boat instability. As far as the overall design is concerned, there are three critical points still to be developed and implemented:

- Design of a robust and foldable rotor, which can adapt to different situations that the vessel can bump into, e.g. storm, excessive rolling, fast change of wind direction, etcetera.
- Aerodynamic optimisation of the rotor to minimise the resistance to the motion due to aerodynamic drag.
- Implementation of a smart design control for an optimal thrust derived from the wind direction and force.

Due to the system's complexity, there is not a specific mathematical relationship of the rotor's spin and the direction and force of the wind with the total generated thrust. In fact, each ship has a specific drag resistance to the motion and the maximum value of thrust or even the optimal working point of the wind and the rotor for maximising the thrust can be different for the same rotor built on for different ships.

Therefore, a reliable relationship between wind characteristics, the velocity of the rotor and the thrust it provides has to be simulated with CFD and validated with real-time measurements. Actually, the two ways of evaluating the Flettner rotor's effect on the ship's power, are interconnected. Through the real data it is possible to understand if the CFD model designed for that particular type of rotor is reliable and, if it is not, it is possible to improve it. In fact, simulating such a complex system needs to assume some simplification that, at the beginning of the work, the researchers don't know if they are assumed in the correct way. Only experience can give an answer and simulating systems programs, built for this type of work, are becoming more and more accurate. Example of CFD programs professionally used are ANSYS CFD, Simcenter STAR-CCM+ and FLOW-3D [51]. They are all based on Navier-Stokes-Fourier equations for viscous fluids and they simulate realistically the behaviour of a fluid, which can be gas, like air, or liquid, like water in a particular system with certain boundary conditions.

## 3 How a cruise ship works

### 3.1 The ship's propulsion system

For more than 50 000 years, since the human being started traveling through water, the thrust sources for the vessels was human power. Only in the early 19<sup>th</sup> century a new mean of marine propulsion was introduced: it was the marine steam engine. During this century, a large variety of reciprocating marine steam engines was developed.

The steam engine was the first choice considered for transports in history. Since the developing of the very first engine by Thomas Newcomen around 1712 and the essential improvements of James Watt in 1775 [52], engineers tried to adapt this technology to every field it could be related to. One of those was the maritime transport.

Today steam turbines are still in use, due to advantages that it provides, compared to other propulsion unit types. Little vibration, low weight, small space required and low maintenance make the marine steam engine still appreciated for some applications, e.g. it is currently adopted in LNG (Liquefied Natural Gas) carrier ships [53]. In fact, for economic reason, it is preferred to use the boiled-off cargo as a fuel, rather than to re-liquefy it. The fuel is used to evaporate water and use the high-pressure steam to run the engine. Moreover, the steam plants are safe, modern and well-established [54]. Another use is in the nuclear marine propulsion system, which takes advantage of the nuclear radiations in order to make the water evaporate and feed the steam plant [55]. Finally, some old ships are still coal-fired, due to the low cost of carbon that does not make investments on more modern power systems attractive.

The steam turbine exploits the kinematic energy of the steam in order to obtain mechanical work. The steam, created by the evaporation of water or liquids due to fuel combustion, hits the turbine at high energy, after being conducted through a nozzle that increases the velocity of the jet. There are two main types of steam engines: the impulse steam engine and the reaction steam engine: the first one is characterised by the jet bumping into the blades, changing the power transmitted with a specific frequency in time, due to the periodically relative movements between the nozzle and the blades. It works at constant pressure and it is used for smaller utilities. The second one is characterised by a ring of fixed blades that conveys the jet from the nozzle to the rotor through a narrowing steam path, which increases the velocity, decreasing the pressure and let the jet run out the rotor with an angle that optimises the efficiency.

During the XX century, the low-efficient and polluting marine steam engine was replaced by diesel engines and gas turbines.

### 3.2 The naval diesel engine

The maritime diesel engine is a particular type of diesel engine that reproduces the surface diesel engine's way of working, adapted for working in a naval environment. They are called reciprocating diesel engines to point out that they work due a system of pistons running in cylinders, supported by piston rods. The pistons activate a system of crankshafts that transmits the torque it produces to the camshaft and, finally, to the propeller. The transmission can be direct or through a reduction gearbox that reduces

the speed of the propeller but increases the torque transmitted to it. The crankshaft can be coupled with an alternator and an electric motor in order to produce electricity, in the case that the power generated by the diesel motor is used to supply electric energy on board. The marine diesel can be classified by:

- 1) The number of strokes per cycle: two-stroke engine or four-stroke engine.
- 2) The speed in the output of the engine: slow, medium or high speed.
- 3) The mechanism used as part of slider-crank linkage: crosshead, trunk or opposed piston.

The functionality of the diesel engine is complex to describe entirely considering every particular aspect. Therefore, it will be described summarily in this thesis.

Basically, it can be stated that it is mainly composed of the following elements:

- The injector, which blows the fuel mixture into the combustion chamber.
- The piston, which is connected to the crankshaft and is moved up and down in the cylinder.
- The combustion chamber, which is the space where the combustion takes place, between the head of the piston and the cylinder head.
- The inlet valve, which is the valve that supplies fresh air for the combustion.
- The exhaust valve, which is the valve through which the exhaust gases are expelled at the end of the cycle.
- The connecting rod, which connects the piston with the crankshaft.
- The crankshaft, which transmits the power to the main shaft.

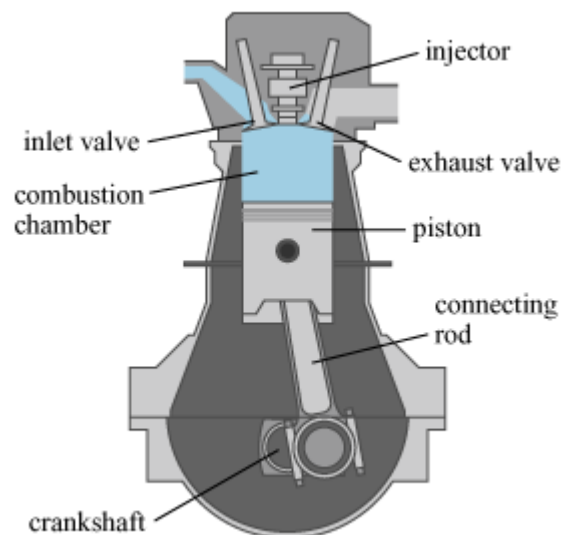


*Figure 10: Scheme of two-stroke diesel engine*

The motor works following the Diesel cycle, proposed by the German inventor and engineer Rudolf Diesel in 1895. Considering an initial point where the cylinder is at the lowest point – the so-called bottom dead centre (BDC), which is the farthest point



from the head of the cylinder –, for the two-stroke engines there are, ideally, four transformations (see Figure 11) :

- a) Isentropic compression, from the point 1 to the point 2: this is the process where the piston is driven from the BDC to the top dead centre (TDC) – the nearest distance from the piston to the cylinder’s top. During the compression, the injection system blows fuel and air inside the combustion chamber. Gas leaks are prevented due to the use of high-performing piston rings, which are lubricated adequately in order to minimise the friction with the cylinder’s walls. At the end of the stroke, the fuel-air mixture compressed achieves high temperature and pressure and the fuel is ignited. In this part of the cycle, ideally the injection valves are completely opened and the relief valve is completely closed, therefore the system does not lose or gain heat.
- b) Reversible isobaric expansion, from the point 2 to the point 3: ideally, the ignition process is seen as heat admission at constant pressure. The point 3 is the point where the highest temperature is reached and the fuel-air mixture expands, transmitting kinetic energy to the piston. Obviously, it is known that in reality the ignition is turbulent and therefore the system cannot be characterised by such a transformation at constant pressure. As can be seen in Figure 11, during the process the gas expands following the constant-pressure line of the pressure–volume diagram (also called PV diagram).
- c) Isentropic expansion, from the point 3 to the point 4: the point 3 is the point where the fuel’s state becomes unstable and it expands, pushing the piston from the TDC to the BDC. After having absorbed the heat from the fuel, the ideal system evolves increasing the volume following an adiabatic process. Also in this case, the system does not exchange heat with the outside. The piston continues the volume expansion until the BDC is reached.
- d) Reversible isochoric process, from the point 4 to the point 1: when the piston reaches its lowest point, the exhaust gases are expelled. The relief valve is completely opened and uses the pressure difference between the internal part and the environment. At the end of this process, the system is at the thermodynamic state indicated in point 1, and the cycle is ended. During this process, heat is lost alongside with the exhaust gases.

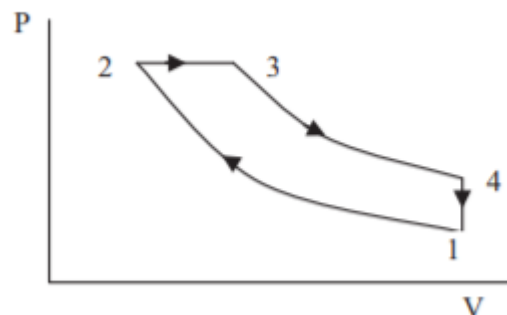


*Figure 11: Ideal Diesel cycle on the PV diagram*

While the ideal cycle is the same for both types of diesel engines, the two-stroke one and the four-stroke one, the corresponding operations of the systems are different. In fact, for the two-stroke engines one cycle corresponds to one rotation of the crankshaft, while, for four-stroke engines, one cycle corresponds to two rotations of the crankshaft. While it corresponds to some differences in the way the system works, the cycle it follows is the same.

Obviously, the real cycle is different from the ideal one. In fact, the assumptions taken into consideration in the ideal cycle cannot describe properly the operation of the machine. For example, the assumption that the ignition of the fuel-air mixture can't be seen as a dilatation under the condition of constant pressure, as well as the relief of the exhaust gases is not accurately described by a phase of pressure drop at constant volume. Furthermore, in the ideal cycle, every transformation is supposed to be reversible, but this assumption is not realistic for the diesel engine. In fact, a thermodynamically reversible process indicates a change of the state of the matter composed by infinitesimal quasi-static variations, during which the matter is in equilibrium with the surroundings. This definition is used in thermodynamic to approximate slow changes of the matter in response to an alteration of its initial condition. In the diesel motor, this type of transformation cannot exist due to the high speed of the movement of the piston and due to the turbulent state of the matter for the compression ignition. Another difference between the ideal and the real diesel cycle is that in the real cycle the fluid condition in the exhaust stroke is not the same as one in the intake stroke, as it is not possible for the engine to reduce the fuel-air mixture to the environment condition.

### 3.2.1 ICE efficiency

In the ideal cycle the efficiency is given by the quality of the cycle, not caused by the mechanical losses or by inefficiencies in the combustion, but only due to the thermodynamic transformation. The efficiency is defined as the output power produced as output by the motor divided by the input power given as input to the motor. It results that:

$$\eta_{id} = \frac{W}{Q_{out}} = 1 - \frac{Q_{out}}{Q_{in}} = 1 - \frac{1}{\varepsilon^{k-1}} \left( \frac{\alpha^k - 1}{k(\alpha - 1)} \right) \quad (1)$$

Where:

- W is the work given by the motor
- Q is the heat
- $\alpha$  is the cut-off ratio, defined as  $\alpha = \frac{V_3}{V_2}$
- $\varepsilon$  is the compression ratio, defined as  $\varepsilon = \frac{V_1}{V_2}$
- k is the value referring to  $k = \frac{c_v}{c_p}$ , where  $c_v$  and  $c_p$  are the specific heat capacities of the fuel-air mixture at constant volume and pressure. While the values of  $c_v$  and  $c_p$  are functions of the temperature, pressure and specific volume of the matter, the value of k, for the Diesel fuel mixture, can be assumed constant as  $k = 1.4$ .

In the real motors, inefficiencies related to the imperfect operation of the machine and the fact that the fluid is not ideal have to be considered. The overall efficiency of the machine is defined as the utility power divided by the potential chemical power of the fuel rate supplied:

$$\eta_u = \frac{P_u}{\dot{m}_b H_i} \quad (2)$$

Where  $\dot{m}_b$  is the fuel rate (kg/s) and  $H_i$  is the lower heating value of the fuel (MJ/kg).

The overall efficiency is relatively easy to calculate measuring the values in input and output, while it is complicated to derive the single causes of the losses of efficiency. Generally, the overall efficiency is considered to be composed of three factors:

- 1) Mechanical efficiency  $\eta_o$ : it is the ratio between the real work in output, transmitted to the shaft, and the work calculated in the indicated thermodynamic cycle. This type of efficiency considers mechanical causes, such as the friction of the piston rings to the cylinder and the energy losses in order to turn on the motor.

$$\eta_o = \frac{W_u}{W_i} \quad (3)$$

- 2) Internal fluid-dynamic efficiency  $\eta_{\theta i}$ : it is the ratio between the work that is reported by the indicated thermodynamic cycle and the work that could be supplied in ideal conditions by the engine if every type of thermomechanical losses were minimised. This type of efficiency considers all the losses that characterise the so called indicated cycle, which can be seen as the real cycle that the machine actually follows. It is called indicated cycle because the physical quantities can be measured by sensors step by step. The losses this cycle takes into consideration are referred to untimely and incomplete combustion, heat exchange with the environment, fluid leakages and work losses for the replacement of working fluid.

$$\eta_{\theta i} = \frac{W_i}{W_{lim}} \quad (4)$$

- 3) Limit cycle efficiency  $\eta_{lim}$ : is the ratio between the  $W_{lim}$  and the potential chemical energy that could be supplied by the fuel. This type of efficiency refers to the so called limited cycle, which is the better cycle that a real fluid can undergo. In this cycle the characteristics of the thermodynamic cycle are ideal (reversible processes, transformation of the fluid following pressure-constant or volume-constant line) but the fluid is seen as real fluid. Therefore the limit cycle efficiency considers the type of the cycle, the compression ratio, the variability of  $c_v$  and  $c_p$  with the temperature and the phenomenon of dissociation. In fact, after the temperature of 1350 K, the inversed chemical reaction from the reagents to the products is not negligible anymore. Therefore part of the fuel does not actually participate in the combustion.

$$\eta_{lim} = \frac{W_{lim}}{m_b H_i} \quad (5)$$

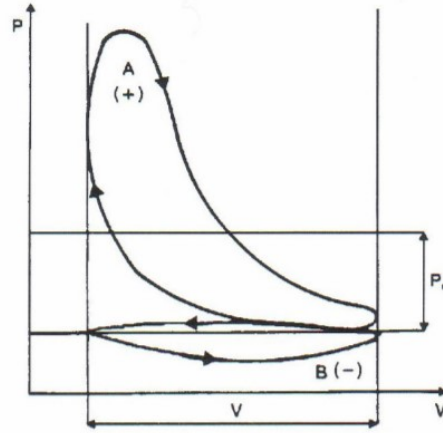


Figure 12: Indicated cycle for diesel engines

The overall efficiency is  $\eta_u = \eta_o \eta_{\theta i} \eta_{lim} = \frac{P_u}{\dot{m}_b H_i}$ . For diesel motors, it is complex to distinguish between internal fluid-dynamic efficiency and limit efficiency. Therefore, engineers usually adopt the term ‘indicated efficiency’ in order to include both at the same value:  $\eta_{indicated} = \eta_{\theta i} \eta_{lim}$ .

Diesel motor’s overall efficiency is around 30%. As  $\eta_o$  and  $\eta_{\theta i}$  are both around 90-80 %, it means that the limit cycle efficiency is the one that impacts the most on the overall machine working. This explain why diesel cycles are preferred to Otto cycle for naval engines: Otto cycle have limitations on the maximum pressure ratio that reduce the maximum power available and decrease the efficiency. By opposite, the Diesel cycle has not limitation in the maximum value, allowing it to supply the high powers that the ship requires and keep the efficiency relatively high. Moreover, due to the necessity of keeping shipping fuel cost the lowest as possible, it is a low-quality product and can’t be used for other purposes: diesel engines are less subjected to the bad effect of the low quality of the fuel than petrol engines.

LNG engines have been implemented in ships for a while. In fact, modern marine engines are so-called dual-fuel engines, which means that they can be operated both on diesel and LNG.

### 3.3 The ship’s topologies

The ship’s topology is that branch of the shipping field of study that studies the possibilities for a ship’s power supply system to be implemented. The power generating systems, effectively, can be complex and composed of several components interfaced to each other in order to provide the power that is needed. Multiple solutions can be found in this field [56].

Generally, there are two big requested power pools that have to be properly satisfied:

- 1) The propulsion power, which is the mechanical power that has to be provided to the thrusters in order to drive the vessel at the required velocity. The engines can be steam engines, internal combustion engines gas turbines or electric motors [57]. As input, they receive pressurised steam (in the case of steam engines), fuel-air mixture (in the case of internal combustion engines), compressed gases (in the case of gas turbines) or electrical power (in case of electric motors). They use a kinematic system in order to transform the potential power into mechanical power, transmitting a value of torque with a certain angular speed to one or more shafts that are connected to the propellers [58].
- 2) The auxiliary power, which is the electrical power needed for allowing the electrical systems on board to run adequately [59]. Electrical power needs to be supplied to the utilities that are integral parts of the electrical, air and water systems. Without going down into details, it has to be considered that pumps, valves, air compression systems and electronic devices are distributed all over the ship in order to regulate the supply and modify the characteristics of air and water flow rates or the right amount of power for the HVAC systems (heating, ventilation and air conditioning) [60]. Furthermore, manoeuvring thruster operation constitutes significant power peaks in auxiliary power demand [61].

The division between the two types of power needed is arbitrary and helps to figure out what challenges the power generating systems have to face. There is not one optimal solution to the problem of power supply and different approaches exist on the market.

Generally speaking, the power is supplied by a set of prime movers, which can be mechanical or electric engines. The formers supply mechanical power in the form  $P_{\text{mech}} = T\omega$ , where  $T$  is the torque in output, measured in [Nm], and  $\omega$  is the angular velocity, measured in [rad/s]; the latter supply power in the form  $P_{\text{elect}} = VI$ , where  $V$  is the voltage measured in [V] and  $I$  is the current measured in [A]. The major issue is to convey mechanical power and electrical power where they are needed, in the right proportions and balancing them. The main actors of all the possible topologies are:

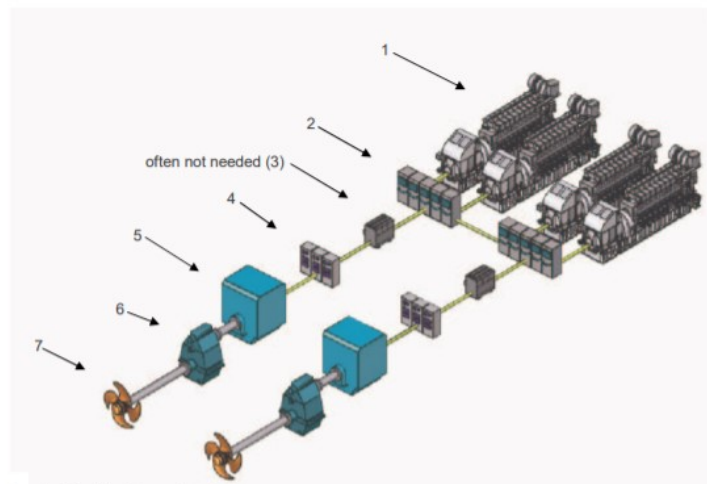
- Propeller-driving engines, or MEs (Main Engines)
- Generator-driving engines, or AEs (Auxiliary Engines)
- Diesel-electric engines, or DEs
- Shaft generators
- Electric power converters
- ESS, most commonly battery

The main effective difference between the three types of engines is the type and the maximum amount of power they can supply. The propeller-driving engines are usually large motors that supply mechanical power. They are generally low-speed engines as they have to furnish high values of torque and are used to directly drive the propellers. Their characteristics can vary substantially according to the manufacturers. The maximum reachable value is more than 10 000 kW [62].

Generator-driving engines are diesel motors that produce electrical power. They are designed to operate at a fixed speed, as the frequency that is supplied must have a

constant value. The engine shaft is connected to an electric generator – which generally is an AC synchronous generator – that transforms the mechanical power into electric power. In the case that the electric power has to be converted into mechanical power in order to drive propellers, a motor drive device needs to interface the generator and the electric motor: the motor drive and the motor are generally seen by naval engine architects as one subsystem for the operational and control interaction between the two [63]. Examples of motor drives are cycloconverters, current/voltage source inverters, DC drives or Pulse Width Modulation (PWM). The last is implemented in the recent power units' architecture and it is the most suitable solution for an optimise use of the overall power system.

Diesel-electric engines are similar to the generator-driving engines, with the difference that, while the formers are used mainly to supply power for the auxiliary system, the latter are used to supply power for both the propulsion and the auxiliary systems. Therefore, the size and the amount of power of diesel-electric engines are considerably higher than the generator-driving engines' ones. New generation diesel-electric systems prefer to adopt the hybrid energy storage system, which consists of the inclusion of batteries: this solution increases the global efficiency of the power unit [64]. The diesel-electric plants can differ from one to the other, according to the manufacturers, but their main structure is the same: they are composed of a diesel engine connected to an electric generator. The main switchboard is connected to the generator, which task is to direct the current to the different units in the ship. The current is supplied finally to the motors that are served by the motor drives, as shown in Figure 13.



Example: Diesel-electric propulsion plant

Legend

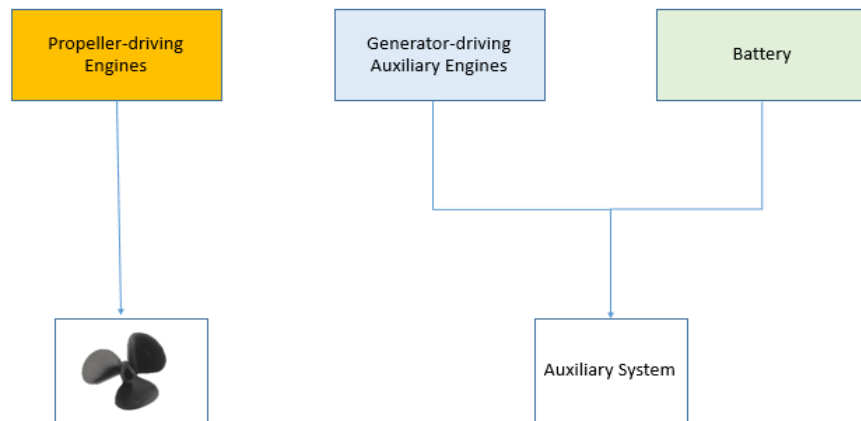
1	Gensets: Diesel engines + alternators
2	Main switchboards
(3)	Supply transformers (optional): Dependent on the type of the converter. Not needed in case of the use of frequency converters with 6 pulses, an Active Front End or a Sinusoidal Drive
4	Frequency converters / Variable speed drives
5	Electric propulsion motors
6	Gearboxes (optional): Dependent on the speed of the E-propulsion motor
7	Propellers / propulsors

Figure 13: Diesel-electric plant [65]

In the naval field, the use of AC electric generators rather than DC ones is preferred. In fact, three phases current allows the generator to provide a higher value of maximum power for the same system size and AC current is easier to generate, transmit and interrupt in case of emergency [66]. The current and the voltage furnished by the generators are meant to be used at different values of voltage, therefore a system of transformers allow to modulate the voltage seen by the different utilities. For example, some large generators can furnish current at very high voltages – up to thousands of Volts –, while normally voltage for customers use works at 220 V [67]. For the conversion, the current is turned form AC form to DC through a system of rectifiers, converted by transformers and finally turned from DC to AC with alternators.

As far as ship topology are concerned, considering what mentioned above, there are mainly three types of logic for the power supplying system:

- 1) The first one, shown in Figure 14, includes a set of propeller-driving diesel engines [68], connected in parallel, supplying the power to the propellers through different shafts, and an auxiliary system composed of generator-driving auxiliary engines [69] that supply auxiliary power for consumer purposes. It is the most common layout and the propellers are connected directly with one or two cross-head engines: this type of configuration is called directly driven propeller shaft [70]. The auxiliary generator system can also include a battery that is able to supply power during the peaks of demand and store energy when its use is not needed, although this inclusion is still quite rare [71]. For the medium and small vessels, it is possible to have two medium speed engines connected to a gearbox that reduces the speed of the propeller: in this case, the propeller is often a controllable pitch propeller. In this first simple configuration, there is no connections between the propulsion power supply system and the auxiliary system.



*Figure 14: First type of ship topology*

- 2) The second is the one that is adopted by recently-built ships and it is composed of diesel direct-driving motors supplying the power to the propellers and auxiliary generators that supply auxiliary power for consumer purposes. The dif-

ference consists in the fact that, in this case, the power supplied by the propulsion side can be transferred to the electrical grid after being converted into electric power through a shaft generator [72]. This configuration, shown in Figure 15, has increased efficiency and the generators/motors system is more versatile. In that case, the main engines can work more constantly at their maximum optimal point, which is around 85% of the maximum load. If the power required for propulsion is less than the power produced, part of it can be sent to the auxiliary services and the power generated by the auxiliary system can be decreased.

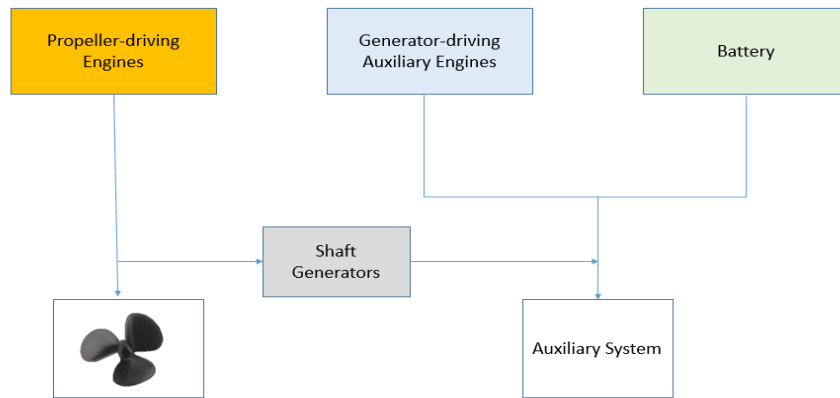


Figure 15: Second type for ship topology

- 3) The third and last case, usually referred to as “all-electric” propulsion unit design, is characterized by no separation between propulsion and auxiliary power sides, as shown in Figure 16. Multiple generator-driving diesel-electric engines provide electric power for all ship operations. Then the power is distributed to the auxiliary system or is converted into mechanical power through electric motors and directed to the propellers. A battery can be used in such a configuration as well to increase the system’s flexibility and shave peaks in power consumption [73].

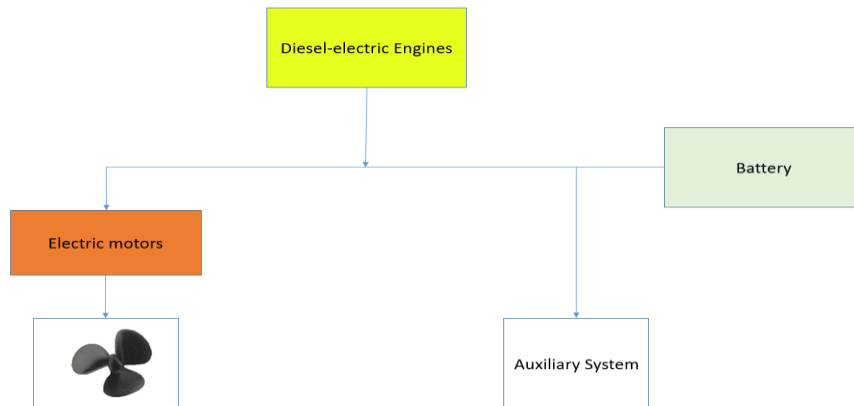


Figure 16: All-electric propulsion system



## 4 Basics of optimisation theory

The aim of the work is to find feasible solutions to a specific optimisation problem. In mathematics, an optimisation problem indicates a problem whose target is to find feasible solutions and to select the best among them. Generally the criteria for finding the best solution is to look for the variables' combinations that maximise or minimise a function called objective function. The variables can be continuous or integer and they are subject to constraints that restrict the possibility of feasible solutions.

In general, the optimisation problem presents itself in the following form:

$$\begin{aligned} & \min h(x) \\ & \begin{cases} f_k(x) \leq 0 \\ g_p(x) = 0 \\ x \in R^n \end{cases} \end{aligned} \quad (6)$$

Where:

- $h(x): R^n \rightarrow R$  is the objective function mentioned above.
- $f_k(x)$  is the  $m$  inequality constraints, with  $k = 1, \dots, m$ .
- $g_p(x)$  is the  $n$  equality constraints, with  $p = 1, \dots, n$ .
- $m, n \in \mathbb{N}$

As can be seen, optimisation problems, by convention, are problems of minimisation. An optimisation problem looking for a maximisation can be transformed into a minimisation problem setting as objective function  $\tilde{h}(x) = -h(x)$ . In fact, it results in

$$\min \tilde{h}(x) = \min[-h(x)] = \max h(x). \quad (7)$$

A first distinction is done between linear and non-linear optimisation problems. In the first category, called Linear Programming (LP), both the objective function and the constraints are linear. Therefore the optimisation problem can be written in the following way:

$$\begin{aligned} & \min c^t x \\ & \begin{cases} Ax \leq b \\ x \geq 0 \\ x \in R^n \end{cases} \end{aligned} \quad (8)$$

Where  $A$  is the matrix of coefficients, while  $b$  and  $c$  are vectors. The algorithms that solve the two different types of problems are deeply different, as different approaches have to be taken in order to find the optimisation solution.

Another distinction is done between convex problems and non-convex problems. The distinction involves the characteristics of the local minimums of the problem: indeed, for a convex problem, a local minimum is always a global minimum. Similarly, a concave problem is a problem where a local maximum is always a global maximum. A linear problem is always a convex problem, while the opposite is not true. The convex problems are solved with the hill climbing technique, which uses incremental changes in the step solutions in order to spot the direction that allows to find the point of minimum.

Another class of optimising problems is Integer Programming (IP). In those cases, all the variables are restricted to be integers. Therefore, the IP problem is defined as follows:

$$\begin{aligned} & \min h(x) \\ & \begin{cases} f_k(x) \leq 0 \\ g_p(x) = 0 \\ x \in Z^+ \end{cases} \end{aligned} \tag{9}$$

IP is an NP-complete class problem, which means that it can be solved using brute-force algorithms. In fact, the integer constraints make the problem non-convex and the complexity of the algorithms sharply increases. The most used algorithm is to solve the LP problem created from the IP problem through the linear relaxation, obtained dropping the integer constraints. After the first LP solution is found, the branch and bound algorithms are applied. The iteration methods are described in Paragraph 6.1.

A subclass of the IP problems is the Integer Linear Programming (ILP) problem, which considers linear programming with integer constraints. ILP present themselves as follows:

$$\begin{aligned} & \min c^t x \\ & \begin{cases} Ax \leq b \\ x \geq 0 \\ x \in Z^n \end{cases} \end{aligned} \tag{10}$$

Even though ILP is linear, the problems are not convex due to the integer constraints.

Finally, the last subclass of optimisation problem is that IP where some variables are integers, other are continuous. For this reason, they are called Mixed Integer Linear Programming (MILP) problems. They are in the following way:

$$\begin{aligned}
 & \min c^t x \\
 & \left\{ \begin{array}{l} Ax \leq b \\ x \geq 0 \\ x_{1 \dots n-q+1} \in R^{n-q} \\ x_{n-q \dots n} \in Z^q \end{array} \right. \quad (11)
 \end{aligned}$$

Where  $q \in Z^+$ . The optimisation models analysed in this work are classified as MILP and will be discussed in Chapter 6.

## 5 Application of the optimisation model on Silja Serenade

The application of the optimisation model to the energy system of Silja Serenade is complex and different actors and constraints have to be considered. For each component, some reasonable simplifications have been chosen, that simplify the simulation and make it possible. Simplifications and their reasonability will be explained in the following paragraphs, relating them to the ship's modality of working and to the optimisation model.

### 5.1 Assumptions over the system's topology – the propulsion unit

The model implemented in Matlab is mainly characterized by two systems: the first one simulates the power unit's behaviour, whose target is to supply the propulsion power transmitted to the propellers, while the second one simulates the operations of the auxiliary electrical power generation, composed of auxiliary engines and the battery.

The propulsion unit supplies the highest amount of power and is used for the ship's main propulsion. Data considering the real amount of propulsion power required by the ship during the journey are given in a time interval of 20 hours and 20 minutes, with a measurement frequency of 10 minutes. The trend is updated to the date 16-12-2018, registered from 16:50:11 to 13:09:59 of the following day. The data registered concern the operational points of the engines installed on board, therefore they take into consideration all the losses that the motors-supplied power has to feed. The data are shown in Figure 17.

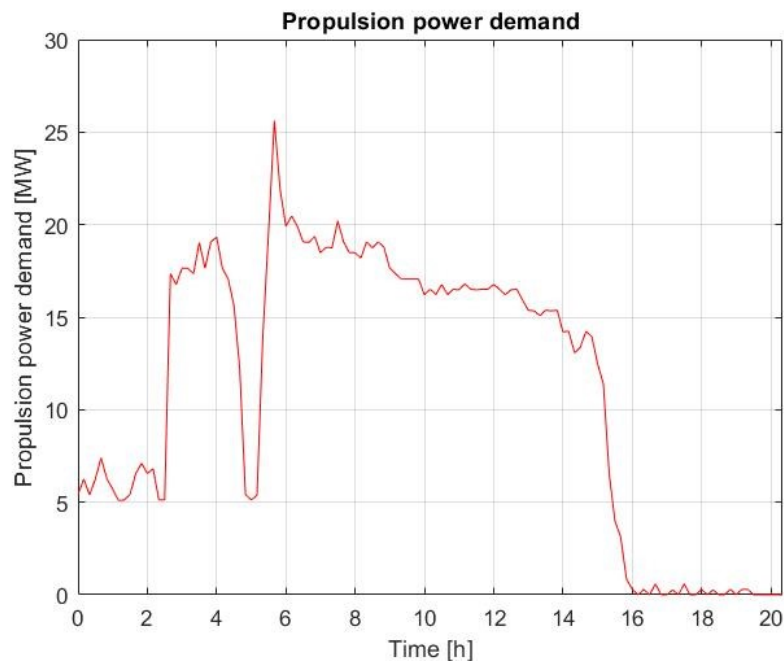


Figure 17: Propulsion Power Demand

Starting from the given data, it is possible to derive the graphic information about the profile of the ship's speed, in order to visualize how the power demand behaves in function of the velocity that it has to provide to the ship. From Figure 18, it is possible to understand that the speed profile can be divided into three big time steps:

- The first time interval lasts 2 hours and 30 minutes; in this step the ship alternates its velocity between 12.5 and 10 knots; the ship is in the archipelago near Stockholm, where the velocity has to be limited.
- The second time interval lasts 14 hours and is characterized by an almost constant speed, at around 18.5 knots. It is characterised by a presence of a sharp fall at the speed profile to 5 knots, related to approaching the port of Mariehamn.
- The last time interval lasts 4 hours and is characterized by the ship being stationary. The reason is that the ship is anchored at the port of Helsinki. The small peaks of power at zero speed are most likely due to measurement error.

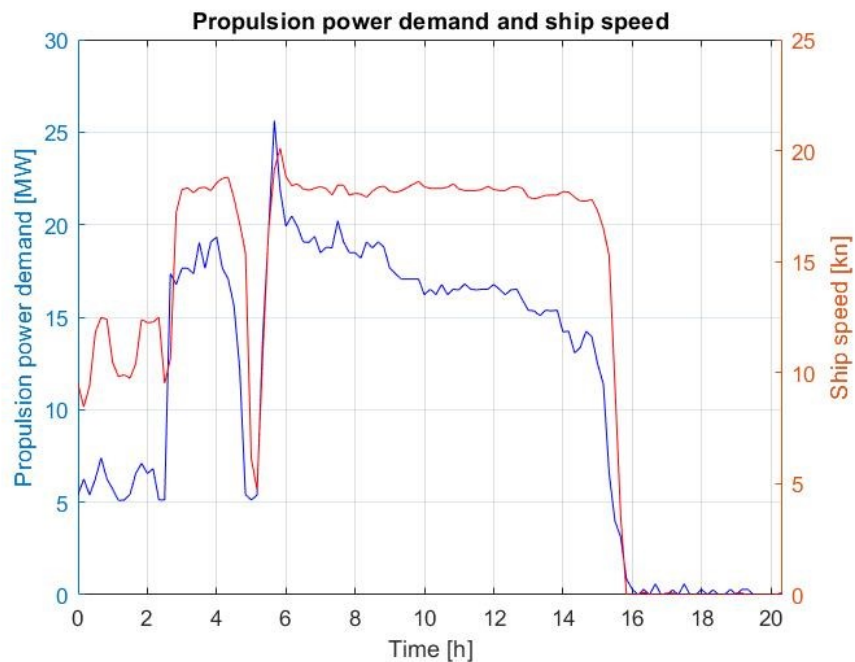


Figure 18: Propulsion power demand compared to the ship speed profile

For the propulsion power unit, a set of four diesel engines connected in parallel has been considered, in pairs of two. In the Silja Serenade case, a set of engines directly connected to the propellers through a reduction gear system are taken into account. They provide mechanical power in terms of torque and speed, therefore they cannot feed the electric grid on board directly. In this work, however, the feasibility of retrofitting a shaft generator to the main engines was studied by simulating and optimising its performance.

Two types of models will be run in order to simulate the behaviour of the whole system. The former will consist of the propulsion and auxiliary power units separated in the way that the two types of engines work independently from one another. The latter

will consider the integration of the two systems through the presence of a shaft generator that allows the propulsion motors to supply additional electrical power to the auxiliary system, in the case the main engines supply a higher amount of power than the requested. Using the last configuration, the overall system is able to be more flexible and its optimal working point increases the efficiency, reducing the global fuel consumption. Both models will be run also in the case of the implementation of a Flettner rotor, as is explained later on.

## 5.2 Assumptions over the system's topology – the auxiliary unit

The auxiliary unit is the power generation unit whose task is to supply electrical power to match the total amount of electric power request from the utilities on the vessel. They include:

- Electricity for the internal and external lighting
- Power for the services (electric components, kitchens, points of charging, etc.)
- Start-up and regulation of the engines
- Work of the manoeuvring thrusters

As mentioned above, the electric grid is furnished with transformers that decrease the high voltages in input in order to adapt them to the different values in use. In general, in fact, it is preferred to generate and transmit electrical power under the condition of high voltage. Actually, the major part of the losses in electrical power transmission is for the so-called Joule effect: the major part of the power is dissipated in heat, whose formula is:

$$P_{diss} = RI^2 \quad (12)$$

Remembering that the formula for the electric power is the product between the transmitted current and the voltage, the equation becomes:

$$P_{diss} = P^2 \frac{R}{V^2} \quad (13)$$

As the resistance R can be reasonably considered as constant, it is derived that the lost power is inversely proportional to the square of the voltage: if it increases, the losses drop. Upstream of the electric grid there is the AEs set, composed of 4 diesel motors that supply the power to the electric grid, supported by a battery. As already explained for the MEs, also the AEs are considered in two pairs, whose maximum power is 3200 kW and 2400 kW.

The data of auxiliary power demand come from a different dataset than the one from the main propulsion. The auxiliary power demand data of measurements for an entire round-trip cruise, which means 48 hours. The measurement frequency was 2 minutes. The graph for the auxiliary power is shown in Figure 19.

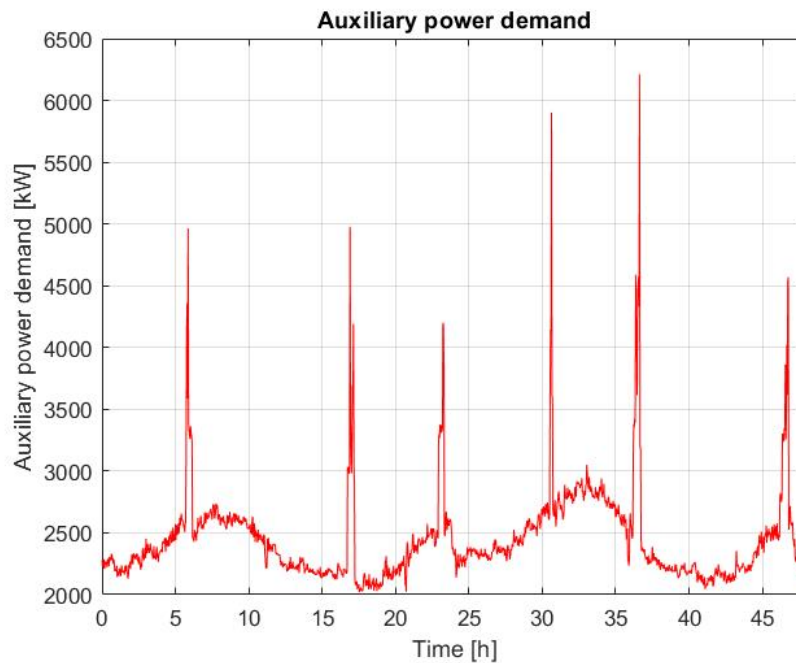


*Figure 19: Auxiliary power demand*

It can be noticed that the power's trend – if peaks are excluded – varies from 2000 to 3000 kW. Cyclically, there are sharp peaks, up to more than 6200 kW. Those peaks are due to the activation of the stern and bow thrusters. In fact, when big cruise ships are in a harbour, it can be very difficult to manoeuvre them only with propellers. Stern and bow thrusters, also called manoeuvring thrusters, are electrically-driven thrusters with lateral propellers that make movements in the harbour – and, generally, in narrow spaces – more fluent. As can be easily thought, the stern and bow thrusters are the main sources of fluctuations in the auxiliary power demand and the power generating system has to adapt to them in order to minimise the consumption in correspondence of the critical peaks [74]. Silja Serenade is furnished with three manoeuvring thrusters, one for each side in the bow and one in the rear.

In order to help the system to react to sharp peaks and to smooth the engines response, which are not easily adjustable in short periods, the system is provided with a battery that is able to release power when it is needed, e.g. when there are peaks or severe fluctuations in the power demand, and store it when the power demand is smooth or it is discharged. In the optimised model for consumption, the engines try to work constantly at their optimal point of efficiency, letting the battery supply the rest of the needed power, if necessary.

From the peaks in Figure 19, it is possible to derive the Silja Serenade journey during the times related to the data. In fact, the 48 hours of measurements are related to the cruise ship roundtrip. As shown in Figure 20, the journey starts from the port of Helsinki from where the ship heads towards Mariehamn to make a quick stop. From Mariehamn, Silja Serenade proceeds directly to Stockholm. The return journey has the same route covered in the outward journey, in the reverse sense.



*Figure 20: Silja Serenade journey*

The peaks in the auxiliary power demand refer to an entry in or exit from the ports. Considering that the trip starts in Helsinki, the first peak is related to the exit from the Helsinki's port, the second one – which is actually composed of two peaks occurring in a short timeframe – stands for the entry and exit from Mariehamn port, the third one is the entry into the port of Stockholm and the fourth one is the exit from it. The following two peaks are related to the return journey, of which one is for the approach to Mariehamn and the other one for the entry in Helsinki's port.

As evident from the two datasets, they do not match each other exactly. In fact, the propulsion data start from the moment in which the ship has left Stockholm and is in the archipelago, while the auxiliary data start from the moment in which the Silja is in Helsinki's port. Therefore, as the aim of this work is to evaluate the total fuel consumption, a decision about the data for the simulation has to be taken. It has been decided to estimate the fuel consumption during the time given by the propulsion data – the shortest one. Thus, the auxiliary power demand data must be fit onto the propulsion power data. As the time steps for auxiliary and propulsion are different, the auxiliary power points will be interpolated on the time steps given by the propulsion data. The only exception will be done for the simulation that considers the two propulsion and auxiliary units separated: in this case, in fact, the auxiliary unit will be simulated for the whole trip, while the consumption in the propulsion time data will be evaluated after that the model find the optimised solution.

### 5.3 The diesel engines

The characteristics of the diesel engines have been taken from the main manufacturers. The motors are diesel that consume HFO (Heavy Fuel Oil), a dark-coloured type of fuel that belongs to the class of residual fuels, which consist of the highly viscous and tar-like residues of the crude oil refining process and typically contains long chains of hydrocarbons and aromatics. For this reason, the HFO is stable in the mass during the time – it does not evaporate – and, as it is resistant to the degradation, it is recognized as an environmental persistent polluting blend.

For the part related to the propulsion system, four diesel motors type ME (Engine driving propeller), Tier II, have been considered. Each pair has the maximum amount of



power of 8125 kW and 7500 kW. The suppliers provide the values of the specific fuel consumption (SFOC – Specific Fuel Oil Consumption) for the values of 100%, 85%, 75% and 50% of the load, which indicates the value of maximum power the engine can supply. The information of SFOC is given in the standard unit of g/kWh; therefore, it indicates the amount of quantity of fuel consumed by the engine per hour (in g/h) for every unit of power in kW supplied by the system.

For the MEs, the SFOC data are reported in Table 2.

Load [%]	Specific fuel consumption, HFO [g/kWh]
50%	185.8
75%	181.4
85%	181.0
100%	183.6

Table 2: SFOC data for ME

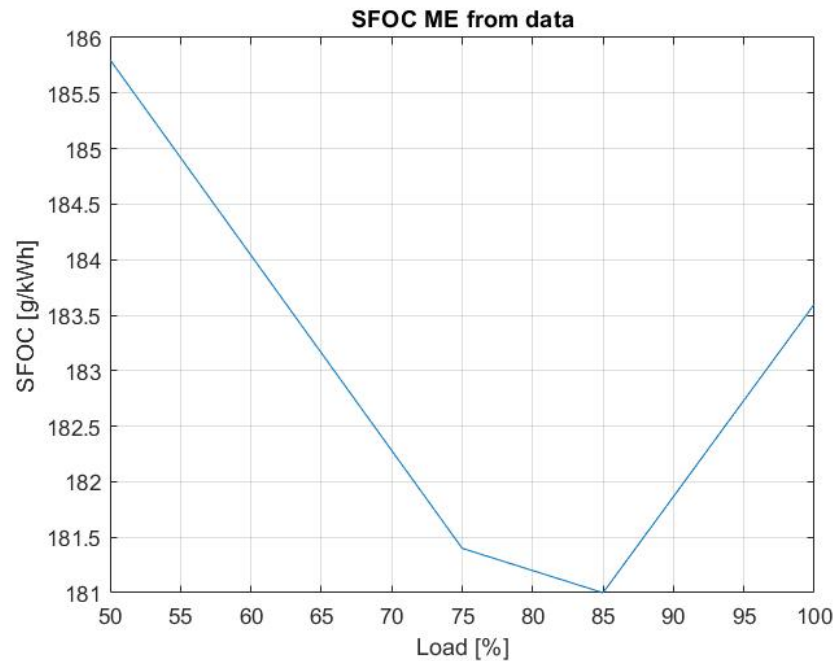


Figure 21: SFOC for ME from data

The function of interest is the value of the fuel flow rate (FFR), indicated in [g/s], in function of the power supplied by the engine. Therefore, the SFOC graph has to be converted into the FFR graphs related to the two different types of engines. The graph shows the fuel flow rate values on the y-axis and the output power on the x-axis. For this purpose, conversions are used:

$$FFR = SFOC * P_{out}/3600 \quad (14)$$

$$P_{out} = Load * P_{max}/100 \quad (15)$$

Applying the conversions, the FFR results are the following:

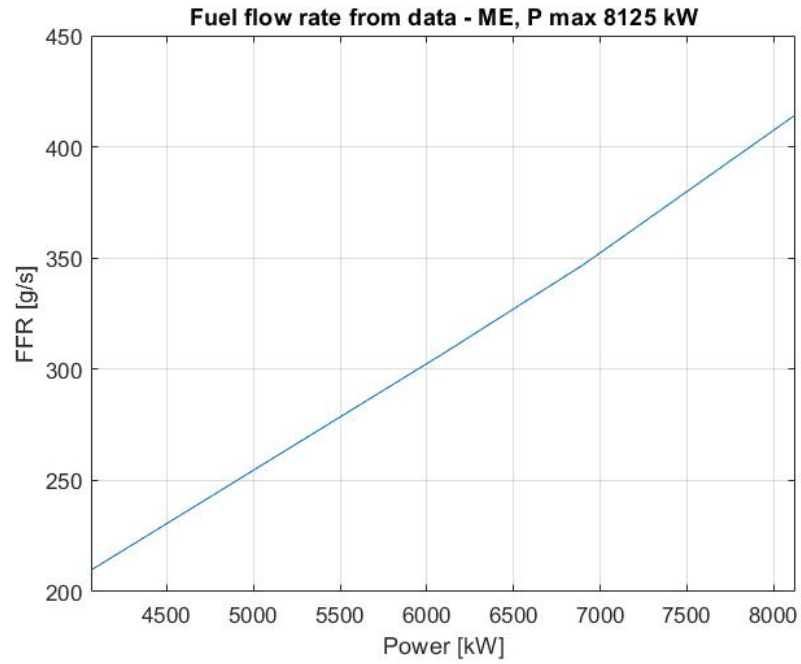


Figure 22: FFR for the ME with maximum power of 8125 kW

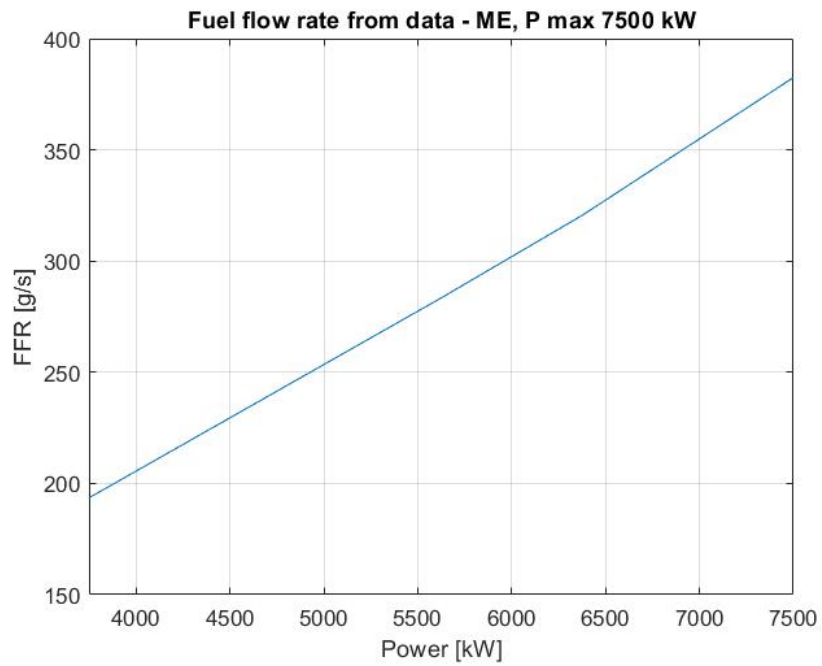


Figure 23: FFR for the ME with maximum power of 7500 kW

For the part related to the auxiliary system, four diesel motors type AE, Tier II have been considered. Two of them can provide a maximum amount of mechanical power of 3200 kW, while the others can supply a maximum power of 2400 kW. The data that concern AEs are shown in Table 3; comparing the values, for the same loads, it is possible to notice that AEs have higher specific fuel consumption than MEs. In fact, that AE type is smaller than MEs, which means that the global efficiency is lower and the specific consumption is higher.

Load [%]	Specific fuel consumption, HFO [g/kWh]
50%	192.3
75%	182.7
85%	182.2
100%	183.3

Table 3: SFOC data for AE

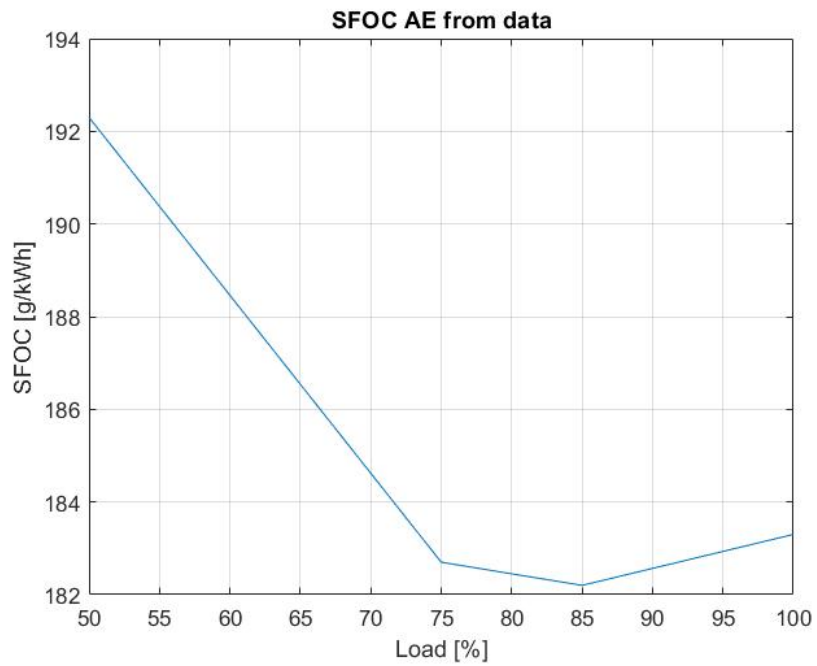


Figure 24: SFOC for AE from data

The previous conversion formulas were used in order to turn the SFOC curves into FRR graphs, as already shown for the MEs. Applying the conversions, FRR graphs for the AEs are the following:

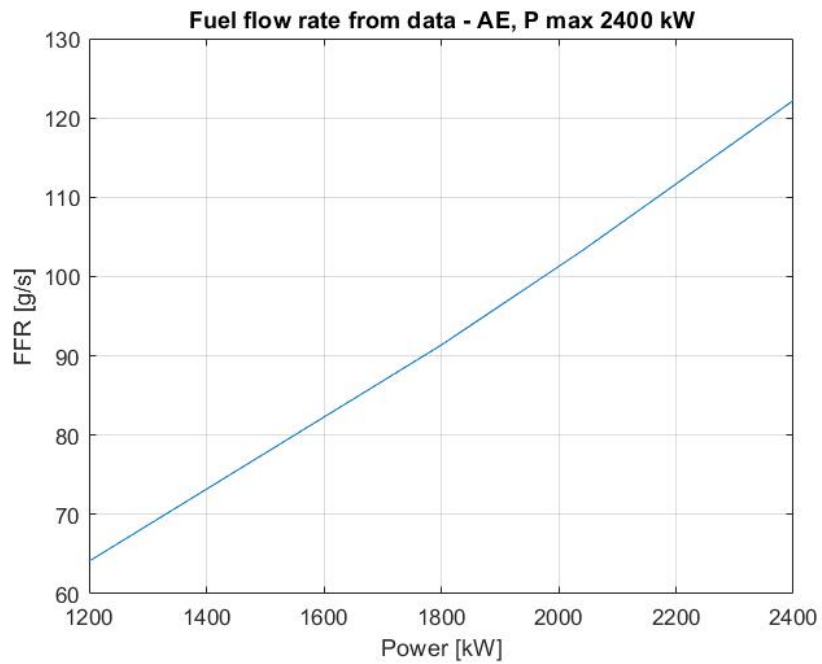


Figure 25: FFR from data for AE with maximum power of 2400 kW

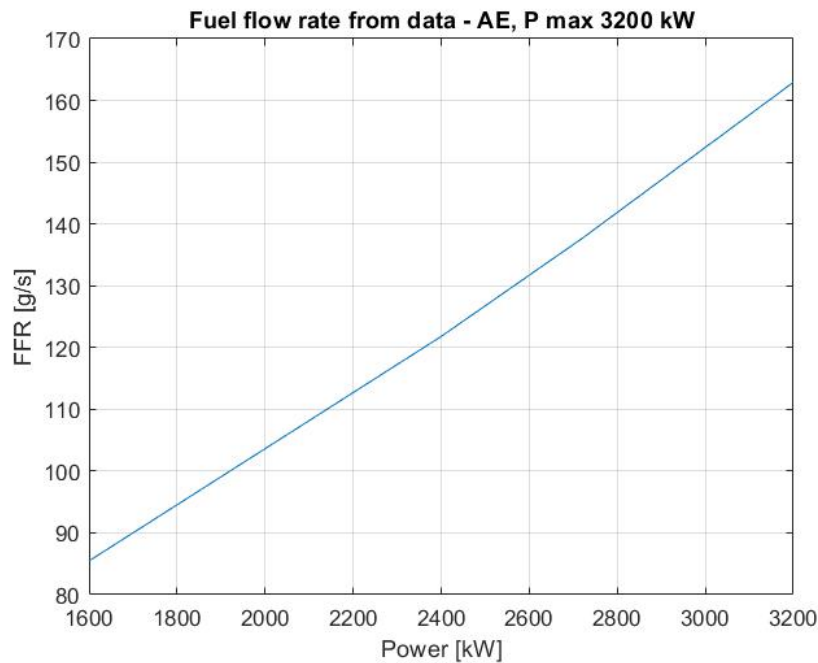


Figure 26: FFR from data for AE with maximum power of 3200 kW

## 5.4 Energy Storage System – the battery

The hybrid energy system proposal of Silja Serenade considers the implementation of a battery for the supply of additional energy when it is needed, e.g. when there are peaks of demanded power. One optimal example, which will be taken into consideration for this thesis, is one of the battery systems commercialised by the naval and industrial Canadian company Corvus Energy, leader for the supply of safe, innovative and reliable energy storage system (ESS). The battery is composed of Li-ion layered polymer cells, set in modules of 24 each. The modules can supply up to 6.7 kWh at the maximum pack voltage of 1100 V. Each pack is composed of 21 modules in series and is connected to a pack controller that controls and regulate power and data referred to the modules. In turn, 11 packs compose an array, which contains in total 231 modules. An array manager computes the data and information for the whole system and interfaces with the ship power management system.

In this model, a specific total capacity of the battery has to be requested to the manufacturers. From the battery data, it is possible to derive the power that the battery is able to release, knowing the C-rate of the system. For the model, the amount of energy selected has been calculated. In fact, it was supposed that the function of the battery was to supply the entire additional energy required during the peaks due to the thrusters' activation. The energy required is the integration of the area subtended by the main peak of the graph of power in Figure 19, excluding the contribution of the auxiliary power that is not related to the thrusters. As data are not distinguished and they refer generally to the on board systems, without specifying the division between bow thrusters and the other systems, in the model the latter term has been approximated as the

power indicated by the graph during the time  $t_1$  or  $t_2$  – which are the times selected for the start and end of the peak. Therefore, if  $P_{thrusters}$  is the amount of power required by the bow thrusters,  $t_1$  and  $t_2$  are the times of start and end of the thrusters' operation, the energy required from the battery is:

$$E_B = \int_{t_1}^{t_2} P_{thrusters} dt \quad (16)$$

For the evaluation of the integral, the Matlab function using the method of trapezoidal integration has been used. For every peak, the points of beginning and finishing of the additional thruster power have been evaluated, after that, the corresponding values of power has been subtracted of the minimal power between the two points. The integration has been evaluated between the two points; the operation has been iterated for each one of the six peaks. Finally, the model adopted the maximum energy value between the calculated ones. Table 4 shows the results for each peak.

N° of peak	Initial time	Final time	Maximum bow thrusters power [kW]	Energy [kWh]
1	5h 36'	6h 10'	2505	496.24
2	16h 38'	17h 18'	2900	645.43
3	22h 14'	23h 22'	1740	432.16
4	30h 28'	30h 48'	3297	317.68
5	35h 54'	36h 46'	3978	1010.67
6	46h 10'	47h 8'	2131	619.65

*Table 4: Evaluation of the peaks*

The result is that the fifth peak is the one that requires the most energy to be completely met. In this case, it can be noticed that the peak that requires more energy is also the peak that reaches the global higher value. To be specific, the peak is referred to the stopover in Mariehamn, characterised, as can be observed in Figure 27, by two relative maximum, referred to the entry and exit from the harbour. The second maximum, that is considerably higher than the other relative maximums referred to the calls at Mariehamn, could be due to adverse weather conditions that require additional auxiliary power to the bow thrusters.

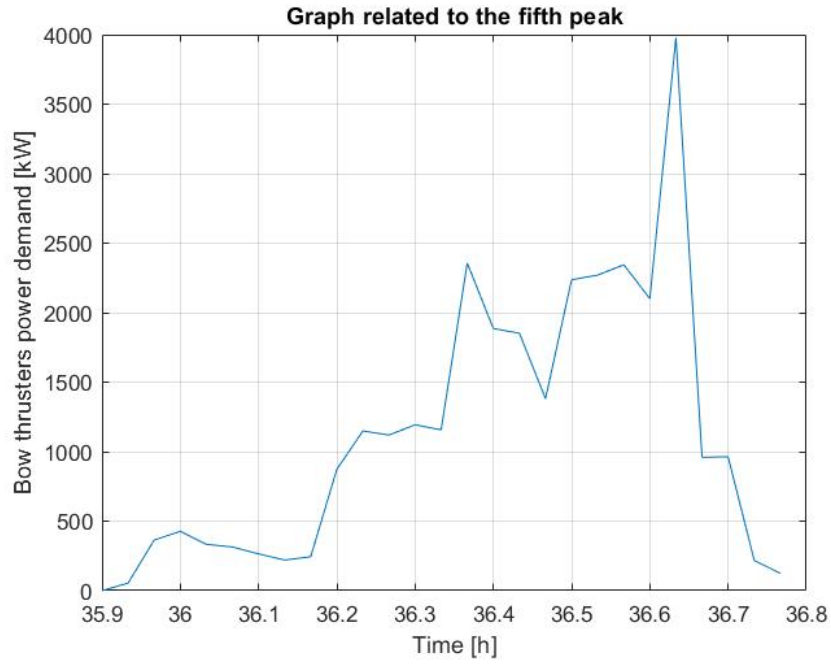


Figure 27: Graph related to the fifth peak

The method for estimating the optimal battery capacity does not consider the ageing process of the battery. If the model wants to be more realistic, it can be done over-dimensioning the battery capacity of a factor of 1.20, which accounts for a prediction of a 20% decrease in battery capacity during its lifetime.

It resulted that the energy required by the battery is 1010.67 kWh – while the energy considering the ageing process is 1212.80 kWh. As the battery has to supply part of all the peaks, a reasonable choice is to select a total capacity that is the double of that one calculated for the highest peak. Considering that the energy of one module is 6.7 kWh, the number of modules is:

$$n_{modules} = \frac{E_{tot}}{E_{module}} = 364 \quad (17)$$

Where  $E_{module}$  is one module's energy and  $E_{tot}$  is the total energy required, considering the ageing process. The number has been rounded up to let the energy required to be met. From here, it is possible to recalculate the global energy that the battery composed of 364 modules is capable of:

$$E_B = n_{modules} * E_{module} = 2438.8 kWh \quad (18)$$

This value considers the incremental factor of 20% for the ageing process. It means that, after the deduction of it, the maximum energy suppliable is equal to 2032.3 kWh.

The data of the selected battery are summed up in the following table:

Maximum Voltage	50.4 V
-----------------	--------

Minimum Voltage	38.4 V
Maximum Pack Voltage	1100 V
Capacity	150 Ah
Energy	6.7 kWh
Scalability	6.7 kWh (1 module) to > 10 MWh (1500 modules)
Cycle Life	>8000 cycles, 80% DoD
C-Rate - Peak	10 C (1500 A) in discharge 5 C (750 A) in charge
C-Rate - Continuous	4 C (600 A) in discharge 3 C (450 A) in charge
C-Rate - RMS	3 C (450 A) if liquid cooled 1.5 C (225 A) if air cooled
Weight	72 kg
Dimensions	59x33x38 cm

Table 5: AT6700 module data

As the whole battery, composed of one array, has 364 modules, it means that the overall weight is 26 208 kg. If at first sight it can seem a big amount of tons, actually, as far as a cruise ship is regarded, it is not a crucial aspect. Instead, the most considered issue during the dimensioning of the battery is the space that is needed for the battery installation. In this work, it would be considered that the size of the battery is feasible.

For the calculation of the maximum power that it is available to supply, the case of continuous operation has to be examined. As shown in Table 5, the values of C-rate for the operations of charging and discharging are different: it results in the energy in charging and in discharging being different. In fact, the relationship between the charging/discharging maximum power and energy is the following:

$$\begin{cases} P_{B,dis,max} = C_{rate,dis} E_{B,max} = 9755.2 \text{ kW} \\ P_{B,cha,max} = C_{rate,cha} E_{B,max} = 7316.4 \text{ kW} \end{cases} \quad (19)$$

Where  $E_B$  is the battery energy,  $P_{dis}$  is the battery discharging power,  $P_{cha}$  is the battery charging power,  $C_{rate,dis}$  is the battery discharging C-rate and  $C_{rate,cha}$  is the battery charging C-rate. The charging and discharging powers evaluated are the maximum discharging and charging powers that characterise the battery.

## 5.5 The Flettner rotors

The logic behind the Flettner rotor's contribution is that it supplies thrust directly on the ship. Traduced in the model's language, its effect is to subtract the additional power supplied from the rotors to the required propulsion power. In this case, both the cases of studied topology can be analysed with the presence of FRs.

Initially, the evaluation of the data is discussed. The data are given from the Norsepower under the form of a polar diagram, valid for the Serenade's speed of 18 knots and true wind's values variable from 0 to 25 m/s. The diagram has to be specific for



Silja Serenade, as the FRs' effect installed on different ships can be considerably different. The data, shown in Figure 28, indicates the numerical values of power supplied considering each combination of true wind's incidence angle and true wind's speed. The data, finally, consider the efficiency of the power transmitting system of 70%.

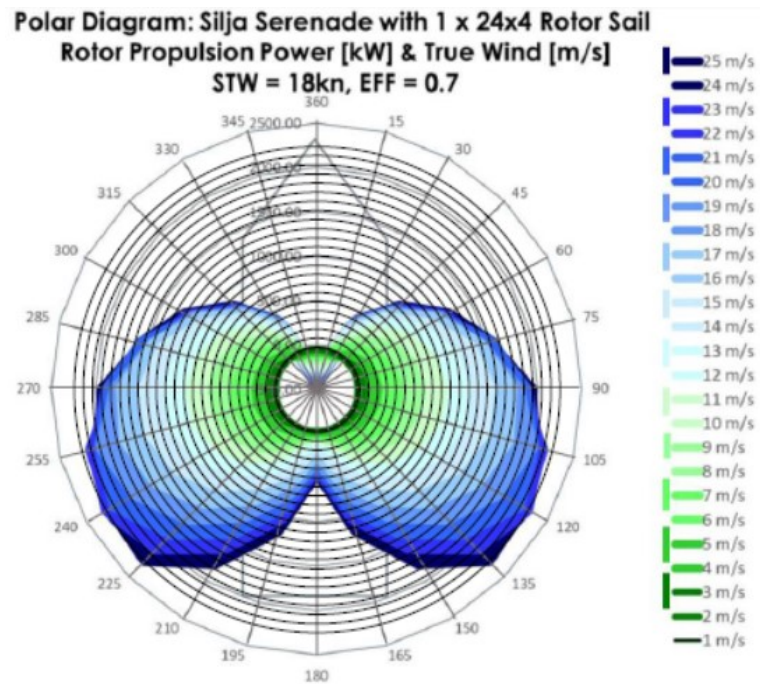


Figure 28: Silja Serenade's polar diagram for the speed of 18 kn

It can be observed that the supplied power goes from -500 kW to 2400 kW. The meaning of the negative power is that, for small angles and high values of true wind, the rotor cannot exploit the Magnus effect to achieve positive thrust. It is interesting to notice that for low-medium true wind's values, the geometry of the contours has 2 symmetries – a vertical one and a horizontal one –, while, for high speeds, there is only one symmetry, as the contours take a stretched form vertically. The vertical symmetry is always preserved as it is assumed that the optimal rotational velocity of the cylinder has the right verse of spinning.

The input in the optimisation model, as far as the FR's obtained power is concerned, are data of true wind and incidence angle, given for each temporal step. Therefore, for each time interval, the additional trust has to be evaluated starting from data figured in Figure 28. Unfortunately, data are only visual, so that they need to be converted numerically. An Excel table was created with the following structure: each column represent an incident angle value, each line a real wind velocity, and for each combination, a value of power has been visually derived and transcribed.

Although numerous, the data are not dense enough for the model, as the pitch angle's step is 15°. Therefore, the 3-dimensional data have been interpolated with a dedicated Matlab script, for angle values and true wind velocities evenly spaced of 1 degree and

0.1 m/s, respectively. It has been decided that a linear interpolation was accurate enough for the interpolation of those data.

The results of the linear interpolation are shown in a 2D plot in Figure 29 and in a 3D plot in Figure 30 and Figure 31.

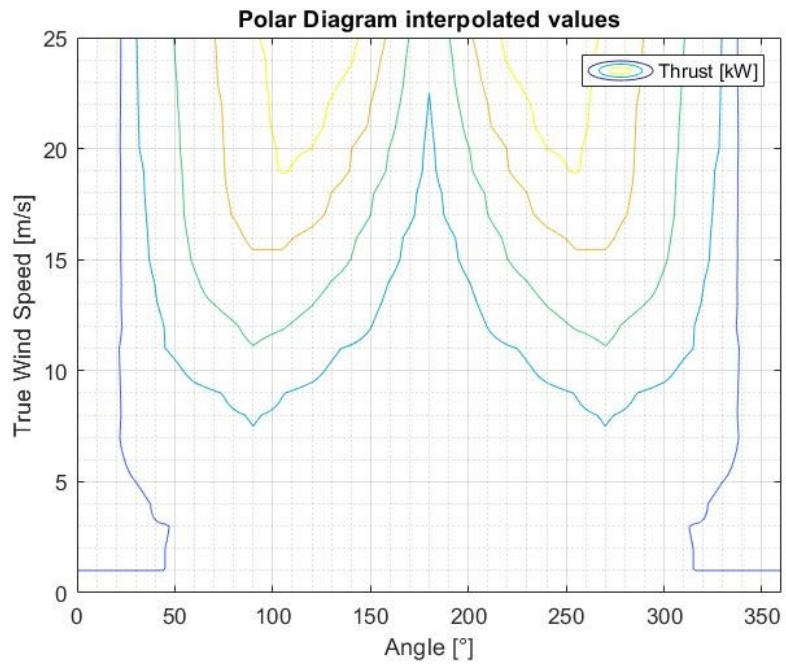


Figure 29: Interpolated polar diagram values in 2D

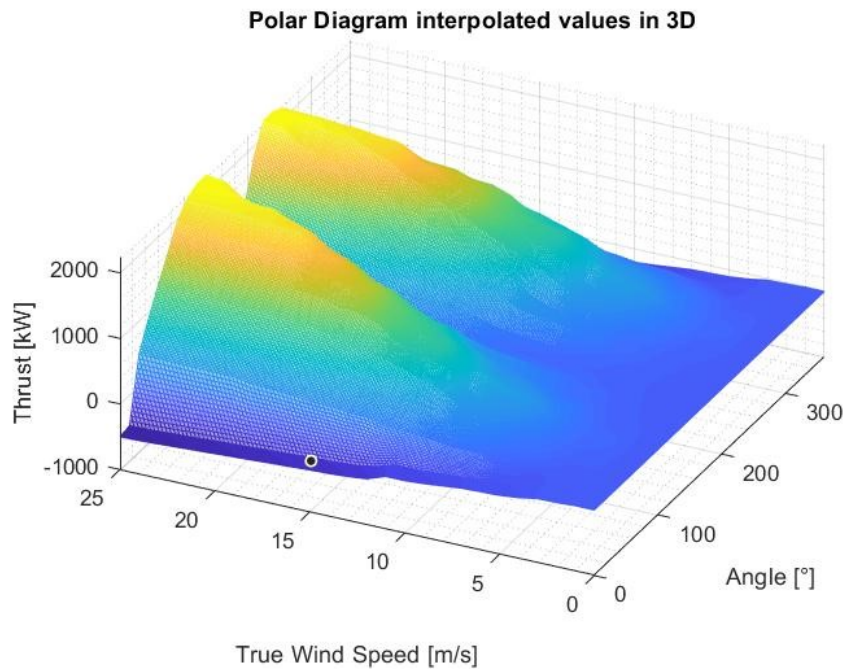
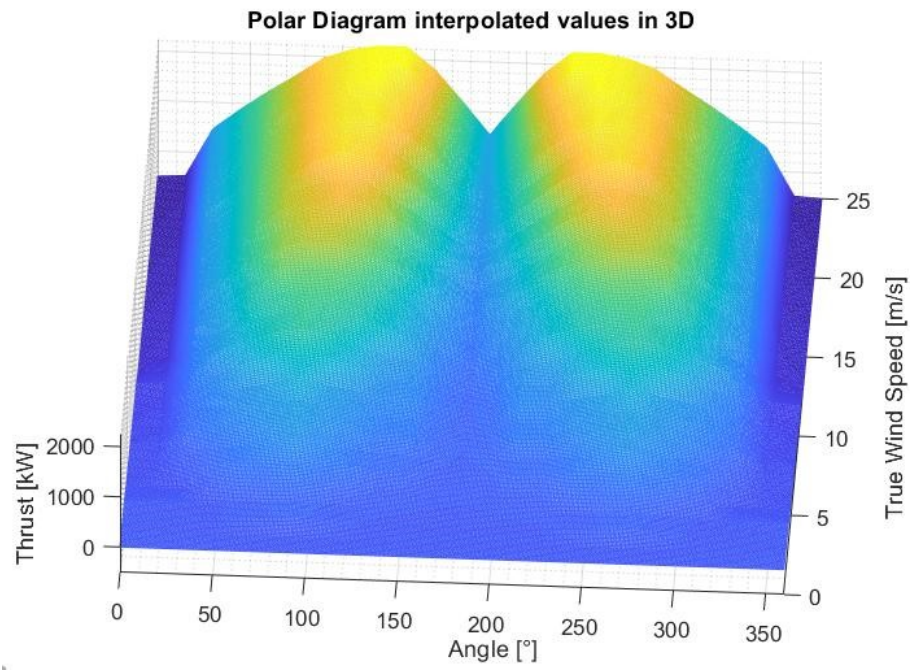


Figure 30: 3D data representation – first view



*Figure 31: 3D data representation – second view*

## 6 Models implementation

### 6.1 Matlab optimisation model

The program used for the simulation of the whole system was Matlab. In fact, the software is furnished with a complete and complex library of simulation tools. Matlab is a powerful and well-known resource and it is currently used by engineers worldwide in order to solve complex problems with the matrix calculation [75]. Nowadays, it has been developed until the point that almost every field related to engineering can be covered through it, from the statistics and optimisation to the data science and deep learning, concerning also the functions of physical modelling about multibody, electrical or fluid dynamic simulations. It can also be used in more remote fields, such as economy, social sciences and applications development [75].

The optimisation toolbox is implemented with functions created in order to find out parameters that minimise or maximise specific functions (called objective functions), meeting the constraints that the developer declares in the script. In general, an optimisation model is set up through the following actors:

- The variables to optimise – they can be single values, vectors or matrix with different dimensions.
- The objective function – it is the function that the developer wants to minimise or maximise. Every variable that is part of the objective function has to be declared as optimisation variable before.
- The constraints – are the conditions that limit the possible combination of the variables in order to reach the target. They can be characterized by mathematical equalities ( $=$ ) or inequalities ( $\leq$ ,  $\geq$ ) between one variable and a fixed value or among more variables.
- The solver – is the algorithm that solves the optimisation problem.

The problem presented is a Mixed Integer Linear Program (or MILP), which means that the objective function and the constraints are linear, while some or all the variables are forced to be integers. Matlab is implemented with an editable optimised series of algorithms to solve the MILP, called with the command *intlinprog*. It involves different types of algorithms, identified under the classes of heuristic cuts and branch-and-bound methods.

The models have been implemented with a Matlab script. The simulations are divided into parts that reflect the optimisation model itself:

- a) model's constant values
- b) optimisation main and auxiliary multidimensional variables
- c) objective function
- d) constraints
- e) problem setup
- f) solving function
- g) graphs of the results.

The chosen method requires the creation of an optimisation model with Matlab function *optimproblem*. By default, the function creates a structure for the optimisation problem composed of the following properties:

- Description of the problem.
- *ObjectiveSense*, which defines if the aim of the model is to minimise or maximise the output.
- Variables, which comprehend all the numeric values that the program has to estimate.
- Objective, which indicates the objective function to maximise or minimise.
- Constraints, which set limits to the variables.

When the *optimproblem* is called, it is initially empty and not defined. It is possible to insert directly the features mentioned above in the *optimproblem* structure. The data created are abstract and are set up in order to be part of an optimisation problem to be solved with specific algorithms, therefore it is not possible to handle them as they are defined – e.g. involving them in algebraic operations.

The created optimising structure is meant to be solved with the *solve* function, set up for Mixed-Integer Linear Programs – it operates the *intlinprog* command. The algorithm that the *solve* function applies to the model aims to simplify the branch-and-bound calculations, which is the rigorous iterative method to calculate the results of the optimisation model. The process expects iterations to quickly pre-examine and spot the futile sub problem candidates and eliminate them in order to run the brunch-and-bound iterations in an easier way.

Firstly, the solve function runs the simulation with the Linear programming (LP) approach, which means that the problem is relaxed, eliminating the constraints involving the integers values and looking for the best numerical solution. The MILP solutions will be greater or equal to the LP solution; during the following simulations the solver would compare, step by step, the numerical solutions of the attempts with the LP solution. After the LP approach, the Cut Generation techniques add the linear constraints to the problem and try to restrict the feasible regions for the final solution. Different types of cuts are executed, depending on the options specified in the ‘solve’ options. Subsequently, the heuristic techniques are applied, before or during the brunch-and-bound iterations, in order to find feasible points faster. As in the case of the Cut Generation techniques, it is possible to edit the heuristic cuts types too. Finally, the algorithm looks for the final solution through the branch-and-bound method. It works building up iteratively sub problems in order to converge to a MILP solution and it is based on giving to the algorithm a sequence of upper bounds to the MILP final solution, which are the feasible solutions found, while the lower bound is the LP solution. The branch-and-bound method calculates iteratively the optimised responses for different combinations of the variables, considering the combination that approximates at best the upper bound to the lower. When the difference between the upper bound and the lower is small enough, the algorithm recognises it and furnish the last upper bound solution as definitive.

## 6.2 Models variables

The model variables consist of main variables and auxiliary variables. The main variables refer to the state of the engines and the battery, consist of discrete variables during the time steps given in the data and they are in the form of multidimensional matrices. They indicate the value of power released on time by each component: once that they are given, it is possible to sum up each of them in order to figure out the total power released by the whole system in the optimised configuration.

The multidimensional matrices consider:

- The number of time step in which the system is analysed:  $i$
- The number of the engine taken into account:  $j$
- The operating engine region:  $k$

They consist of:

- ✓ The engine power given as output by each engine:  $P_E$
- ✓ The battery charging power:  $P_{B,cha}$
- ✓ The battery discharging power:  $P_{B,dis}$
- ✓ The battery charge status:  $E_B$

Every power considered is expressed in kW, while the battery charge is expressed in kWh. All the variables are matrices where each line considers the discrete time steps, while each column coincides with the engine that the value is related to. In the case of the battery, the variable has one column as one battery is considered.

The auxiliary variables are variables that do not represent a form of power or energy, but they are artificially made up in order to make the system respect the constraints and, in this case, to count the number of times a single engine is turned on. The explanation of why this factor has to be taken into consideration is given in the Paragraph 7.3. They consist of:

- ✓ TurnOn: it is a binary variable that indicates when a single engine is turned on and in what time step. As explained later in details, it is composed of 1, if the engine is turned on, and 0, if it does not happen.
- ✓ engOn: it is a binary variable that detects if the engine is turned on in a specific time step. It has the same dimensions of  $P_E$  and it is used to evaluate the TurnOn optimisation variable comparing two subsequent values on engOn for the same engine.
- ✓ SOC: it is the battery state of charge. It is used to evaluate the energy state of the battery for each time step and to impose the constraints over the battery action.

## 6.3 Objective function

The objective function is the function to minimise, which in the analysed case is the function that evaluates the total fuel consumption. Some assumptions have to be taken into account. First of all, in order to make the model more realistic, a penalty term is associated with the engines start-up. If  $m_{add}$  is the additional equivalent mass of fuel

that is consumed and  $t_{start}$  is the time that the engine takes to reach the nominal speed, the formula for deriving the additional consumption can be stated as:

$$m_{add} = \int_0^{t_{start}} SFOC(t) * Power(t) dt \quad (20)$$

As the value of  $m_{add}$  is complex to calculate mathematically, it is rule of thumb to test the engine for assuming the value. In the model, an additional mass of 3600 grams has been considered for the MEs, while for the AEs, which are smaller, a value of 2000 grams has been considered.

If the FFR values in function of power are approximated as a straight line, the equation of the interpolated FFR is in the form:

$$FFR = A * P_E + A_0 \quad (21)$$

Where A is the angular coefficient and  $A_0$  is the constant term of the interpolating line. The objective function to minimise is therefore:

$$OF = \sum_{i \in I} \sum_{j \in J} \left\{ \sum_{k \in K} [(A_{i,j,k} * P_{E_{i,j,k}} + engOn_{i,j,k} * A_{0_{i,j,k}}) \Delta t] + TurnOn_{i,j} * m_{add} \right\} \quad (22)$$

Where I is the set of time steps, J is the set of engines, K is the set of engine operation regions and T is the time step. The objective function is the sum of the contributions of each term of powers related to each time interval, engine and operating region of the considered engine. The reason why different working regions for the engine are considered will be explained later on.

The relationship between power and fuel consumption contains a coefficient and a constant term that are different for each of the two regions considered for the engine. In fact, if the SFOC curve is approximated with a piecewise linear function, the coefficients characterising the straight lines are different. The contribution given by the additional starting consumption is summed up to the fuel consumption of the engines. It is to be noticed that the term  $TurnOn_{i,j}$  does not consider the working region k: in fact, the engine's turning-on condition is independent from the power it operates after the turning. Implementing the objective function, the model needs to interpolate the FFR values through a piecewise function. This particular choice is taken in order to allow the optimisation model to be linear: non-linear FFR curves, in fact, would make the model non-linear, increasing drastically its complexity and solving time.

In order to assume a reasonable time for the simulation and considering that, generally, the most optimised point of working for ICEs is around 85%, it has been decided to use two straight lines for the interpolation of the values, divided at the load point of 85%. As the manufacturers provide information about the SFOC only until 50% of the nominal load, it is reasonable to consider a range of functionality of the motor from

20% of the load to a full power capacity. Furthermore, the manufacturers do not recommend to operate the engines below 20% of the nominal power. Finally, an interpolation with a third grade polynomial shows graphically the goodness of the piecewise interpolation – it is demonstrated that the third grade polynomial interpolates point reducing the error according to the least squares method. The curves that are derived by the process are present in Figure 32, for the ME whose maximum power is 8125 kW, and Figure 33, considering the ME’s maximum power of 7500 kW.

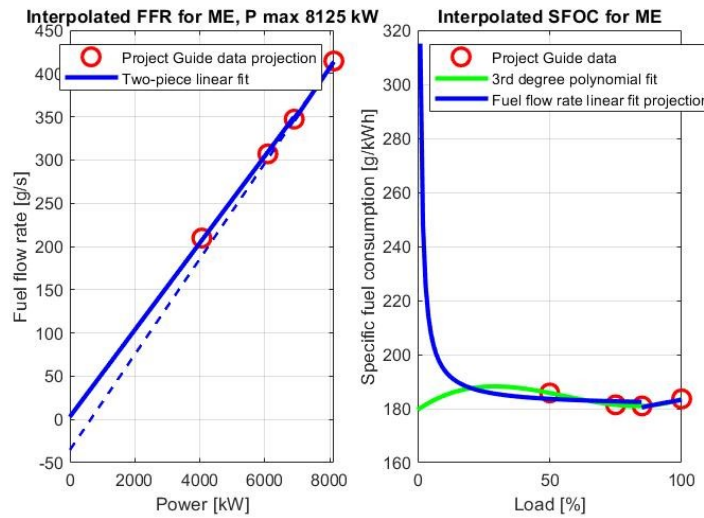


Figure 32: Interpolated FFR and SFOC for ME with max power 8125 kW

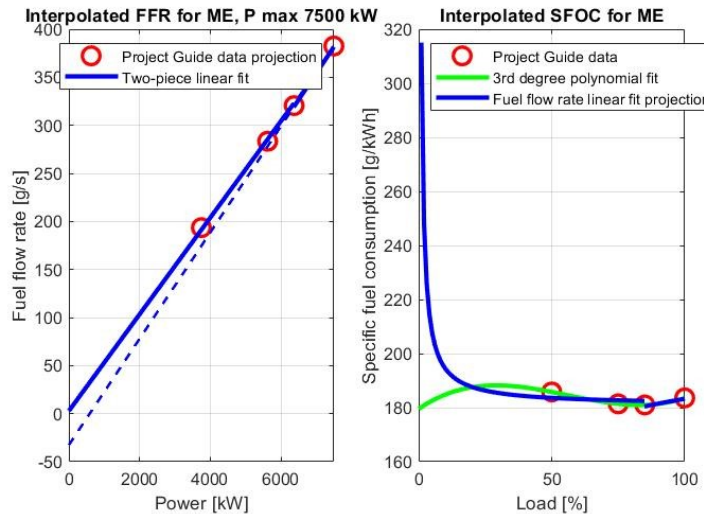


Figure 33: Interpolated FFR and SFOC for ME with max power 7500 kW

The figures show the FFR interpolated values for the two types of ME, drawn with a continuous straight line. The function is piecewise and not continuous, in fact it has a discontinuity of the first kind at the point of 85% of the load. This is the result of the function of interpolation, which does not consider the continuity between the pieces of



the function; the lines are derived from Matlab using the least squares method. This method is a mathematical algorithm that allows any kind of function to be set in order to minimise the global distance between the points and the interpolating function. Therefore, the algorithm does not expect to impose the continuity of the functions at the point of 85% of the load.

In the right part of the picture, the SFOC values have been calculated from the FRR interpolated values with the formula:

$$SFOC = \frac{FRR * 3600}{Power} \quad (23)$$

The red dots are the points of nominal working provided by the manufacturers. It is possible to notice that the two types of interpolation methods (the linear piecewise and the third-grade polynomial) are very close until the valued of load that is near the point of 20%. For lower loads, the two curves clearly diverge: this effect is due to the lack of interpolated points in the range between 0% and 50% of the load.

The same proceeding has been undergone in order to evaluate the FRR related to the AEs. As shown in Table 3, the values of SFOC are slightly higher, as smaller engines have lower efficiency, as a general rule. The curves that are derived by the process are figured in Figure 34 and Figure 35.

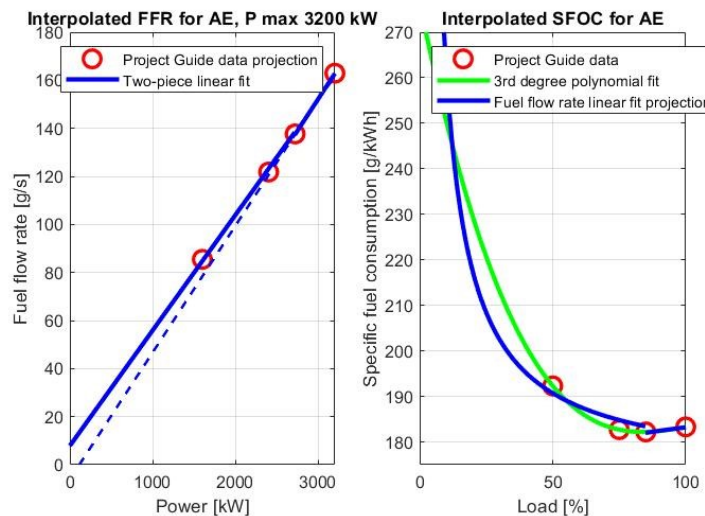


Figure 34: Interpolated FFR and SFOC for the AEs with max power of 3200 kW

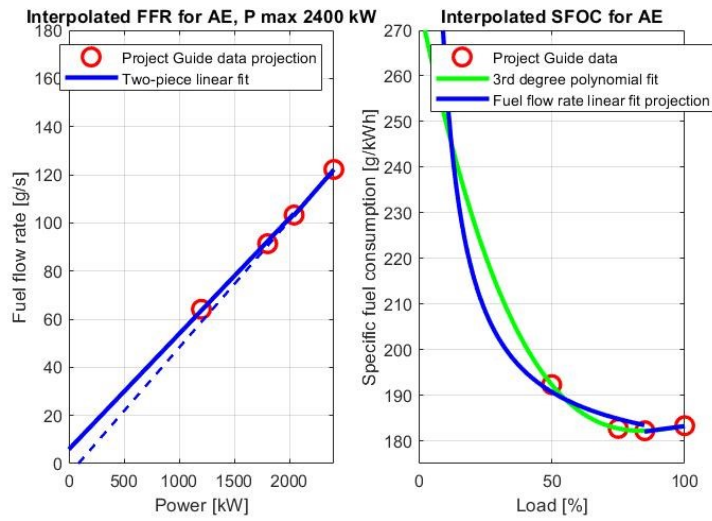


Figure 35: Interpolated FFR and SFOC for the AEs with max power of 2400 kW

It is possible to derive from the graphs that also for this case the FRR interpolation is reasonable, as the third-grade polynomial curve and the SFOC curve follow the same trend. The difference is noticeable only at low powers – below the 20% of nominal power; however, the model considers a minimum point of functioning that is above this percentage. The red dots are the points of nominal working provided by the manufacturers.

As can be seen in Figure 36, the lack of data brings to a very high estimation of the consumptions at low powers.

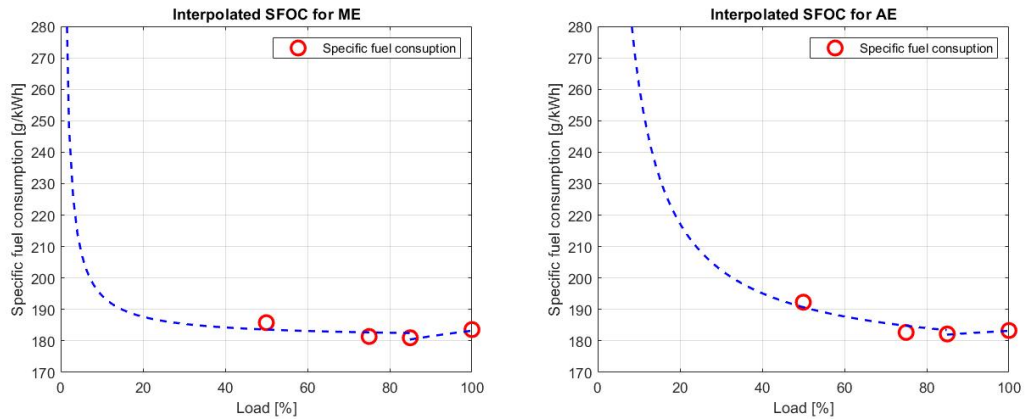


Figure 36: Interpolated SFOC for MEs and AEs

For the previous reasons, the model should consider a minimum value for the actual power that is not far from the last point of working pointed out by the manufacturers. Actually, even though a linear trend has been assumed for the FFR interpolation, it is complex and unclear about how to evaluate a likely behaviour of such a complex machine without official experimental data. Furthermore, an optimised model should avoid the engines to work at low-power points as it means lower efficiency and higher

consumption. Considering the considerations mentioned above, for the simulation model it has been considered a minimum load of 20% for both MEs and AEs.

## 6.4 Constraints

The constraints are the conditions that determine the operation field of the optimising variables. They can be set on both main and auxiliary variables and considers the maximum and power of the engines, the evaluation of the binary variables or the essential condition of the minimum global power that is the output from the model for each time step.

The first constraint is the minimum power that the power unit needs to supply. The essential condition is that, for each time step, the power furnished by the power unit is equal or bigger than the power demanded, indicated as  $P_{D,i}$ . The balance equation does not consider only the sum of all the power from the motors, but also the contribution of the charging or discharging power from the battery. Arbitrary efficiency coefficients have been considered for the discharge and charge state. The constraint is the following:

$$\sum_{j \in J} \sum_{k \in K} P_{E,i,j,k} - \frac{P_{B,cha,i}}{\eta_{cha}} + \eta_{dis} P_{B,dis,i} \geq P_{D,i} \quad (24)$$

The values of  $\eta_{cha}$  and  $\eta_{dis}$  are set in the model as 0.97 and 0.98 respectively.

One other constraint concerns the maximum and minimum power for each engine. If the factor  $engOn_{i,j,k}$  is added to the effective power, the result is that the power is always zero if  $engOn_{i,j,k}$  is zero. If  $P_{E,max}$  and  $P_{E,min}$  are respectively the maximum and minimum power from the engines, and  $\theta_{max,k}$  and  $\theta_{min,k}$  are respectively the upper and lower thresholds for the operation region  $k$ , the constraint can be written in the following way:

$$engOn_{i,j,k} \theta_{min,k} P_{E,min,i,j,k} \leq P_{E,i,j,k} \leq engOn_{i,j,k} \theta_{max,k} P_{E,max,i,j,k} \quad (25)$$

From the model, the previous equation is read as:

$$\begin{cases} \theta_{min,k} P_{E,min,i,j,k} \leq P_{E,i,j,k} \leq \theta_{max,k} P_{E,max,i,j,k} & \text{if } engOn_{i,j,k} = 1 \\ P_{E,i,j,k} = 0 & \text{if } engOn_{i,j,k} = 0 \end{cases} \quad (26)$$

Actually, the use of  $engOn_{i,j,k}$  allows the programmer to include two conditions into one constraint in order to make the optimisation problem linear.

A constraint closely related to the factor  $engOn_{i,j,k}$  is that, for the same values of  $i$  and  $j$ , the sum of the factors has to be less or equal than one. In fact, an engine can work only in one interval of the graph SFOC/Power per time. Nonetheless, if, for a specific value of  $k$ , the factor  $engOn_{i,j,k}$  is on, the other has to be off. Therefore:

$$\sum_{k \in K} engOn_{i,j,k} \leq 1 \quad (27)$$

An ulterior constraint considers the  $TurnOn_{i,j}$  factor. This multidimensional binary variable is set to 1 if the system detects that the engine is turned on in the instant  $i$ , or is set to 0 if the condition is not detected. As the system tries to minimise its value, its constraint can be set as follows:

$$TurnOn_{i,j} \geq \begin{cases} \sum_{k \in K} (engOn_{i,j,k} - engOn_{i-1,j,k}) & \text{if } i > 1 \\ \sum_{k \in K} engOn_{i,j,k} & \text{if } i = 1 \end{cases} \quad (28)$$

The previous constraint evaluates the difference of the operating binary value of each motor in each instant and compares it with the same value in the previous time. As all the motors are supposed to be turned off in the first time step, when Silja Serenade is anchored in the Helsinki's harbour, the  $TurnOn_{i,j}$  variable considers only the sum on  $k$  of  $engOn_{i=1,j,k}$  at the start point. As the model minimises the  $TurnOn_{i,j}$  values, they will be set as one if the engine is turned on from a turned-off state, or zero if it is not.

The constraints for the battery consider the maximum power, the minimum power and the battery SOC. The logic behind them is that the output power has to respect a specific range, indicated by the manufacturers. Besides, it has to be considered that the battery SOC can vary between a specific range of percentages of the battery capacity. For each instant, the battery power has to respect the following constraints:

$$\begin{cases} P_{B,cha,i} \leq P_{B,cha,max} \\ P_{B,dis,i} \leq P_{B,dis,max} \end{cases} \quad (29)$$

Once that the battery charging and discharging power is evaluated, the SOC can be derived directly from those value and the SOC in the previous time step, knowing the time between one state and the following one. In order to evaluate the SOC trend during the cycle, an initial constraint has to be supposed. In the model the condition considered is that the SOC at the first step is at its full capacity, as in the Helsinki harbour it is able to recharge directly from a charge point. Therefore, the constraints are:

$$E_{B,i} = \begin{cases} E_{B,max} + \frac{P_{B,cha,i} - P_{B,dis,i}}{E_{B,max}} \Delta t & \text{if } i = 1 \\ E_{B,i-1} + \frac{P_{B,cha,i} - P_{B,dis,i}}{E_{B,max}} \Delta t & \text{if } i > 1 \end{cases} \quad (30)$$

Finally, the last constraint involving the battery requires that the SOC, normalised by the maximum battery energy, has to be between 1 and 0, which mean respectively that the ESS is full-charged or completely discharged. Actually, the battery has to prevent from being fully drained in order to avoid damages; on the other side, for technical reasons it is not possible to fully charge it. For those reasons, the feasible values for the SOC are established between 95% and 20%:

$$20\% \leq SOC \leq 95\%$$

(31)

## 6.5 Implementation of the model with the shaft generator

The model that includes the shaft generator needs to have the propulsion and the auxiliary data implemented in the same script. The presence of the shaft generator allows the exceeding mechanical power – generated by the propulsion power unit – to be converted into electrical power in order to reduce the consumption over the auxiliary power supplying system.

Shaft generators are electric generators that exploit the rotational speed of the shaft in order to derive current. A permanent magnet is fixed on the shaft, while the stator is provided by wires that collect the current generated by the relative movement of the shaft and the stator. The alternate current they supply to the vessel electrical grid can be provided with constant frequency if the solution with adopted is PTO/CFE (Power take-off/constant frequency electrical), which is furnished with a slow running alternator with electrical control equipment.

In the configuration that is taken into account, the low speed main engine driven shaft generator is expected to be after the gearbox, where the speed is low and the torque transmitted is high. The shaft generator relates with only a couple of engines. In fact, there could be another one, in order to cover all the four MEs, but the solution would be too much expensive.

The model implemented for the simulation considers the functioning of the propulsion power system during a specific time lapse. In this case, the data refer to the time lapse used for the evaluation of the propulsion power, between the departure from Stockholm and the permanence in Helsinki's port.

Both the power demand values, the propulsion and the auxiliary ones, have been evaluated in the selected amount of time. They are shown, plotted, in Figure 37.

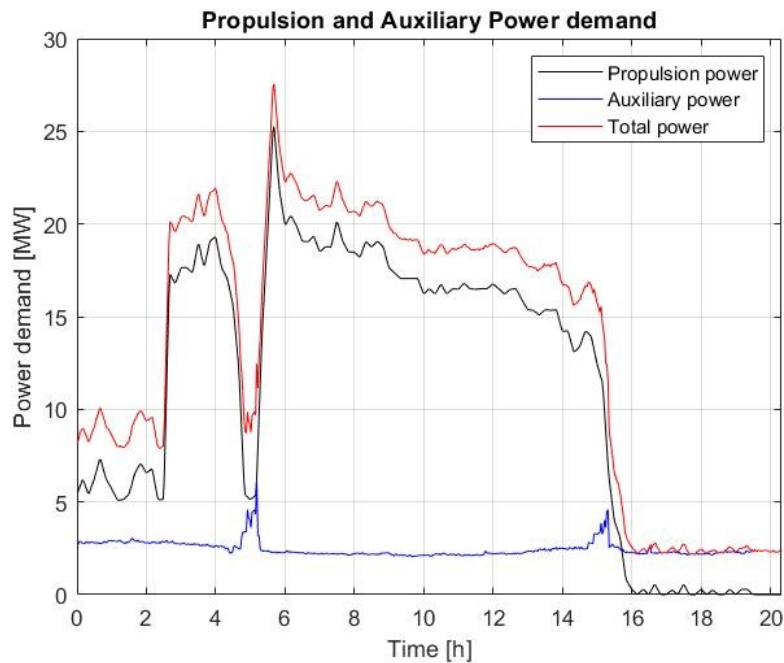


Figure 37: Propulsion and auxiliary power demand

It is evident now that the auxiliary power demand, even the bow thrusters' demand, is actually low compared to the propulsion demand. The adopted logic for the setting of the optimisation was that the power that is furnished by the MEs in excess can be used by the electric grids once that it is converted into electrical power. The production of power from the shaft generator allows the AEs to generate power to satisfy a lower amount of power demand. Firstly, the propulsion power unit is simulated, considering the nominal power need. After that, the difference between the actual generated power and the propulsion power demand is calculated, for each time step. This power difference is exploited by the shaft generator, which powers the electric grid and reduces the need for electric power.

There are assumptions to be taken for the shaft generator operations. One assumption is on the maximum power that it can convert. In fact, according to the manufacturers, the maximum power can reach up to 3.5 MW. This value will be considered for the simulation. Besides, the functionality is not ideal, but there are losses from the power conversion. The indicated values fluctuate between 81% and 92%; a value of 85% is considered in the model.

## 6.6 Optimised model with the Flettner rotor

The current paragraph will discuss the implementation, in the simulation model, of the Flettner rotor on board. This solution refers to the polar diagram shown in Figure 28. According to the main FRs manufacturers, only one Flettner rotor could be installed on the deck due to the lack of available open space.

The model will simulate the behaviour of the vessel's power unit topologies with the contribution given by the Flettner rotors. As they provide thrust directly on the ship,

the model will assume that the power indicated by the polar diagram provided powers directly the propulsion power demand. In addition to this, the values of power indicated refer to the simulations on Silja Serenade and consider the output power directly, as the model does not have to consider any further efficiency.

Another assumption is taken for the speed related to the journey. As shown in Figure 18, the most common velocity is about 18 knots, which is the reference ship speed that the power values related to the polar diagram rely on. However, there are some tracts where the speed is considerably lower. To take this factor into account, a multiplication factor of 0.8 has been considered for the speed during the archipelago navigation – at the medium velocity of 14 knots – while for the last part, where the ship is still in Stockholm’s port, the thrust values have been halved.

Data about the wind speed and the relative angle of the wind during each time step are needed in order to simulate the generated thrust. As it was not possible to gain the exact data for a particular journey, large sinusoidal data for both the factors have been considered, as shown in Figure 38.



Figure 38: Data for the case of FR installation

The data consist of the true wind speed – which is the absolute speed of the wind – and the relative angle between the ship direction and the wind speed vector. The wind speed is assumed to be oscillating between 25 m/s and 10 m/s, while the relative angle covers all the possibilities from 0° to 360°. The sinusoidal functions are assumed to be characterised of a random phase displacement.

## 7 Optimised results for the hybrid power system

As first attempt, the propulsion power unit and the auxiliary power unit have been simulated separately. This type of working reflects the first configuration introduced in Paragraph 3.3, which considers the two types of power supplying separated. As the problems are non-convex, a maximum time of simulation has been set up due to the fact that the iterations do not converge in a reasonable time ( $> 1$  hour). After that, a second model has been simulated, which is similar to the first configuration with the addition of a shaft generator; it allows the mechanical power supplied in surplus to be converted into electrical power in order to feed the auxiliary system. The Matlab codes implemented for all the cases can be found on Github at the link [https://github.com/alexmaruccia/Ship\\_Optimisation.git](https://github.com/alexmaruccia/Ship_Optimisation.git).

### 7.1 Results for the propulsion power unit

In the first instance, the propulsion power unit has been simulated. To allow the problem to be linear, it is not possible to write the objective function as indicated in Paragraph 6.3 : in fact, considering that the coefficients  $A_{i,j,k}$  and the constant terms  $A_{0,i,j,k}$  are variables depending on the power generated by the engines, the system has to differentiate the power regions' coefficients, in order to detect to what region the power belongs to and to set to zero the powers of the other region, as each engine can have only one power as output. In the considered case, there are two power regions, one from 0% to 85% of load and the other one from 85% to 100% of load. Therefore the objective function for the Matlab script is:

$$OF = \sum_{i \in I} \sum_{j \in J} \{ [A_{i,j,1} * P_{E_{i,j,1}} + engOn_{i,j,1} A_{0,i,j,1}] + [A_{i,j,2} * P_{E_{i,j,2}} + engOn_{i,j,2} A_{0,i,j,2}] \} \Delta t + TurnOn_{i,j} * m_{add} \quad (32)$$

Where the subscript 1 is related to the straight line interpolating the data of the FFR from 0% to 85% and 2 is related to the straight line interpolating the data of the FFR from 85% to 100%.

The options for the cut generation and the heuristic methods have been set on 'advanced', which implies the strongest algorithms for the research of the solutions. The final solution is shown in Figure 39 and Figure 40.



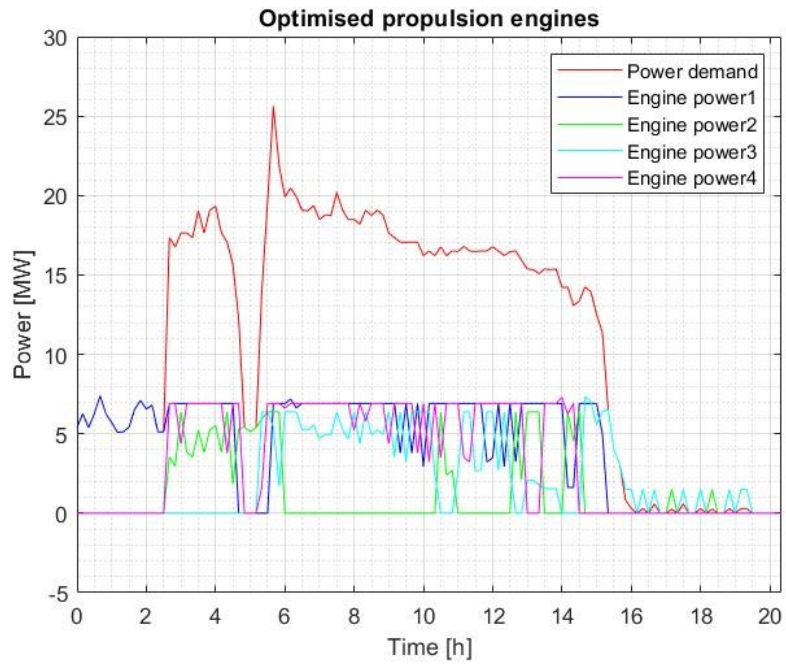


Figure 39: Results for the propulsion power unit simulation

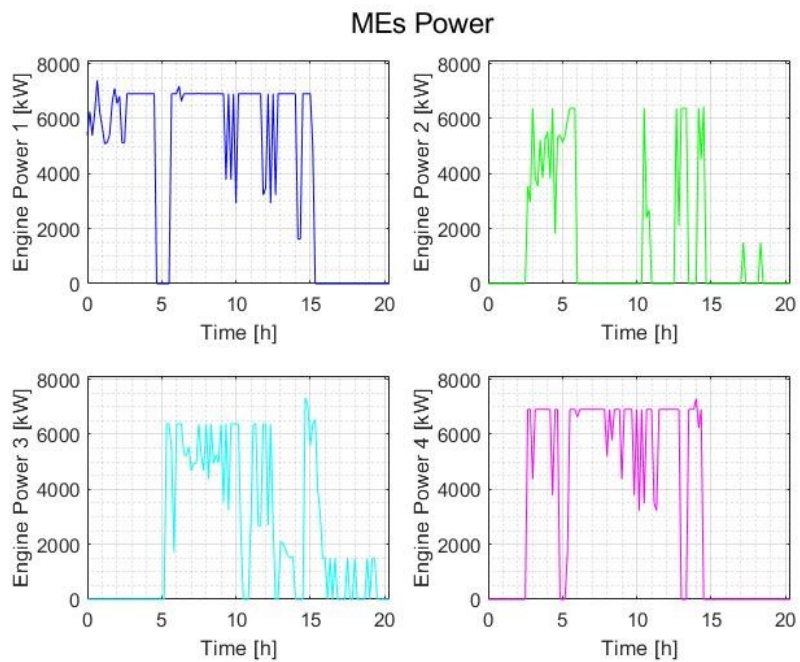


Figure 40: Optimised power plotted for each propeller-driving engine

The results show that, for most of the time, the engines work at the optimised load of 85%, equal to a power of 6906 kW. This happens because, for this value, the SFOC is at its minimum. Furthermore, it can be observed that, to allow some of the engines to run constantly at their optimal point, other engines are characterized by oscillating

behaviour, in the points where the required power oscillates. This behaviour cannot be avoided, as there is no other power source except from the diesel engines, which has a minimum load of 20%. In the case of the auxiliary system, it will be seen that the presence of the battery, which is able to supply electrical power in a wider range, reduces the instantaneous peaks of the motors.

The total consumption resulting is 42 067 kg, chosen between 18 optimal solutions found by the simulator, exploring 43 111 knots; the gap between the branch-and-bound solution, which is the one plotted, and the LP solution, which is the optimal objective value, is 0.29%, therefore the solution can be accepted. Even though the total consumption can seem a very high amount, it is in the reasonable range for Silja Serenade for the time interval indicated by the data.

## 7.2 Results for the auxiliary power unit

After the propulsion power unit, the auxiliary power unit has been simulated. The simulation model is similar to the propulsion one, with differences for the presence of the battery and for the lower engines' maximum power. The results are plotted in Figure 41 and Figure 42.

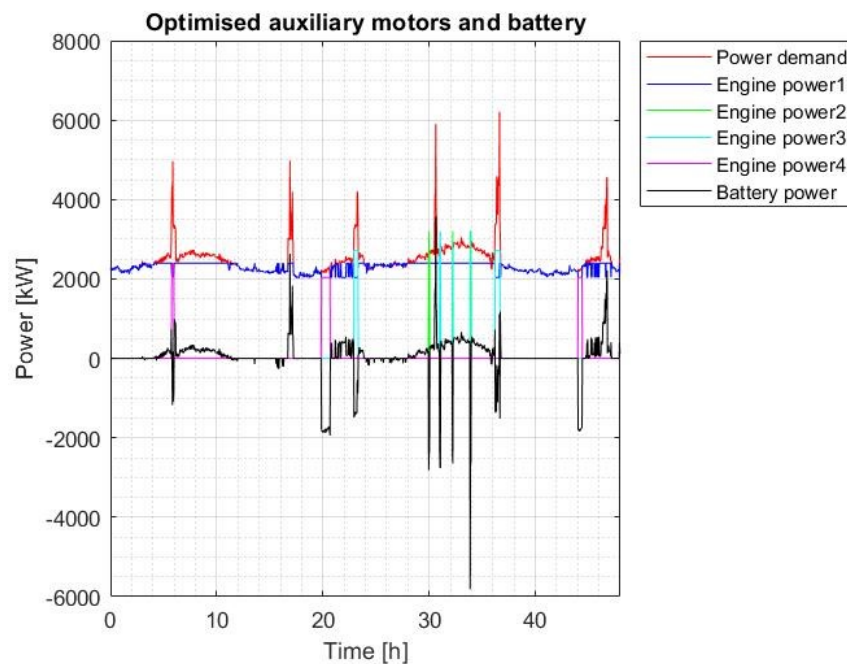


*Figure 41: Results for the auxiliary power unit simulation*

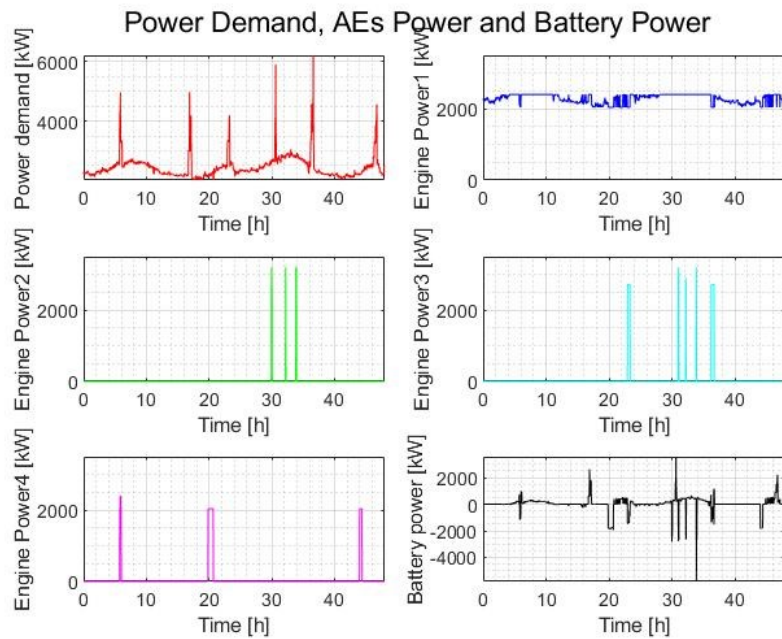
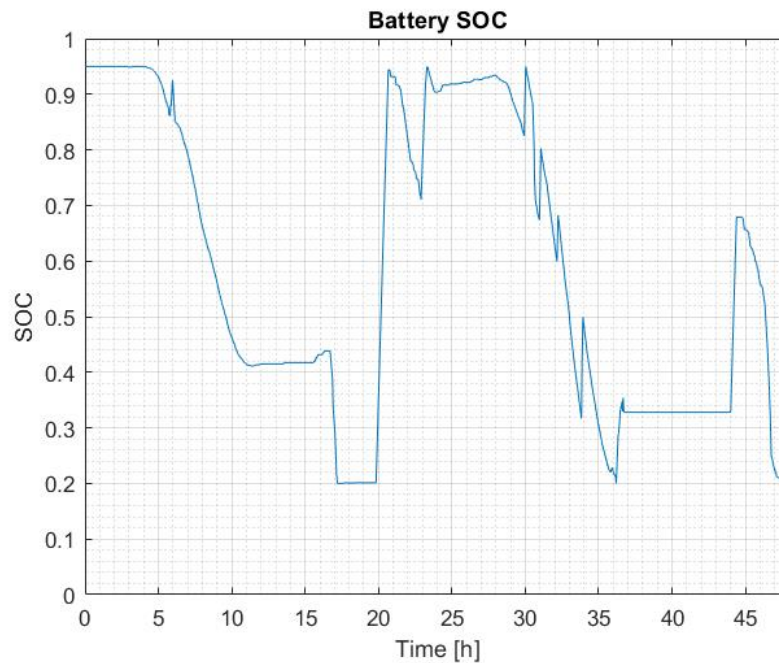


Figure 42: Optimised power plotted for each motor-driving engine

It can be stated that the behaviour of the simulated propeller-driving engines is different from the one of the motor-driving engines. In fact, the first engine has a continuous functioning at the high powers, between 2000 and 2400 kW, supplies most of the demanded power: it works stably at the highest efficiencies. The other engines supply power occasionally, when the demanded power is characterised by peaks and the battery's SOC is not enough to let the battery supply the right amount of power.

Looking at the battery, its power is used partly to supply power during the peaks demand, partly to supply power when the request is higher than the first engine's maximum power, while it charges when the engines' power is high and overcomes the power demand. The SOC of the battery is shown in Figure 43.



*Figure 43: Battery SOC*

It can be noticed that the battery recharges during the third requested power peak, where two engines are turned on, supplying more power than the one requested: the battery recharges. In the between of the two peaks related to the entry and the exit in/from the Helsinki's port, all the peak demands are at least partially satisfied by the discharging action of the battery. In the specific, the second, the fourth and the last peaks are totally powered by the battery, while the remaining are partially powered by the battery and partially by the engines. It is to be noticed that the battery is supposed to be recharged during its stay in the Helsinki's port.

The auxiliary system optimised consumes 21 315kg of fuel during its cycle, with a gap of 0.71% from the LP solution. It has to be considered that the time considered for the auxiliary power supply is 48 hours, while the cycle considered for the propulsion cycle is only 20 hours and 20 minutes.

In order to evaluate the consumption in the considered time for the global simulation, the model has to consider the period identified in Paragraph 5.2. Plotting the power values referred to that time interval, the results are the ones shown in Figure 44 and Figure 45.

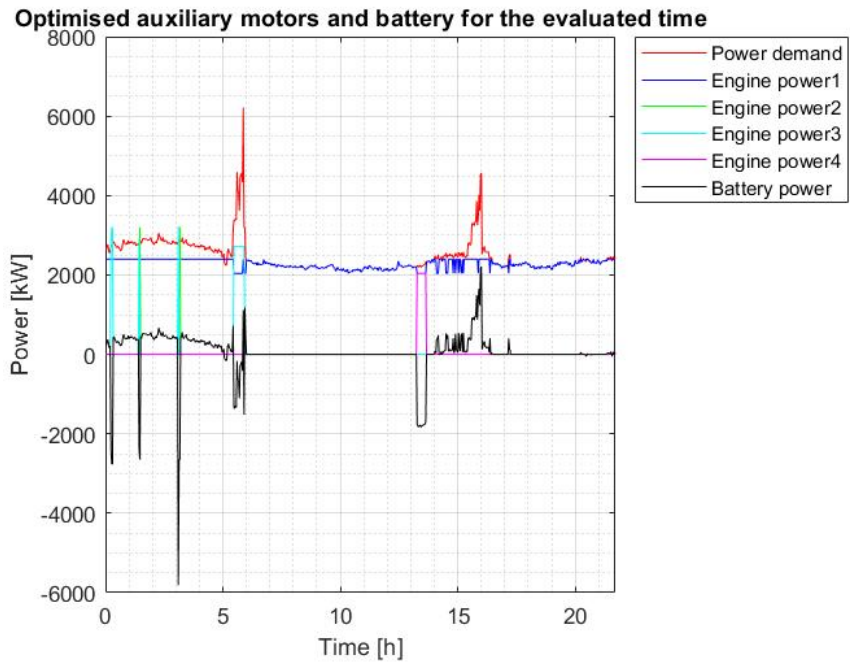


Figure 44: Results for the auxiliary power unit simulation for the evaluated time

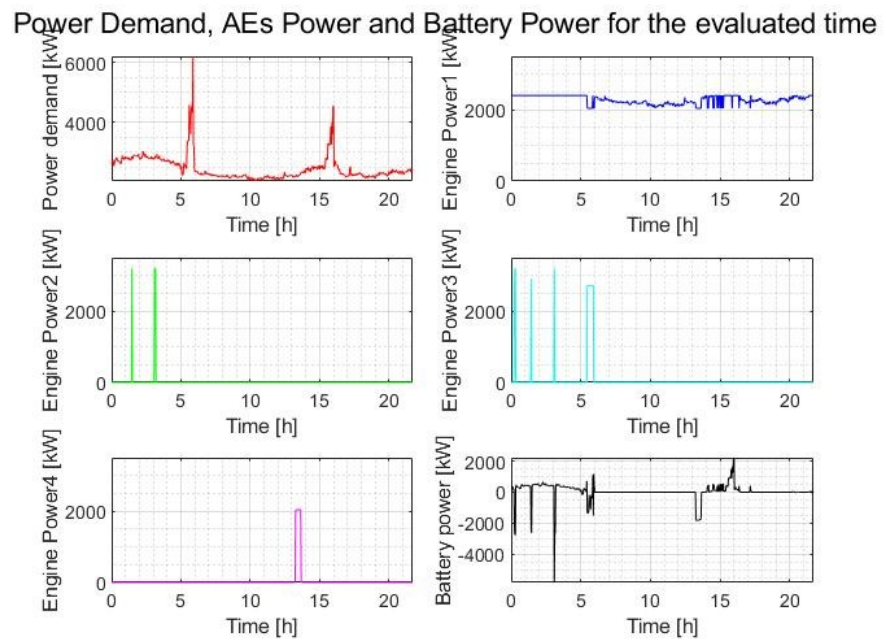


Figure 45: Optimised power for each motor-driving engine for the evaluated time

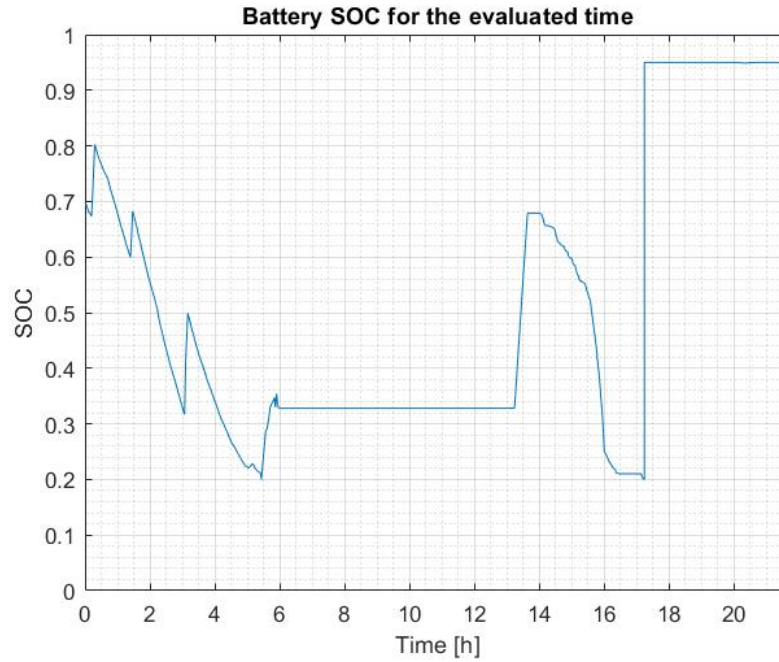


Figure 46: Battery SOC for the evaluated time

The fuel consumption in the evaluated period is of 9 638 kg. It will be considered, alongside the propulsion consumption, in order to make comparisons between the different ship's topologies.

### 7.3 Results with the implementation of the shaft generator

The presence of the shaft generator is simulated in the model through the creation of an additional optimisation variable in the model. As, for this case, the propulsion system and the auxiliary system are interconnected, the two categories of matrixes – related respectively to the propulsion power generating unit and the auxiliary power generating unit – are implemented in bigger matrixes that considers both types, in order to simplify and optimise the solving algorithms. In fact, the integration of the two types of engines with the relative constraints makes the model stiff to solve.

The maximum power assigned to the simulated shaft generator is equal to 3.5 MW, while its global efficiency has been set up to 0.85, in order to assume the worse condition; in fact, generally the shaft efficiency is higher, but in the model other types of efficiency – e.g. the losses due to the shaft friction – are neglected.

The integrated model considers the constraint for the propulsion system under the following formula:

$$\sum_{j \in J} \sum_{k \in K} P_{E\_prop,i,j,k} - P_{shaft,i} \geq P_{D,i} \quad (33)$$

Where the  $P_{shaft,i}$  is the power conveyed to the shaft. The power converted by the shaft generator is conveyed to the electric grid considering the shaft efficiency, therefore the power constraints for the auxiliary system is:

$$\sum_{j \in J} \sum_{k \in K} P_{E\_aux,i,j,k} - \frac{P_{B,cha,i}}{\eta_{cha}} + \eta_{dis} P_{B,dis,i} + \eta_{shaft} P_{shaft,i} \geq P_{D,i,aux} \quad (34)$$

In the view of the previous consideration, the shaft generator can be seen as a system that regenerates the extra power from the propulsion unit into electrical power to supply to the auxiliary system. Therefore the power generation by the propulsion unit is the same of Paragraph 7.1, but the power generation from the auxiliary unit decreases. It can be expected that, in optimised conditions, two or more AEs do not work for a considerable amount of time or even at all.

The simulation has been run considering different starting additional consumptions for MEs and AEs. The time set for the simulation is 300 s. The results are given in Figure 48 for the MEs and in Figure 50 for the AEs, while Figure 51 and Figure 52 show the shaft generator's power and the battery's SOC.

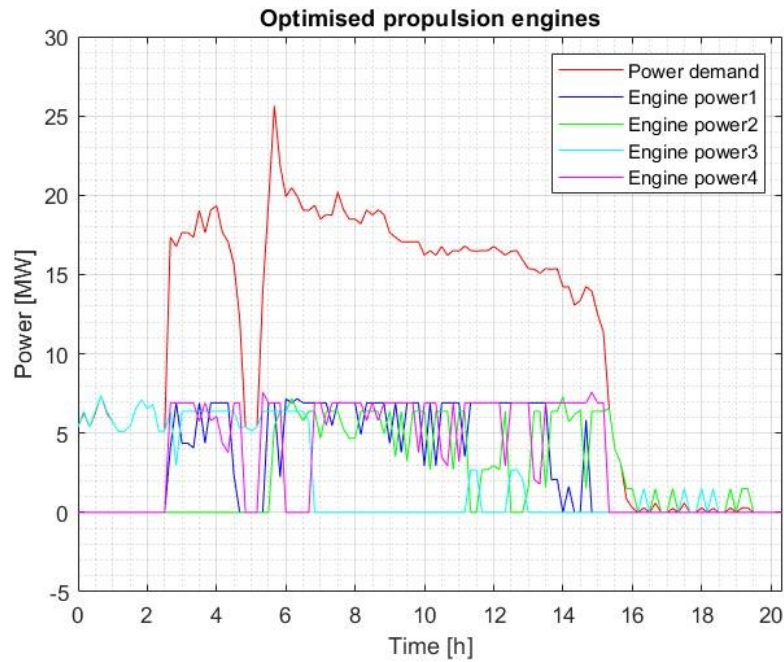


Figure 47: Optimised propulsion engines with shaft generator

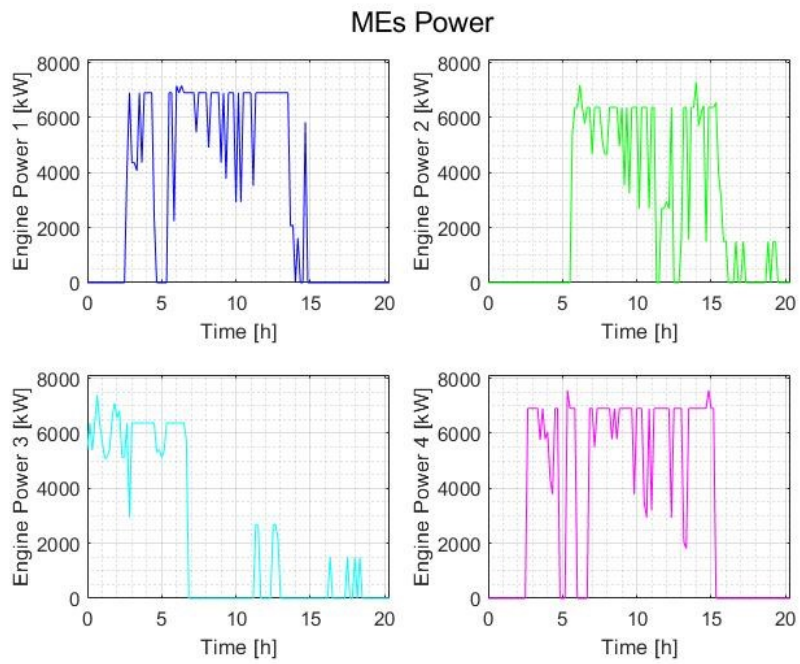


Figure 48: Optimised MEs powers with shaft generator

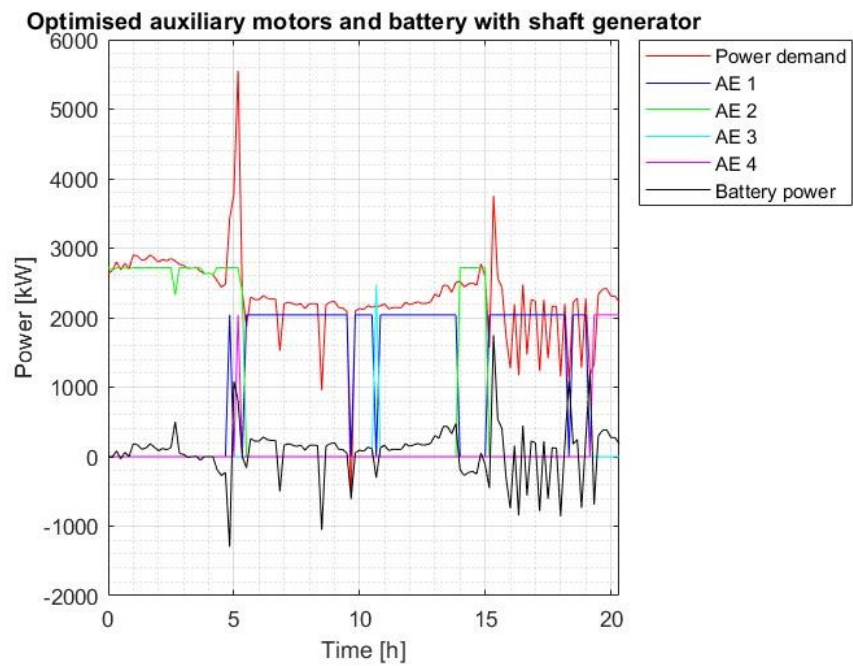


Figure 49: Optimised auxiliary AEs and battery with shaft generator



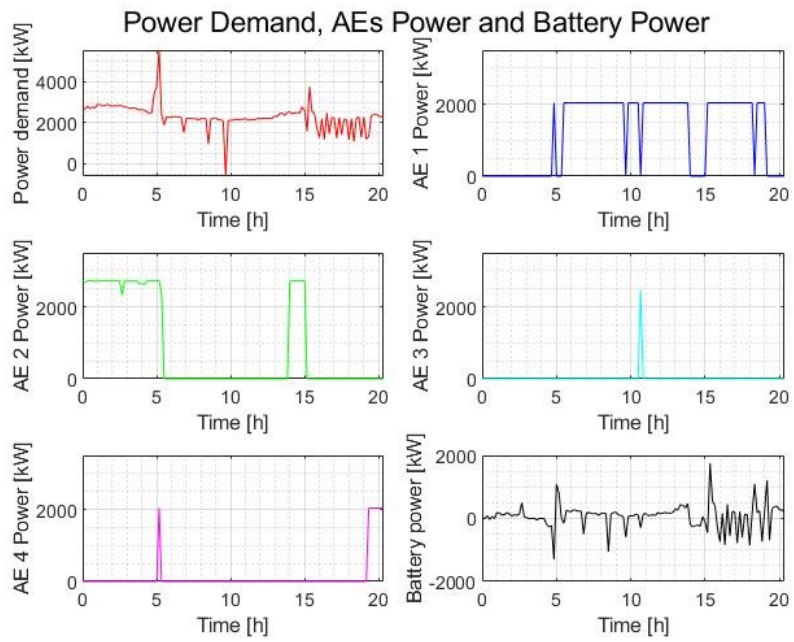


Figure 50: Optimised AEs and battery powers with shaft generator

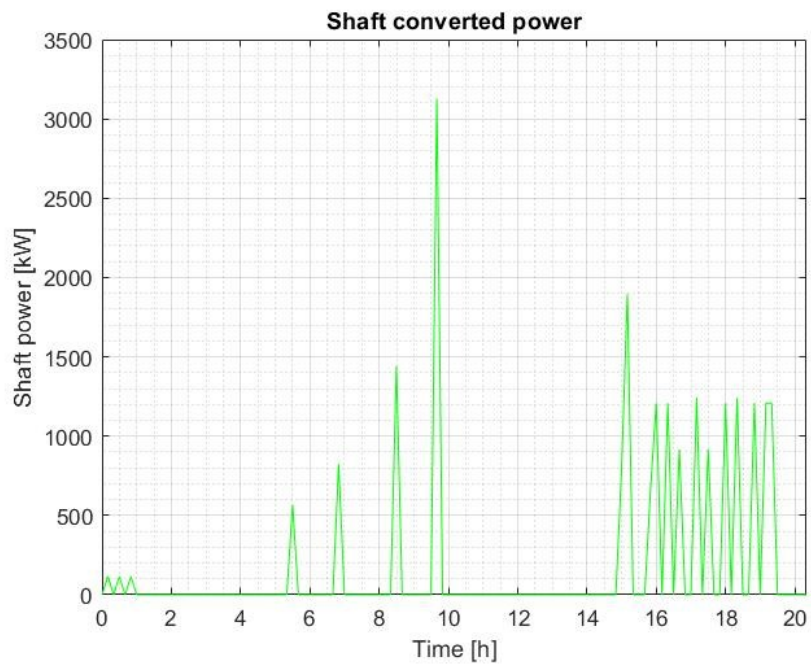
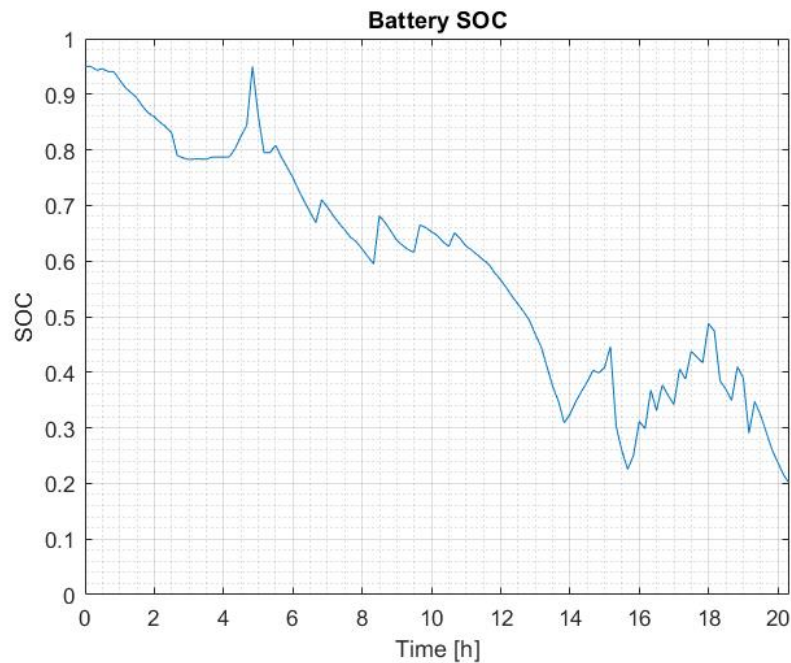


Figure 51: Power converted through the shaft generator (input)



*Figure 52: Optimised battery SOC with the shaft generator*

From the results, it can be stated that this topology let the auxiliary power unit run with more regular trend. The first and second engines run almost constantly at their maximum efficiency, for a considerable part of the total time. The third and fourth engines are, instead, characterised by few instantaneous peaks, supplying power when it is necessary. The battery works intensively with the logic explained in Paragraph 7.2.

The total fuel consumption optimised by the model is 50 756 kg. Therefore, this solution is more convenient than the typology where the propulsion and the auxiliary units are separated as it allows to save 309 kg of fuel, which is remarkable if it is considered that Silja Serenade can take up to more than one hundred trips per year.

#### 7.4 Effects of the Flettner rotor on the propulsion system

As first try, the FR has been implemented in the propulsion system's simulation. The starting mass of 3500 grams has been held, while the simulation time is 300 s.

A specifically-created function simulates the function of the Flettner rotors and evaluates the values of thrust, in terms of power, given by the FR. The value is then subtracted to the propulsion power demand profile. The FR's supplied thrust has the profile given in Figure 53.

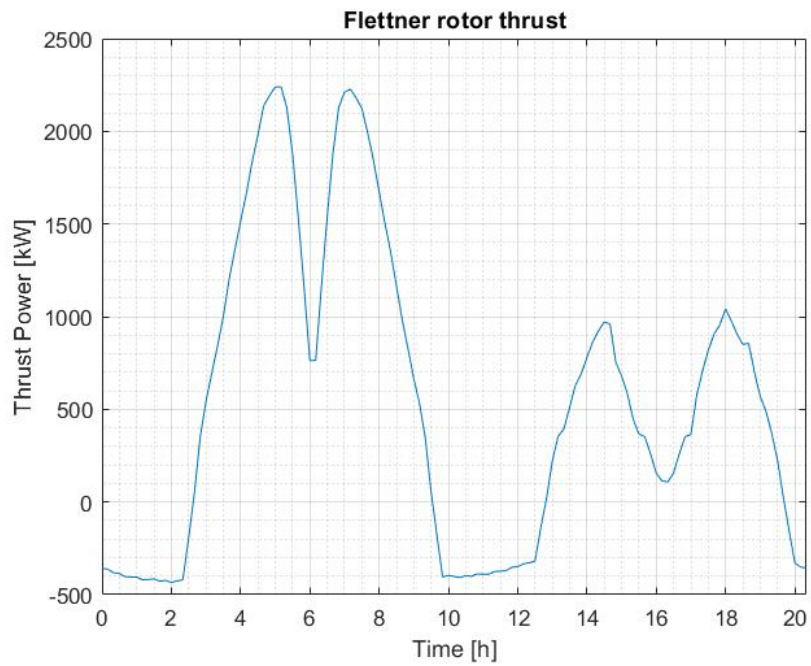


Figure 53: FR's thrust contribution

Figure 54 shows the initial power demand, the generated thrust and the evaluation of the net power demanded by the engines. It can be observed that the FR contribution flats the peaks of power demand, therefore they are made less critic.

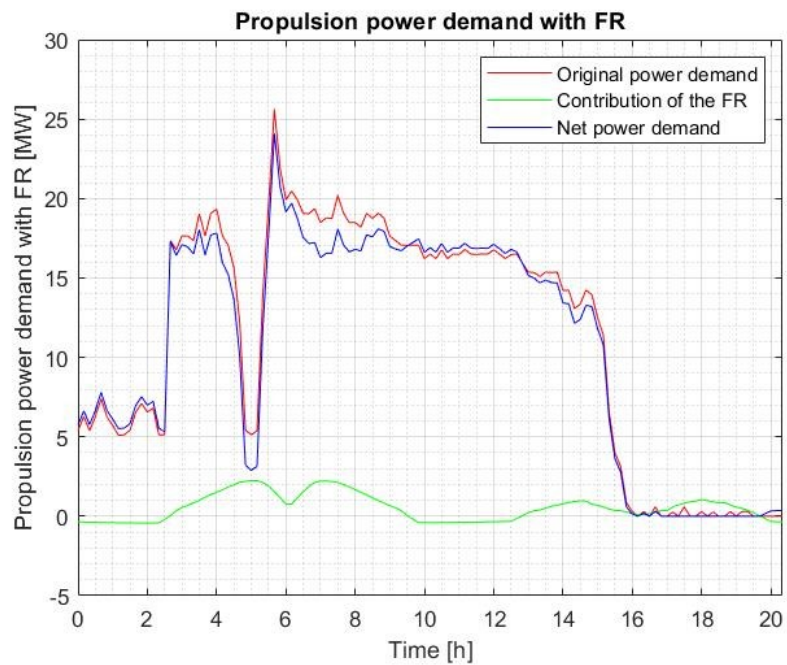


Figure 54: Powers related to the system

The net power demand is the value of power that the engines have to supply to the thrusters in order to keep the roadmap. It can be noticed that in some cases the additional thrust is negative, therefore the new power demand is higher: it is the case of small angle of incidence of the wind from the ship's bow, where the rotors are not able to exploit the wind force, which instead resists to the vessel's movement.

In the simulated case the FR's thrust originates two peaks that shave the tortuous power profile from the point of approach to Mariehamn to few hours after leaving Stockholm. The calculation of the thrust is done with the support of a Matlab-implemented function that calculates the thrust for each time step working on the values of the wind's true speed and incidence angle, using the interpolated data derived from Figure 28.

The simulation's results are shown in Figure 55 and Figure 56.

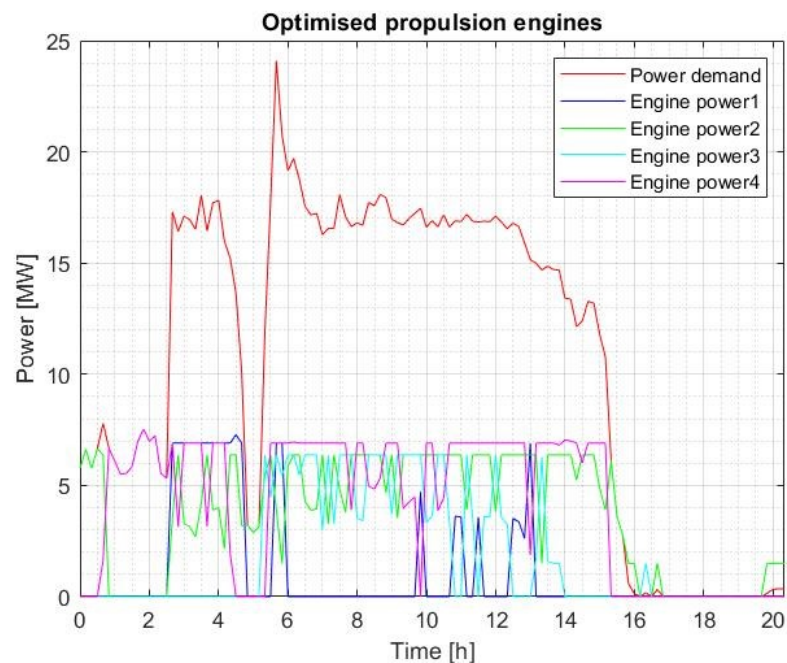
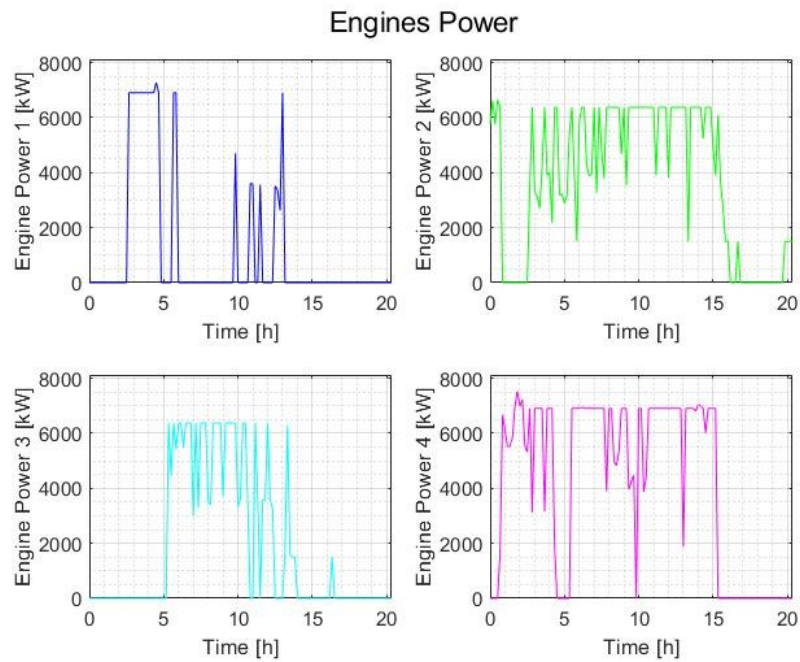


Figure 55: Optimised MEs in case of FR installation



*Figure 56: Behaviour of MEs in case of FR installation*

The oscillations of the optimised workloads of the engines are due to the instability of the optimised behaviour of the engines in case of the oscillation of the power demand, as is shown also in Figure 40. Moreover, the oscillations are denser as the model is heavier than the case described in Paragraph 7.1. Basically, this unstable behaviour intensifies with the complexity of the model, as the branch-and-bound algorithms have difficulties to spot feasible solutions. In fact, additional constraints increase the model's stiffness.

### 7.5 Effects of the FR on the shaft generator's powering topology

Finally, the behaviour of the last topology is simulated: this case includes both the presence of the shaft generator, which considerably decreases the need for the AEs work, and the Flettner rotor, which instead decreases the need for the mechanical power generation. The implementation of those systems largely increases the model's stiffness, as it increases the number of optimisation variables and the constraints, but, if well-implemented, it is able to minimise the global fuel consumption.

The model actually reflects completely the modern ship's topology, built with the aim of reducing pollution. Increasing-efficiency systems integration is the main drive that big companies, specialised in naval buildings, are trying to achieve. Shaft generator and Flettner rotors are two of the main systems that are appealing nowadays, and big efforts and researches are done through this direction.

The simulation has been run with the advanced options for the simulation solving algorithms and the simulation's time of 500 s.

The results of the final simulation are shown in Figure 57 and Figure 58 for the MEs, Figure 59 for the converted power by the shaft generator, Figure 60 and Figure 61 for the AEs and, finally, Figure 62 for the battery's SOC.

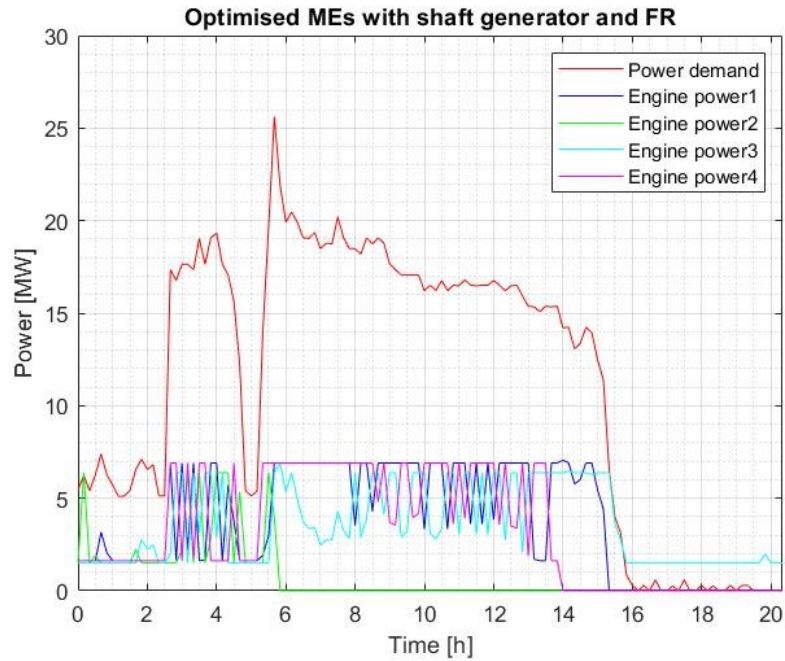


Figure 57: Optimised MEs in case of shaft generator and FR installation

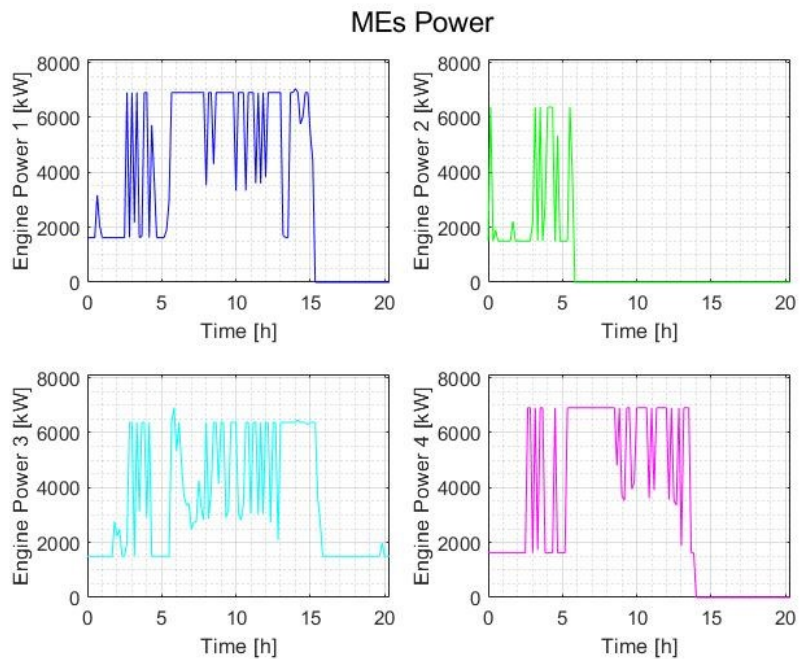


Figure 58: Behaviour of MEs in case of shaft generator and FR installation

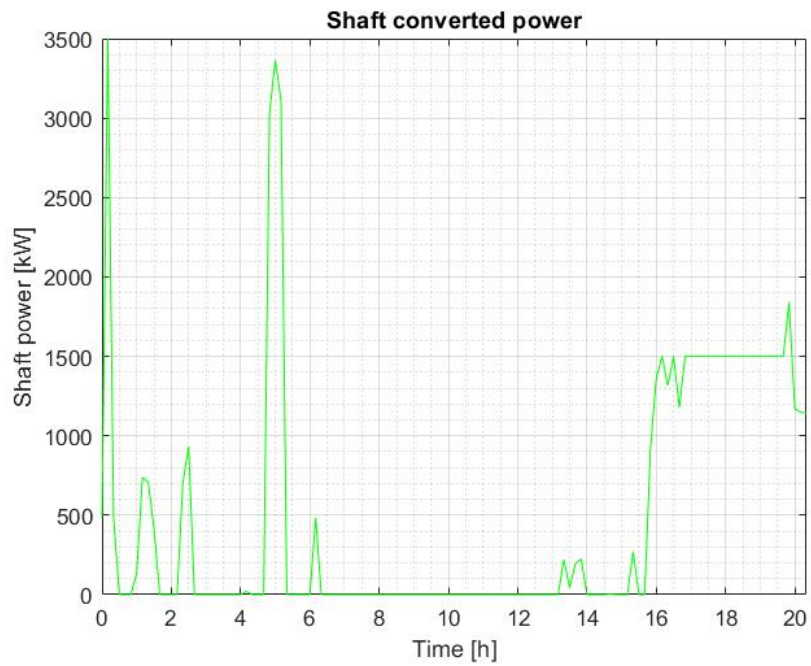


Figure 59: Optimised shaft power in case of shaft generator and FR installation

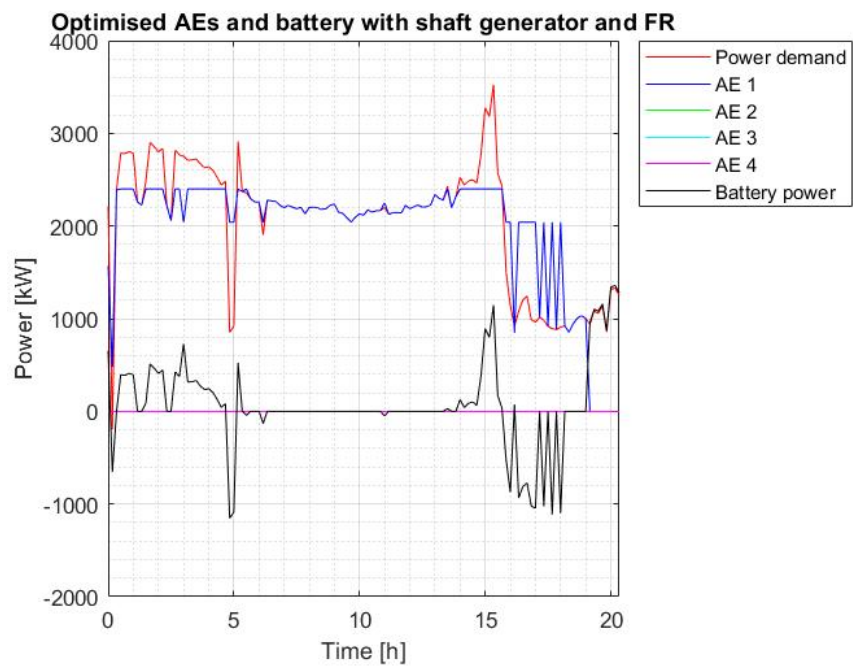


Figure 60: Optimised AEs in case of shaft generator and FR installation

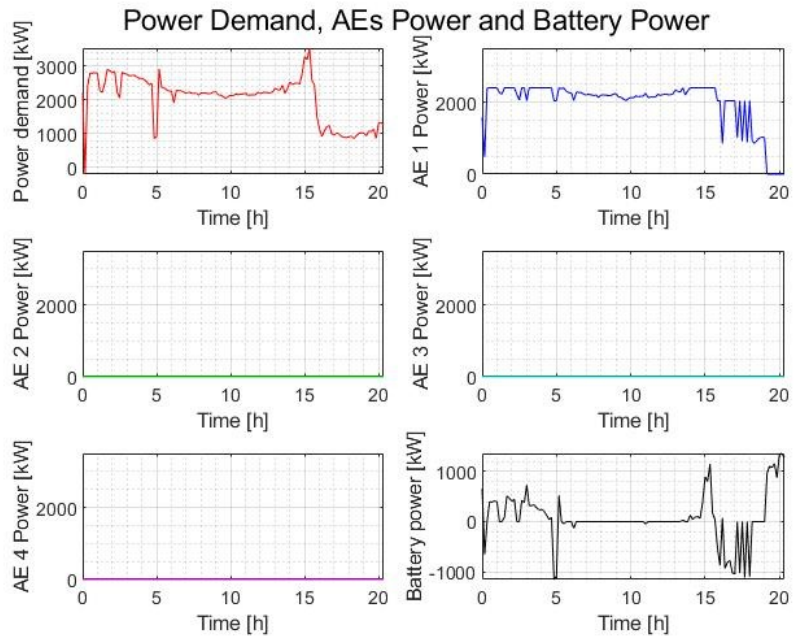


Figure 61: Behaviour of AEs in case of shaft generator and FR installation

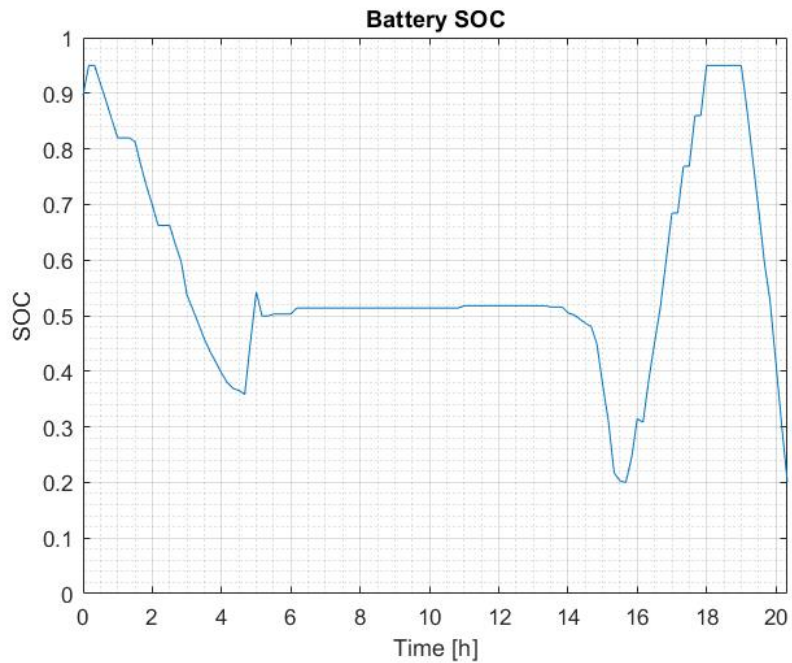


Figure 62: SOC trend in case of shaft generator and FR installation

In the MEs graphs it can be noticed that, in the period between 2 and 5 hours, the engines' powers oscillates continuously. This effect, as already explained in Paragraph 7.4, is due to the model's instability related to the fast oscillations of the demanded power. Compared to the results of the simulation of the model with the only FR (Figure 56), it can be noticed that the engines are working with more stability. Most of the differences with the previous model are related to the AEs: in fact, only one engine is



enough to supply the totality of the required power, alongside with the battery. All the other engines are shut-off for all the trip. This result is very different from the results in Paragraph 7.3, where all the engines had to be turned on at least once during the simulation. However, it should not be forgotten that the simulation simulates the values related to the wind speed and the incidence angle, therefore the results can change easily depending on the weather conditions.

## 8 Conclusions

Considerations on the fuel saving can be drawn out of the run simulations. The optimised models allow to minimise the global fuel consumption, though considerable differences can still be noticed simulating different cases of the Silja Serenade's topology.

The first simulation, considering the propulsion and auxiliary power-generating units separated, results in fuel consumption of 42 067 kg for the propulsion system and 9 638 kg for the auxiliary system, for global consumption of 51 705 kg for each round trip.

The second simulation considers the presence of a shaft generator, which closely connects the propulsion and auxiliary power unit. Decreasing the global fuel consumption, reducing the actual auxiliary power demand, the result of the total consumption is 50 756 kg, which means a fuel – and related pollution – saving of 949 kg during one trip.

The third simulation simulates the implementation of one FR on board, with the effect of reducing the propulsion power demand. In this case, as for the first one, the propulsion and auxiliary power generating units are considered to be independent. The propulsion unit simulation gives fuel consumption of 40 213 kg, which increases up to 49 851 kg if the AEs' independent simulation is included.

Finally, the model provided by FRs and shaft generator should be the one that allows to save the biggest quantity of propellant. It simulates the optimal behaviour for MEs and AEs resulting in a total fuel consumption of 49 781 kg, which means saving 975 kg of combustible compared to the only-shaft-installed case, 70 kg compared to the only-FR-installed case and 1 924 kg compared to the model considering the propulsion and auxiliary system separated, which is approximately the 3.72% of the overall consumption. The values are shown in Table 6, where the saved fuel refers, as comparisons, to the first-analysed topology case.

Case	Fuel consumption [kg]	Saved fuel [kg]	Saving [%]
Prop. and Aux. systems independent	51 705	-	-
Only shaft generator	50 756	949	1.84%
Only FRs	49 851	1854	3.59%
FRs and shaft generator	49 781	1924	3.72%

*Table 6: Fuel consumptions and savings for different solutions*

From the previous data, it is possible to draw out some conclusions. Firstly, it is clear that the implementation of the Flettner rotor does not allow the huge percentage that technology could achieve. In fact, there are nowadays cases with percentages that go from 25% up to 40% of fuel saving, but those are the cases of relatively small ships

furnished with multiple Flettner rotors, where the amount of power demand is considerably lower than the Silja Serenade case. In fact, FRs have some technologic constraints and, as it is easy to understand, their power does not increase with the ship's size. Therefore flat, large ships can be powered by few engines and contain up to four FRs, allowing them to supply a considerable percentage of power, while cruise ships, with less space on the deck and higher, can't be provided with the same effect.

Nevertheless, in absolute terms, the implementation of it – without considering the shaft generator – can lead to save 1854 kg of fuel in one period of 20 hours. According to the International Energy Agency, in Sweden, in the month of May 2019, the HFO costs 1025.06 USD/tonne, which, converted in euro at the change of the same month, is 912.30 €/tonne [76]. Therefore, it results that the implementation of one FR could allow to save 1691.40 € of fuel during the selected time period of 20 hours. As a conclusion, it can be seen that a small percentage of the total consumption actually refer to a reasonable amount of money and saved fuel.

It is worth to notice that the two types of topologies considering the FR or the combination of FR and the shaft does not bring to a reasonable change in the fuel saving. In fact, the difference in the savings is only 70 kg. Nevertheless, it has to be kept in mind that the FR solution does not always allow the same performance, while the implementation of a shaft generator assures convertibility between the mechanical power and the electrical power in every case. Furthermore, it is a good practice to install those systems together in order to better control the trend of the generated powers and avoid large waste.

As a conclusion, it can be stated that the implementation of the Matlab models that simulate the behaviour of different topologies meet the expectations as far as numerical results, comparisons and logic are concerned. The fuel consumptions evaluated in Chapter 7 shows clearly that the installation of a Flettner rotor brings a considerable quantity of saved fuel, for both the simulations with the FR or FR alongside with the shaft generator. Instead, the installation of the only shaft generator brings to savings of around half of the previous case. The Matlab optimisation models have been optimised in order to reduce the needed computing power and to facilitate the convergence of the found solutions.

Further studies could be done collecting experimental data and comparing them with the ones that are given as output from the models. In this way, it would be easy to establish if the simulations are likely or to spot if some of the assumptions are not correct. Moreover, it can be noticed that the simulations do not converge exactly to the minimum result, as time limits are set up in the options: therefore, it is possible that Matlab will release in the next future versions with updated optimisation toolbox that will enable the script to solve the problem with a better logic and to converge in a shorter time.

## References

- [1] European Commission, “2020 climate & energy package,” 2017. [Online]. Available: [https://ec.europa.eu/clima/policies/strategies/2020\\_en](https://ec.europa.eu/clima/policies/strategies/2020_en). [Accessed: 02-Feb-2019].
- [2] 2nd International conference on modelling and optimisation of ship energy system Proceedings of Moses 2019 Conference, “Feasibility analysis of a battery system for a passenger ferry,” pp. 1–2, 2019.
- [3] M. Kaushik, “Bow Thrusters: Construction and Working,” *Marine Insight*, 2019. [Online]. Available: <https://www.marineinsight.com/tech/bow-thrusters-construction-and-working>. [Accessed: 10-Mar-2019].
- [4] N. B. Clausen, “Marine Diesel Engines. How Efficient can a Two-Stroke Engine be?,” Copenhagen, DE, 2009.
- [5] Damian Carrington, “Global pollution kills 9m a year and threatens ‘survival of human societies,’” *The Guardian*, 2018. [Online]. Available: <https://www.theguardian.com/environment/2017/oct/19/global-pollution-kills-millions-threatens-survival-human-societies>. [Accessed: 03-Feb-2019].
- [6] WHO, “How air pollution is destroying our health,” 2019. [Online]. Available: <https://www.who.int/air-pollution/news-and-events/how-air-pollution-is-destroying-our-health>. [Accessed: 02-Feb-2019].
- [7] EIA, “Energy and the Environment Explained: Where Greenhouse Gases Come From,” 2018. [Online]. Available: <https://www.eia.gov/>. [Accessed: 02-Feb-2019].
- [8] WHO, “CLEAN AIR FOR HEALTH: Geneva Action Agenda,” 2018. [Online]. Available: <https://www.who.int/phe/news/clean-air-for-health/en/>. [Accessed: 02-Feb-2019].
- [9] IMO, “Third IMO GHG Study 2014: Executive Summary and Final Report,” Suffolk, UK, 2015.
- [10] R. Kantharia, “Top 7 Green Ship Concepts Using Wind Energy,” *Marine Insight*, 2017. [Online]. Available: <https://www.marineinsight.com/green-ship/top-7-green-ship-concepts-using-wind-energy/>. [Accessed: 07-Feb-2019].
- [11] R. Ionescu, I. Szava, S. Vlase, M. Ivanoiu, and R. Munteanu, “Innovative solutions for portable wind turbines, used on ships,” *Procedia Technology*, 2015.
- [12] Eco Marine Power Co., “Technologies for Sustainable Shipping,” 2013.
- [13] A. Chemistry, L. Johansson, J. Kukkonen, A. Brink, and J. Kalli, “Extension of

an assessment model of ship traffic exhaust emissions for particulate matter and carbon monoxide,” *Atmos. Chem. Phys.*, pp. 2015–2018, 2011.

- [14] H. I. Copuroglu and E. Pesman, “Analysis of Flettner Rotor ships in beam waves,” *Ocean Eng.*, vol. 150, no. January, pp. 352–362, 2018.
- [15] GloMEEP, “Flettner Rotors,” 2018. [Online]. Available: <https://glomeep.imo.org/technology/flettner-rotors/>. [Accessed: 02-Feb-2019].
- [16] B. Krause, “Silja Serenade,” 2009. [Online]. Available: <http://www.faergelejet.dk/faerge.php?id=788>. [Accessed: 03-Feb-2019].
- [17] P. Nuttall, “The Magnus Effect and the Flettner Rotor : Potential Application for Future Oceanic Shipping,” vol. 36, no. 2, pp. 161–182, 2016.
- [18] Kasper Skaarhoj, “The Flettner Rotor – An Invention Ahead of Its Time?,” 2019. [Online]. Available: <https://sdtb.de/museum-of-technology/exhibitions/1623/>. [Accessed: 03-Feb-2019].
- [19] W. Seufert and U. Seufert, “New Scientist: Critics in a spin over Flettner’s ships,” London, UK, pp. 656–659, 1983.
- [20] W. H. Phillips, “JOURNEY IN AERONAUTICAL RESEARCH, A Career at NASA Langley Research Center,” vol. 12, 1998.
- [21] F. Walker, *Ships and Shipbuilders: Pioneers of Design and Construction*. Barnsley, UK: MPG Books Group, 2010.
- [22] K. Kornei, “Spinning metal sails could slash fuel consumption, emissions on cargo ships,” *Science (80-. )*, Sep. 2017.
- [23] A. Moseman, “Cargo Ships Are Turning Back to Wind Power—But Don’t Expect Big Triangular Sails,” *Pop. Mech.*, 2018.
- [24] THiiiNK, “History of windpower,” 2019. [Online]. Available: <http://www.thiink.com/history-of-flettner-rotor/>. [Accessed: 04-May-2019].
- [25] P. J. Marsh, “The Flettner Rotor Makes a Comeback!,” *Marsh’s Maritime Media*, 2017. [Online]. Available: <https://sea-to-summit.net/the-flettner-rotor-makes-a-comeback/>. [Accessed: 07-Feb-2019].
- [26] J. Fagerberg, “Technology and Competitiveness,” *Oxford Rev. Econ. Policy*, vol. 12, no. 3, pp. 39–51, 1996.
- [27] S. Salter, G. Sortino, and J. Latham, “Sea-going hardware for the cloud albedo method of reversing global warming,” *Philos. Trans. R. Soc.*, vol. 366, no. Mathematical physical and Engineering Sciences, pp. 3989–4006, 2008.
- [28] J. Kuepper, “How to Invest in the Global Shipping Sector,” *Int. Invest.*, 2018.

- [29] J. Rifkin, “The Third Industrial Revolution: How the Internet, Green Electricity, and 3-D Printing are Ushering in a Sustainable Era of Distributed Capitalism,” *World Financ. Rev.*, 2012.
- [30] N. Georgescu-Roegen, “The Entropy Law and the Economic Process in Retrospect,” *Eastern Economic Journal*, 1986.
- [31] H. Daly, “Towards A Steady-State Economy,” College Park, UK, 2008.
- [32] J. Lee, “A Fire’s Carbon Footprint,” 2007. [Online]. Available: <http://idahoptv.org/outdoors/shows/wildfire/carbonfootprint.cfm>. [Accessed: 23-Apr-2019].
- [33] T. Altenburg and C. Assmann, *Green Industrial Policy. Concept, Policies, Country Experiences*, First. Geneva, Bonn, 2017.
- [34] A. S. Nada, “Renewable energy will power the green economy, innovation will drive it,” *The National*, 2014. [Online]. Available: <https://www.thenational.ae/opinion/renewable-energy-will-power-the-green-economy-innovation-will-drive-it-1.264720>. [Accessed: 09-Feb-2019].
- [35] International Institute for Labour Studies, “Policy options and instruments for a green economy,” 2011.
- [36] J. Kanter, “Is Nuclear Power Renewable?,” *The New York Times*, 2009. [Online]. Available: <https://green.blogs.nytimes.com/2009/08/03/is-nuclear-power-renewable/>. [Accessed: 20-May-2019].
- [37] ENERCON, “Enercon E-Ship 1. A Wind-Hybrid Commercial Cargo Ship,” *4th Conference on Ship Efficiency*, 2013.
- [38] M. Schuler, “Wind Propulsion Vessel E-Ship 1 – Interesting Ship of The Week,” *gCaptain*, 2008. [Online]. Available: <https://gcaptain.com/interesting-ship-of-the-week-e-ship-1/>.
- [39] T. Craft, N. Johnson, and B. Launder, “Back to the Future ? A Re-examination of the Aerodynamics of Flettner-Thom Rotors for Maritime Propulsion Back to the Future ? A Re-examination of the Aerodynamics of Flettner-Thom Rotors for Maritime Propulsion,” *Flow Turbulence Combust.*, vol. 92, pp. 413–427, 2014.
- [40] D. R. Pearson, “The use of Flettner rotors in efficient ship design,” London, UK, 2014.
- [41] M. D. A. Al-falahi, T. Tarasiuk, S. G. Jayasinghe, Z. Jin, H. Enshaei, and J. M. Guerrero, “AC Ship Microgrids: Control and Power,” Basel, Switzerland, 2018.
- [42] Bore, “Successful trial-phases for Norsepower’s Rotor Sail System onboard

M/V Estraden,” 2015. [Online]. Available: <https://www.bore.eu/successful-trial-phases-for-norsepowers-rotor-sail-system-onboard-mv-estraden/>. [Accessed: 11-Feb-2019].

- [43] J. Stansfield, “New Ship Rotor Sail Wind Power Technology Successfully Tested,” *VesselFinder*, 2015. [Online]. Available: <https://www.vesselfinder.com/news/3506-New-Ship-Rotor-Sail-Wind-Power-Technology-Successfully-Tested>. [Accessed: 11-Feb-2019].
- [44] eZ Systems, “Norsepower and Bore Successfully Test Wind Power Technology for Ships,” *NAPA - Solutions for Design and Operation of Ships*, 2015. [Online]. Available: <https://www.napa.fi/News/Press-Releases/Norsepower-and-Bore-Successfully-Test-Wind-Power-Technology-for-Ships>. [Accessed: 11-Feb-2019].
- [45] Z. Guangrong, “Ship energy efficiency technologies - now and the future,” Espoo, FI, 2017.
- [46] S. Modeva, “Norsepower’s Rotor Sail Solution Wins Prestigious ‘Innovation of the Year’ Award,” 2016. [Online]. Available: <https://www.vesselfinder.com/news/6535-Norsepowers-Rotor-Sail-Solution-Wins-Prestigious-Innovation-of-the-Year-Award>. [Accessed: 11-Feb-2019].
- [47] J. Stansfield, “Norsepower receives €2.6M funding to develop the world’s largest Rotor Sail,” *VesselFinder*, 2016. [Online]. Available: <https://www.vesselfinder.com/news/7038-Norsepower-receives-26M-funding-to-develop-the-worlds-largest-Rotor-Sail>. [Accessed: 11-Feb-2019].
- [48] M. Schuler, “Maersk Tanker to Be Fitted with Flettner Rotor Sails.,” *gCaptain*, 2017. [Online]. Available: <https://gcaptain.com/maersk-tanker-fitted-flettner-rotor-sails/>. [Accessed: 08-Apr-2019].
- [49] C. Mims, “‘Albedo Yachts’ and Marine Clouds: A Cure for Climate Change?,” *Scientific American*, 2009. [Online]. Available: <https://www.scientificamerican.com/article/albedo-yachts-and-marine-clouds/>. [Accessed: 02-Apr-2019].
- [50] P. K. Shea and T. F. Radke, “Foldable Flettner Rotor for Small Sailing Boats Foldable Flettner Rotor for Small Sailing Boats Focus Project,” Zürich, 2014.
- [51] T. Glatzel *et al.*, “Computational fluid dynamics ( CFD ) software tools for microfluidic applications – A case study,” *Comput. Fluids*, vol. 37, pp. 218–234, 2008.
- [52] R. Woods, “Thomas Newcomen and the Steam Engine,” *Mechanical Engineering Magazine*, 2003. [Online]. Available: [https://ethw.org/Thomas\\_Newcomen\\_and\\_the\\_Steam\\_Engine](https://ethw.org/Thomas_Newcomen_and_the_Steam_Engine). [Accessed: 04-Apr-2019].

- [53] E. Lewis, Ed., *Principles of Naval Architecture*, Second edit. Jersey City, NJ: The society of Naval Architects and Marine Engineers, 1988.
- [54] A. Rowen, “Machinery consideration,” in *Ship Design & Construction*, First edit., T. Lamb, Ed. Jersey City, NJ: Society of Naval Architects and Marine Engineers, 2003, pp. 20–21.
- [55] MI News Network, “Understanding Nuclear Marine Propulsion,” *Marine Insight*, 2017. [Online]. Available: <https://www.marineinsight.com/main-engine/understanding-nuclear-marine-propulsion/>. [Accessed: 08-Mar-2019].
- [56] M. Jaurola, A. Heidin, S. Tikkanen, and K. Huhtala, “Optimising design and power management in energy-efficient marine vessel power systems: a literature review,” *J. Mar. Eng. Technol.*, 2018.
- [57] A. L. Rowen, “Machinery Consideration,” in *Ship Design & Construction*, First edit., T. Lamb, Ed. Jersey city, NJ: Society of Naval Architects and Marine Engineers, 2003, pp. 1–6.
- [58] S. Ghosh, “Understanding Design Of Ship Propeller,” *Marine Insight*, 2017. [Online]. Available: <https://www.marineinsight.com/naval-architecture/design-of-ship-propeller/>. [Accessed: 22-Mar-2019].
- [59] A. Molland, *The Maritime Engineering Reference Book - A guide to ship design, construction and operation*, First edit. Burlington, USA: Elsevier, 2008.
- [60] A. Molland, *The Maritime Engineering Reference Book - A guide to ship design, construction and operation*, First edit. Burlington, USA: Elsevier, 2008.
- [61] T. Sinha, “Electric generators and motors: An overview,” *Marine Insight*, 2017. [Online]. Available: <https://www.marineinsight.com/naval-architecture/introduction-to-tunnel-thrusters-ships/>. [Accessed: 01-Mar-2019].
- [62] N. Goyal, “World’s Most Powerful Marine Diesel Engine Puts Out Nearly 109,000 HP!,” *Industry Tap*, 2015. [Online]. Available: <http://www.industrytap.com/worlds-powerful-marine-diesel-engine-puts-nearly-109000-hp/27177>. [Accessed: 04-May-2019].
- [63] R. M. Calfo, J. A. Fulmer, and J. E. Tessaro, “Generators for use in Electric Marine Ship Propulsion Systems,” Chicago, IL, USA, 2002.
- [64] Wärtsilä, “Diesel-Electric Propulsion Systems,” 2016.
- [65] MAN AG, “Diesel-electric Drives,” 2016. [Online]. Available: <https://marine.mandieselturbo.com/docs/librariesprovider6/marine-broschures/diesel-electric-drives-guideline.pdf>. [Accessed: 04-May-2019].
- [66] I. Boldea, “Electric Generators and Motors : an overview,” *CES Trans. Electr. Mach. Syst.*, vol. 1, pp. 3–12, 2017.



- [67] A. Wankhede, “How is Power Generated and Supplied on a Ship?,” *Marine Insight*, 2017. [Online]. Available: <https://www.marineinsight.com/marine-electrical/how-is-power-generated-and-supplied-on-a-ship/>. [Accessed: 01-Mar-2019].
- [68] D. Stapersma and H. Woud, “Matching propulsion engine with propulsor,” *J. Mar. Eng. Technol.*, vol. 4177, 2014.
- [69] K. Valkeejärvi, “The ship’s electrical network, engine control and automation,” *R. Belgian Inst. Mar. Eng.*, 2006.
- [70] P. Wu and R. Bucknall, “Marine propulsion using battery power,” University College London, 2016.
- [71] W. Schäfer, “Ship drive with a drive engine and directly driven propeller shaft,” US 6,183,317 B1, 2001.
- [72] R. D. Geertsma, R. R. Negenborn, K. Visser, and J. J. Hopman, “Design and control of hybrid power and propulsion systems for smart ships : A review of developments,” *Appl. Energy*, vol. 194, pp. 30–54, 2017.
- [73] J. M. Apsley *et al.*, “Propulsion Drive Models for Full Electric Marine Propulsion Systems,” *IEEE Trans. Ind. Appl.*, vol. 45, no. 2, pp. 676–684, 2009.
- [74] B. Palczynska, L. Spiralski, and J. Wyszowski, “Electromagnetic Field Measurements of Bow Thruster Drive with Frequency Converter,” in *5th International Conference-Workshop*, 2007.
- [75] eduCBA, “Uses Of Matlab,” 2019. [Online]. Available: <https://www.educba.com/uses-of-matlab/>. [Accessed: 05-May-2019].
- [76] International Energy Agency, “Key World Energy Statistics,” 2019. [Online]. Available: <https://www.iea.org/statistics/kwes/prices/>. [Accessed: 12-May-2019].